

38599

INTERACTION OF VITAMIN E WITH CHOLESTEROL-CONTAINING  
PHOSPHOLIPID MODEL MEMBRANES: AN FTIR STUDY

A Master's Thesis

Presented by

BAYKAL, Ülkü

to

the Graduate School of Natural and Applied Sciences

of Middle East Technical University

in Partial Fulfillment of the Degree of

MASTER OF SCIENCE

in

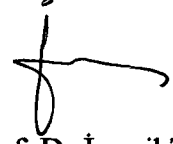
BIOTECHNOLOGY

MIDDLE EAST TECHNICAL UNIVERSITY

ANKARA

January, 1995

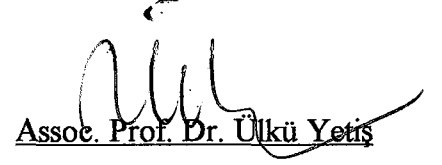
Approval of the Graduate School of Natural and Applied Sciences



Prof. Dr. İsmail Tosun

Director

I certify that this thesis satisfies all the requirements as a thesis for the degree of Master of Science.



Assoc. Prof. Dr. Ülkü Yetiş

Chairman of the Department

We certify that we have read this thesis and in our opinion it is fully adequate, in scope and quality, as a thesis for the degree of Master of Science in Biotechnology.



Prof. Dr. Şefik Süzer

Co-Supervisor



Prof. Dr. Feride Severcan

Supervisor

Examining Committee in Charge

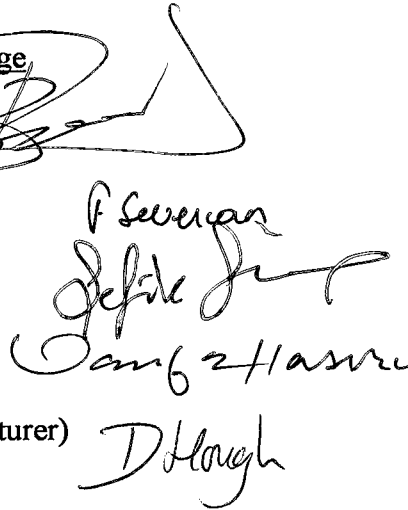
Prof. Dr. Lemi Türker

Prof. Dr. Feride Severcan

Prof. Dr. Şefik Süzer

Prof. Dr. Vasif Hasırcı

Dr. David Hough (Senior Lecturer)



## ABSTRACT

### INTERACTION OF VITAMIN E WITH CHOLESTEROL-CONTAINING PHOSPHOLIPID MODEL MEMBRANES: AN FTIR STUDY

BAYKAL, Ülkü

M.S. in Biotechnology

Supervisor: Prof. Dr. Feride Severcan

Co-Supervisor: Prof. Dr. Şefik Süzer

January, 1995, 101 sayfa

Effect of  $\alpha$ -Tocopherol which is the major component of Vitamin E, on cholesterol-containing Dipalmitoyl Phosphatidylcholine (DPPC) multilamellar liposomes has been investigated by FTIR spectroscopic technique at different temperatures.

The investigation of  $\text{CH}_2$  stretching bands reveals that, when both  $\alpha\text{T}$  and cholesterol are present together in the system, in the gel phase, they exhibit additive effect on acyl chain organization by increasing the number of gauche rotamers. On the contrary, in the liquid crystalline phase,  $\alpha\text{T}$  reduces the effect of cholesterol by increasing the number of gauche rotamers in the system. Effect of  $\alpha\text{T}$  concentration on cholesterol-membrane interaction is that, effect of  $\alpha\text{T}$  is dominant and effect of cholesterol on DPPC liposomes decreases gradually with increasing  $\alpha\text{T}$  concentration.

Investigation of  $\text{CH}_3$  asymmetric stretching mode implies that, the addition of  $\alpha\text{T}$  into cholesterol-containing liposomes introduces an additional stiffness in the deep interior of the bilayer.

Infrared spectra of  $\text{CH}_2$  scissoring bands reveals that, when  $\alpha\text{T}$  and cholesterol are present in the system an increase in the conformational disorder and chain rotation is observed. Joint effect of  $\alpha\text{T}$  and cholesterol on  $\text{C}=\text{O}$  stretching mode is that, in the gel phase  $\alpha\text{T}$  makes stronger OH bonding with DPPC head group and has dominant effect relative to cholesterol. In liquid crystalline phase, system behaves as if there is no cholesterol in the system.

Key Words: Vitamin E, Cholesterol, DPPC, Liposome, Phospholipid Membrane, Membrane Structure, Membrane Dynamics, FTIR.

Science code: 401.02.00

ÖZ

VİTAMİN E' NİN KOLESTEROL İÇEREN FOSFOLİPİD MODEL HÜCRE  
ZARLARIYLA ETKİLEŞMESİ: BİR FTIR ÇALIŞMASI

BAYKAL, Ülku

Yüksek Lisans Tezi, Biyoteknoloji Anabilim Dalı

Tez Yöneticisi: Feride Severcan

Yardımcı Tez Yöneticisi: Şefik Süzer

Ocak, 1994, 101 sayfa

Vitamin E'nin en önemli bileşeni olan  $\alpha$ -tokoferolün, kolesterol içeren çok tabakalı DPPC lipozomları ile etkileşmesi, farklı sıcaklıklarda, FTIR spektroskopik tekniği ile incelenmiştir.

$\text{CH}_2$  gerilme bantlarının incelenmesi gösterir ki,  $\alpha$ T ve kolesterol, ikisi birden sistemde oldukları vakit, jel fazda gauche rotamerlerinin sayısını artırarak hidrokarbon zincir organizasyonuna önemli bir etki yapar. Buna karşılık, sıvı kristal fazda,  $\alpha$ T sistemdeki gauche rotamerlerin sayısını artırarak kolesterolün etkisini azaltır.  $\alpha$ T konsantrasyonunun kolesterol-membran etkileşmesine etkisi şudur:  $\alpha$ T etken olup, DPPC lipozomları üzerine kolesterolün etkisi  $\alpha$ T konsantrasyonu arttıkça azalır.

$\text{CH}_3$  asimetrik gerilme modunun incelenmesi, kolesterol içeren lipozomlara  $\alpha\text{T}$  katılması ile lipozomların iç derinliklerinde ilave sertlik meydana geldiğini gösterir.

$\text{CH}_2$  makaslama bandının infrared spektrumları incelendiğinde, kolesterol ve  $\alpha\text{T}$ 'ün sistemde birarada olmasıyla, konformasyonel düzensizlikte ve zincir dönmesinde artış göstermiştir.

$\alpha\text{T}$  ve kolesterolün  $\text{C}=\text{O}$  gerilme modu üzerindeki müşterek etkisi, jel fazda  $\alpha\text{T}$ 'ün kolesterole göre daha etken olduğu ve DPPC baş grubu ile daha kuvvetli bir OH bağlanması yaptığı şeklindedir. Sıvı kristal fazda ise, sonuçlar sistemde kolesterol yokmuş gibidir.

Anahtar Kelimeler: Vitamin E, Kolesterol, Fosfolipid Model Membran, Membran Yapısı, Membran Dinamiği, FTIR

Bilim Dalı Sayısal Kodu: 401.02.00

## ACNOWLEDGEMENTS

I am grateful to Prof. Dr. Feride SEVERCAN and Prof. Dr. Şefik SÜZER for their interest and encouragements throughout this study.

I would like to thank Prof. Dr. Saim ÖZKAR for providing me with FTIR spectrometer, Assoc. Prof. Ceyhan KAYRAN and Ayşin TEKKAYA for their valuable help during this study.

My gratitudes go to my brother, Şevket A. BAYKAL for his valuable help during preparation of the manuscript.

I would like to thank my family for their continuous support and encouragements throughout the study.

## TABLE OF CONTENTS

ABSTRACT.....	iii
ÖZ.....	v
ACKNOWLEDGEMENTS.....	vii
LIST OF TABLES.....	x
LIST OF FIGURES.....	xi
CHAPTER I: INTRODUCTION.....	1
1.1 Importance of Biological Membrane Studies and Aim of This Study.....	1
1.2 Basic Theory of Biological Membranes.....	2
1.2.1 Molecular Motions in Membranes.....	5
1.2.2 Thermotropic Phase Transitions in Membranes.....	9
1.2.3 Lipid Asymmetry and Lateral Phase Separation.....	10
1.3 Structure and Function of Cholesterol.....	13
1.4 Structure and Function of Vitamin E.....	17
1.5 Responsible Forces Governing The Bilayer Formation.....	23
1.6 Infrared spectroscopy.....	27
1.6.1 The Basic Theory.....	27
1.6.2 Advantages of FTIR Spectroscopy to Other Biophysical Techniques..	32
CHAPTER II: MATERIALS AND METHODS.....	34
2.1 Reagents.....	34
2.2 Model Membrane Preparations.....	34
2.3 Instrumentation.....	35
2.3.1 Dispersive Instruments.....	35
2.3.2 Fourier Transform Infrared (FTIR) Spectrometer.....	36
2.4 Sample Handling.....	37



2.5 Infrared Spectral Regions Used in This Study.....	41
2.6 Spectrum Handling.....	42
2.7 Empirical Rules Used in FTIR Spectroscopic Membrane Research.....	51
CHAPTER III: RESULTS AND DISCUSSION.....	53
3.1 Spectral Characteristic of the Acyl Chains.....	53
3.1.1 Vitamin E-Membrane Interactions.....	55
3.1.2 Cholesterol Membrane Interactions.....	64
3.1.3 Vitamin E-Cholesterol-Membrane Interactions.....	67
3.1.3.1 CH <sub>2</sub> Stretching Modes.....	67
3.1.3.2 CH <sub>3</sub> Asymmetric Stretching.....	78
3.1.3.3 CH <sub>2</sub> Scissoring Mode.....	80
3.1.3.4 Head Group Vibration: C=O Stretching Mode.....	86
CHAPTER IV: CONCLUSION.....	92
REFERENCES.....	97

## LIST OF TABLES

Table 1. Lipid compositions of some biological membranes.....	3
Table 2. The hydrocarbon chain modes often used in the study of aqueous lipid assemblies. ....	41



## LIST OF FIGURES

Figure 1. Schematic illustration of amphiphile structures. ....	4
Figure 2. A general model for the structure of biological membranes.....	5
Figure 3. Flip-flop transition of lipid molecules.....	7
Figure 4. Structure of 1,2-diacylphosphatidylcholine molecule emphasizing the relative orientation and conformation of the head group and of the acyl chain. The lower part of the figure illustrates an alkyl chain in an all-trans and part-gauche conformations. The Newman projections for the trans and gauche conformations are also shown. ....	8
Figure 5. Schematic illustration of the lamellar bilayer phases. ....	10
Figure 6. Schematic illustration of possible structures of a spherical bilayer composed of two types of lipids (a) A homogeneous bilayer. (b) Asymmetric compositions of two surfaces. (c) Lateral phase separations of both surfaces. (d) Lateral phase separation off the inner surface only. ....	11
Figure 7. Schematic illustration of lateral phase separation in the plane of a lipid bilayer membrane. ....	12
Figure 8. Structure of cholesterol shown in two different conventions. ....	14
Figure 9. Possible models for the lateral packing of phospholipid + cholesterol 1:1 (left) and 1:2 (right) viewed perpendicular to the plane of the lamellar phase.....	16
Figure 10. Partial phase diagram for cholesterol/DPPC mixtures. ....	17
Figure 11. Schematic illustration of $\alpha$ -Tocopherol. ....	18
Figure 12. The vitamin E cycle enzymic and non-enzymic recycling interactions of water and lipid soluble antioxidants with vitamin E radicals in human erythrocyte membranes.....	20
Figure 13. Vitamin E as a biological response modifier.....	21
Figure 14. Potential energy diagrams. (1) Harmonic oscillator, (2) anharmonic oscillator. ....	29

Figure 15. Types of normal vibrations in a linear (A) and a non-linear (B) triatomic molecule.....	31
Figure 16. Infrared spectrum of $\text{CaF}_2$ .....	38
Figure 17. Infrared spectrum of DPPC multibilayer liposomes with (a) and (b) without spacer.....	40
Figure 18. Infrared spectrum of the air.....	43
Figure 19. Infrared spectrum of liquid water.....	44
Figure 20. Water vapor bands on the infrared spectrum of a DPPC sample in the region of C=O stretching mode at 50°C.....	46
Figure 21. FTIR spectrum of aqueous DPPC multilamellar liposomes at 30°C (a) before and (b) after water subtraction.....	47
Figure 22. FTIR spectra of DPPC liposomes at different water concentration.(a) 90%, (b)80% hydration.....	49
Figure 23. FTIR spectrum of DPPC multilamellar liposomes in $\text{D}_2\text{O}$ .....	50
Figure 24. Temperature dependence for the C-H stretching region of the FTIR spectrum of pure DPPC multilamellar liposomes at different temperatures.....	54
Figure 25. Frequency of the $\text{CH}_2$ antisymmetric stretching mode of DPPC multilamellars versus temperature for DPPC multilamellar liposomes-containing 0 mol% $\alpha\text{T}$ , 6mol% $\alpha\text{T}$ , 12 mol% $\alpha\text{T}$ , and 20 mol% $\alpha\text{T}$ .....	56
Figure 26. Frequency of the $\text{CH}_2$ symmetric stretching of DPPC multibilayers versus temperature for DPPC multilamellar liposomes-containing 0 mol% $\alpha\text{T}$ , 6 mol% $\alpha\text{T}$ , 12 mol% $\alpha\text{T}$ , and 20 mol% $\alpha\text{T}$ .....	57
Figure 27. Temperature dependence frequency of $\text{CH}_2$ antisymmetric stretching mode of DPPC liposomes in the absence and in the presence of 20 mol% $\alpha\text{T}$ for $\text{H}_2\text{O}$ hydration.....	59
Figure 28. Temperature dependence frequency of $\text{CH}_2$ antisymmetric stretching mode of DPPC liposomes in the absence and in the presence of 20 mol% $\alpha\text{T}$ for $\text{D}_2\text{O}$ hydration.....	60

Figure 29. Temperature dependence of the bandwidth at 0.75x peak height of the CH <sub>2</sub> antisymmetric stretching mode of DPPC multilamellar liposomes containing-0 mol% αT, 6 mol% αT, 12 mol% αT, and 20 mol% α.T.....	62
Figure 30. Temperature dependence of the bandwidth at 0.75x peak height of the CH <sub>2</sub> symmetric stretching mode of DPPC multilamellar liposomes containing 0 mol% αT, 6 mol% αT, 12 mol% αT, and 20 mol% αT.....	63
Figure 31. Temperature dependence frequency of CH <sub>2</sub> symmetric stretching mode of DPPC multilamellar liposomes containing-0 mol% cholesterol, 20 mol% cholesterol,and 40 mol% cholesterol. ....	65
Figure 32. Temperature dependence of the bandwidth at 0.75x peak height of the CH <sub>2</sub> symmetric stretching mode of DPPC multilamellar liposomes containing 0 mol% cholesterol, 20 mol% cholesterol, and 40 mol% cholesterol.....	66
Figure 33. Temperature dependence frequency of CH <sub>2</sub> antisymmetric stretching mode of DPPC multilamellar liposomes containing 0 mol% cholesterol + 0mol% αT, 20 mol% cholesterol, 20 mol% αT, 20 mol% cholesterol + 20 mol% αT.....	68
Figure 34. Temperature dependence frequency of CH <sub>2</sub> symmetric stretching mode of DPPC multilamellar liposomes containing-0 mol% cholesterol + 0mol% αT, 20 mol% cholesterol, 20 mol% αT, 20 mol% cholesterol + 20 mol% αT.....	69
Figure 35. Temperature dependence of the bandwidth at 0.75x peak height Of CH <sub>2</sub> antisymmetric stretching mode of DPPC multilamellar liposomes containing-0 mol% cholesterol + 0 mol% αT, 20 mol% cholesterol, 20 mol% αT, 20 mol% cholesterol + 20 mol% αT.....	71
Figure 36. Temperature dependence of the bandwidth at 0.75x peak height of CH <sub>2</sub> symmetric stretching mode of DPPC multilamellar liposomes containing-0 mol% cholesterol + 0 mol% αT, 20 mol% cholesterol, 20 mol% αT, 20 mol% cholesterol + 20 mol% αT. ....	72
Figure 37. Temperature dependence of the CH <sub>2</sub> antisymmetric stretching mode of DPPC multilamellar liposomes containing-0 mol% cholesterol + 0 mol% αT, 20 mol% cholesterol, 20 mol% αT, 20 mol% cholesterol + 6 mol% αT, 20 mol% cholesterol + 12 mol% αT, 20 mol% cholesterol + 20 mol% αT.....	74

Figure 38. Temperature dependence of the CH <sub>2</sub> symmetric stretching mode of DPPC multilamellar liposomes containing-0 mol% cholesterol + 0 mol% αT, 20 mol% cholesterol, 20 mol% αT, 20 mol% cholesterol + 6 mol% αT, 20 mol% cholesterol + 12 mol% αT, 20 mol% cholesterol + 20 mol% αT.....	75
Figure 39. Temperature dependence of the bandwidth at 0.75x peak height of CH <sub>2</sub> symmetric stretching mode of DPPC multilamellar liposomes containing-0 mol% cholesterol + 0 mol% αT, 20 mol% cholesterol, 20 mol% αT, 20 mol% cholesterol + 6 mol% α, 20 mol% cholesterol + 12 mol%αT, 20 mol% cholesterol + 20 mol% αT.....	77
Figure 40. Temperature dependence of the frequency of the asymmetric CH <sub>3</sub> stretching mode of DPPC multilamellar liposomes containing 0 mol% cholesterol + 0 mol% αT, 20 mol% cholesterol, 20 mol% α T, and 20 mol% cholesterol + 20 mol% αT.....	79
Figure 41. Infrared spectra of the CH <sub>2</sub> scissoring band of DPPC multibilayers at different temperatures.....	81
Figure 42. Acyl chain crystal-packing patterns: A, orthorhombic or monoclinic; B, hexagonal and C, triclinic. In all cases, the long axes of the chains are projecting from the page. In the case of hexagonal packing, the torsion about the long axes is such that the orientations of chains relative to each other at a given moment are random.....	82
Figure 43. CH <sub>2</sub> scissoring mode of spectra of DPPC multibilayer liposomes containing (1) 0 mol% cholesterol + 0 mol% αT, (2) 20 mol% cholesterol, (3) 20 mol% αT, (4) 20 mol% cholesterol + 20 mol% α T at 32°C.....	83
Figure 44. CH <sub>2</sub> scissoring mode of spectra of DPPC multibilayer liposomes containing (1) 0 mol% cholesterol + 0 mol% αT, (2) 20 mol% cholesterol, (3) 20 mol% αT, (4) 20 mol% cholesterol + 20 mol% α T at 39°C.....	84
Figure 45. CH <sub>2</sub> scissoring mode of spectra of DPPC multibilayer liposomes containing (1) 0 mol% cholesterol + 0 mol% αT, (2) 20 mol% cholesterol, (3) 20 mol% αT, (4) 20 mol% cholesterol + 20 mol% α T at 49°C.....	85
Figure 46. Infrared spectra in the C=O stretching region of DPPC multilamellar liposomes at six temperatures (24, 32, 36, 39, 41.2, and 49°C) in decreasing intensity.....	87

- Figure 47. Infrared spectra in the C=O stretching region of DPPC multilamellar liposomes containing (1) 0 mol% cholesterol + 0 mol%  $\alpha$ T, (2) 20 mol% cholesterol, (3) 20 mol%  $\alpha$ T, (4) 20 mol% cholesterol + 20 mol%  $\alpha$ T at 42°C. .... 88
- Figure 48. Temperature dependence frequency changes of C=O stretching mode for DPPC multilamellar liposomes containing 0 mol% cholesterol + 0 mol%  $\alpha$ T, 20 mol% cholesterol, 20 mol%  $\alpha$ T, and 20 mol% cholesterol + 20 mol%  $\alpha$ T. .... 89
- Figure 49. Temperature dependence of the bandwidth at 0.75x peak height of C=O stretching mode of DPPC multilamellar liposomes containing 0 mol% cholesterol + 0 mol%  $\alpha$ T, 20 mol% cholesterol, 20 mol%  $\alpha$ T, 20 mol% cholesterol + 20 mol%  $\alpha$ T. .... 91



## INTRODUCTION

### CHAPTER I

#### 1.1 Importance of Model Membrane Studies and the Aim of This Work

Biological membranes contain different lipid-protein-polysaccharide compositions, and they have quite complex structures. It is usually very difficult to give a completely satisfying explanation about the lipid interactions occurring between membrane components in biological membranes[1]. Synthetic membranes, made from a double-chain phospholipid amphiphile, have many of the basic characteristics of natural biological membranes[2]. In this case, it is possible to change membrane composition, concentration and experimental conditions. Therefore model membrane studies are very important in membrane research. Real biological membranes are in the form of unilamellar liposomes which are of larger dimensions. The extruder is the best equipment at present to obtain unilamellar liposomes, but the largest diameter that we can obtain is around 400 nm which is still far from the real systems. In addition to this, harmful effect of sonication and pressure on membranes should be considered. For these reasons MLV systems are suitable for the investigation of many structural and functional questions concerning the bilayer phase, except for transport studies[3].

Maintenance of ionic gradients, transmembrane potentials, activities of membrane-bound enzymes, interactions between membrane proteins, transmembrane signal transmission, intercellular communication, manifestation of cellular development and cell transformation, all depend on the structure and fluidity of the



lipid bilayer[2]. For these and other reasons, studies on the structure and dynamics of phospholipid model membranes have become particularly important in recent years.

Although vitamin E is used in the protection and treatment of several diseases, the exact molecular mechanism behind such diverse functions of vitamin E is not clearly known. The present study was done to examine the interaction of  $\alpha$ T with model membranes in the presence of cholesterol, in order to provide better understanding of the molecular mechanism of action of  $\alpha$ T, especially in the treatment and prevention of cardiovascular disorders. Although numerous studies appeared in the literature on interaction of  $\alpha$ T or cholesterol with saturated and unsaturated lipid membranes [4-12], interaction of  $\alpha$ T with model membranes in the presence of cholesterol has not been reported to date. To achieve this goal, the effect of  $\alpha$ T on cholesterol-containing liposomes has been investigated by using FTIR spectroscopic technique.

## 1.2 Basic Theory of Biological Membranes

Membranes are the most common cellular structures in both plants and animals. They are now recognized as being involved in almost all aspects of cellular activity ranging from motility or food entrapment in simple unicellular organisms, to such complex functions as energy transduction, immunorecognition, or biosynthesis in higher organisms. Such diverse functions are mediated and regulated by and through membrane. Thus, an understanding of the physical principles that govern the molecular organization of membranes is essential for identification of their physiological roles since structure and function are strongly interdependent in membranes[13].

Membranes are composite structures which are essentially composed of proteins(50%-60%) and lipids(40%-50%). The lipid portion is derived from cholesterol, phosphoglycerides and sphingomyelins. The lipid composition of some biological membranes is given in table 1

Table 1. %Lipid compositions in some biological membranes.

Lipid	Human erythrocyte	Human myelin	Beef-heart mitochondria	E. coli
Phosphatidic acid	1.5	0.5	0	0
Phosphatidyl choline	19	10	39	0
Phosphatidyl ethanolamine	18	20	27	65
Phosphatidyl glycerol	0	0	0	18
Phosphatidyl inositol	1	1	7	0
Phosphatidyl serine	8.5	8.5	0.5	0
Cardiolipin	0	0	22.5	12
Sphingomyelin	17.5	8.5	0	0
Glycolipids	10	26	0	0
Cholesterol	2.5	26	3	0

In phosphoglycerides and sphingomyelins polar group residues (e.g, ethanolamine, choline, serine, inositol, glycerol,etc.) are bound to phosphoric acid. The result is an amphipathic molecule with a polar head and a nonpolar hydrophobic tail.

The crucial physical characteristic of the double-chain amphiphile is its tendency to form bilayers in aqueous dispersions, in the form of single vesicles or

multilamellar structures. The amphiphiles arrange themselves with polar head groups exposed to the aqueous phase and the hydrocarbon moieties clumped together generating their own hydrophobic environment. The bilayer acts as a membrane, separating components encapsulated on the inside of the vesicle from those on the outside. Clearly the thickness of the bilayer will depend on the length and stiffness of the hydrocarbon moieties of the lipids. Fig.1 shows the schematic representation of amphiphile structures[1].

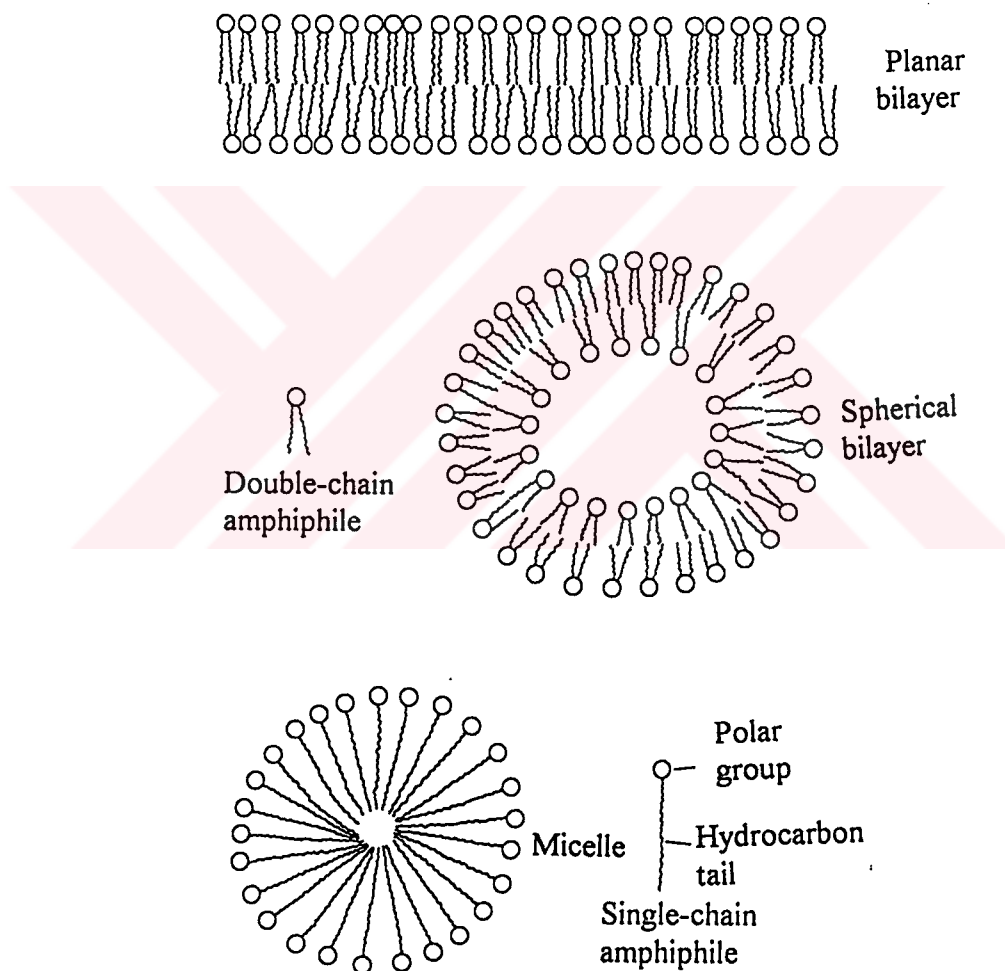


Figure 1. Schematic illustration of amphiphile structures. The planer bilayer and spherical bilayer.(vesicle) are formed from double-chain amphiphiles. The micelle is formed from a single-chain amphiphile.

The most popular model for the structure of biological membranes is the fluid mosaic model which was proposed by Singer and Nicholson[1]. This model is shown in Fig.2.

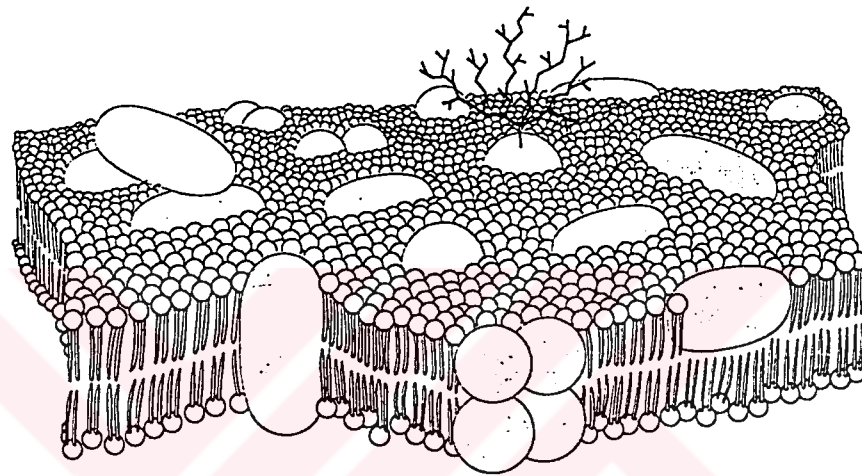


Figure 2. A general model for the structure of biological membranes.

According to this model, the phospholipid bilayer is accepted as a fluid matrix  $60\text{\AA}$  to  $100\text{\AA}$  thick in which various integral proteins are implanted. Some proteins protrude through only one side. Most peripheral proteins are expected to be located on the surface of the membrane.

### 1.2.1 Molecular Motions in Membranes

The motions of lipid molecules in natural and artificial bilayers have been investigated in detail at the molecular level employing such physical methods of study

as ESR, NMR, fluorescence, infrared and raman spectroscopy, in spite of the remaining discrepancies concerning interpretations and conclusions, regarding lipid dynamics and membrane organization, obtained from these studies.

It is known that the membrane has a dynamic nature. Lipid and protein components are in motion. Several types of molecular motion are experienced by the components within the constraints of the bilayer organization. Rotation of molecules along their axes perpendicular to the plane of the membrane occurs every 0.1-100 nsec for lipids and 0.01-100 msec for proteins; segmental motions of acyl chains (0.01-1 nsec) gives rise to an increased disorder toward the center of the membrane.

Two types of motion have been described namely, intramolecular movements of a part of a molecule with respect to another (e.g. rotational and torsional motions about single bonds and motions of individual acyl chains) and whole molecule motions. Whole molecule motions involve two types of motions: rotation and translation. Translation can be further subdivided into lateral translation and transbilayer migration. Translational motion can take place in two ways in the bilayer systems. Translation of lipids in the plane of bilayer, a motion limited to one monolayer of the bilayer, comprises the first type of the translational motion. The second is the transverse migration across the bilayer from one monolayer to other. This type of motion is referred to as flip-flop (Fig.3). It is very rare and slow. Its occurrence takes several hours. These motions are considered when dealing with such fundamental properties of biomembranes as thermotropic phase transitions, lipid-lipid and lipid-protein interactions and bilayer viscosity. The reason for the slowness of the flip-flop motion of lipid molecules is that it is energetically unfavorable because it requires insertion of the polar groups into nonpolar regions and exposure of the

apolar groups to the polar regions. Such motions might be essential for carrying out many of the functions associated with membranes.

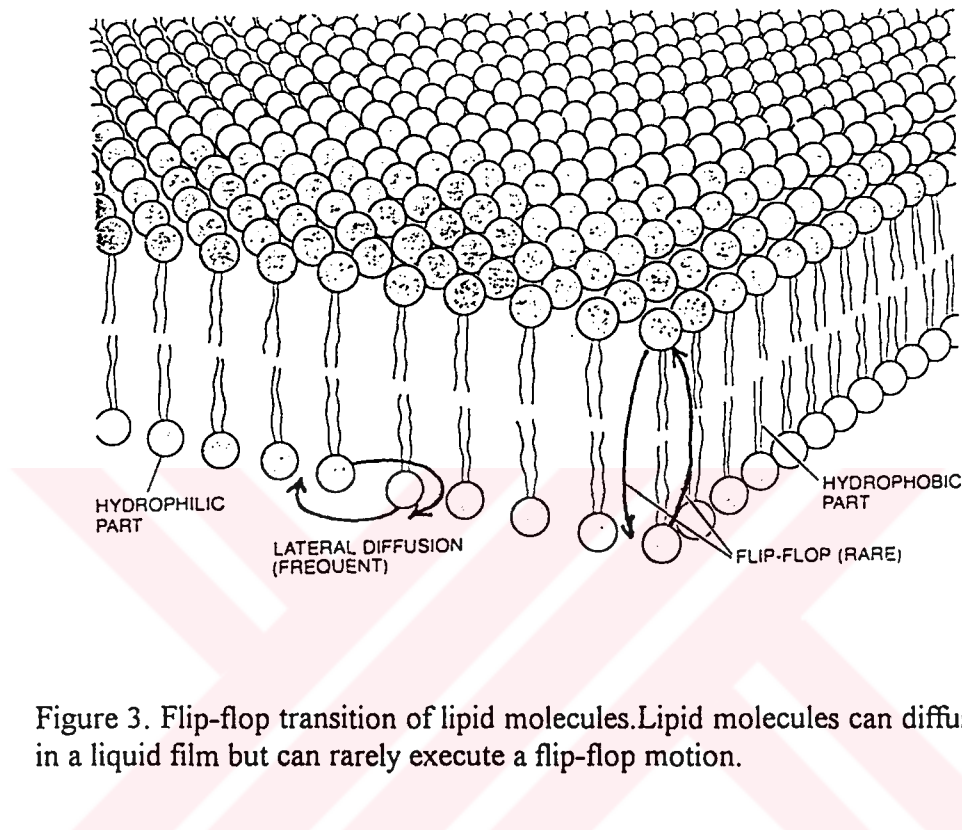


Figure 3. Flip-flop transition of lipid molecules. Lipid molecules can diffuse laterally as in a liquid film but can rarely execute a flip-flop motion.

Intramolecular motions involve rotations of groups about single bonds, segmental and long-range swinging motions of fatty acyl chains, and polar head group conformational changes. These motions are closely related to the chemical structure of lipids[1,2].

Orientation of a phospholipid molecule in a bilayer implies strong anisotropic constraints for its orientation, conformation, and motion. For example rotation along the long axis of phospholipids is much more facilitated than it is along other axis. Traditionally two parameters have been used to characterize the general state of disorder in bilayers: (i) The orientation and conformation of acyl chains and

(ii) the motion of the chain that determines the dynamic properties like rotation, lateral diffusion, permeation of solutes. Thus, conformation and dynamics of acyl chains play an important role in determining the properties of bilayers[2].

There is always rotation about C-C bonds (Fig.4). The two higher energy minima corresponding to the dihedral angles of  $120^\circ$  g(+) and  $240^\circ$  g(-) between the alternate bonds give rise to gauche (g) conformers. The free energy of such gauche conformers is higher than that of trans (t) conformers because of the greater steric hindrance. In a close-packed bilayer a single g conformer in an acyl chain causes a large change in the length, width, and packing ability of the neighbouring acyl chains.

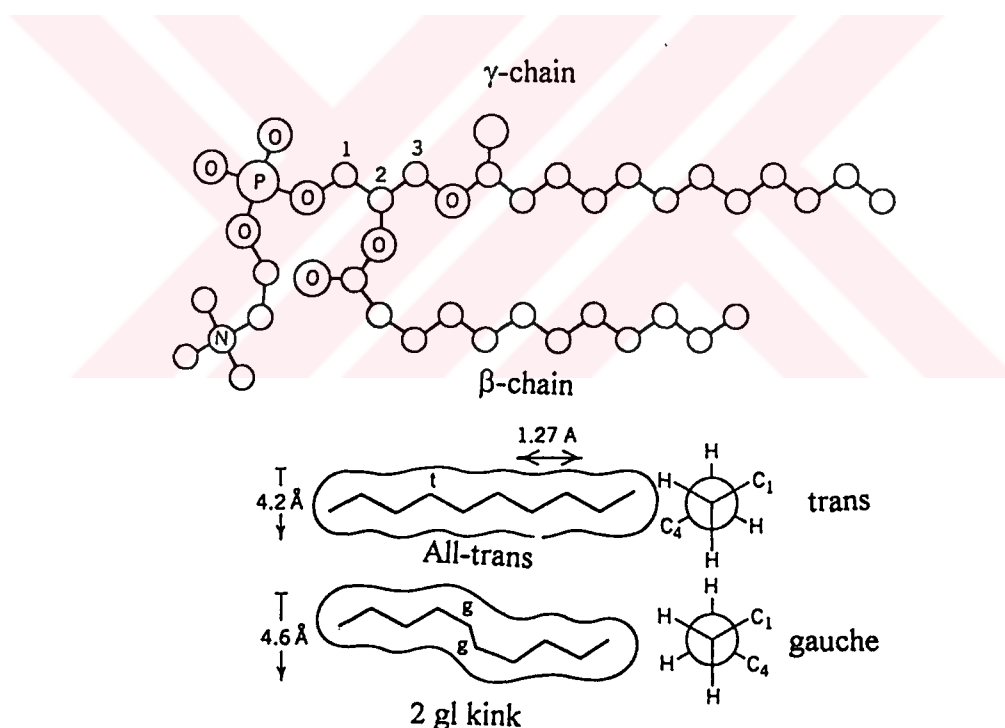


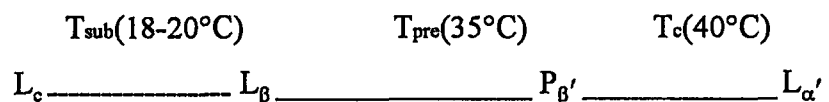
Figure 4. Structure of 1,2-diacylphosphatidylcholine molecule emphasizing the relative orientation and conformation of the head group and of the acyl chain. The lower part of the figure illustrates an alkyl chain in an all-trans and part-gauche conformations. The Newman projections for the trans and gauche conformations are also shown.

### 1.2.2 Thermotropic Phase Transition in Membranes

The behaviour of lipid molecules in bilayers is strongly influenced by temperature. At sufficiently low temperatures, the lipid molecules are solidlike. They show little translational motion, and in many ways their properties resemble those of hydrocarbon crystals. As the temperature is raised, the properties of bilayers show abrupt changes at one or more temperatures. The abrupt small increase in the phase transition curve corresponds to the pretransition associated with the tilting of the hydrocarbon chains and the abrupt larger increase corresponds to the main transition of hydrated phospholipids from the gel to the liquid crystalline phase which is associated with complete melting of the hydrocarbon chain[8].

In the disordered fluid state of bilayers, the phospholipid molecules retain an average orientation perpendicular to the layer surface. Rapid rotational transitions occur along the long axis of the polymethylene chain (Fig.4). Due to coupled trans-gauche-trans isomerizations, the chains remain extended and essentially parallel to each other[2].

It is known that DPPC liposomes undergo the following three phase transitions [14-16].



where  $L_{\text{c}}$ ,  $L_{\beta}$ ,  $P_{\beta'}$ ,  $L_{\alpha'}$  correspond to crystalline gel, gel, rippled gel and liquid crystalline bilayer structures respectively. Fig.5 shows the schematic illustration of the lamellar bilayer phases. Very little is known about the ripple phase[2]. Researchers



are mainly concerned with the liquid crystalline and the gel phases. Further research is necessary to find out the properties of the ripple phases.

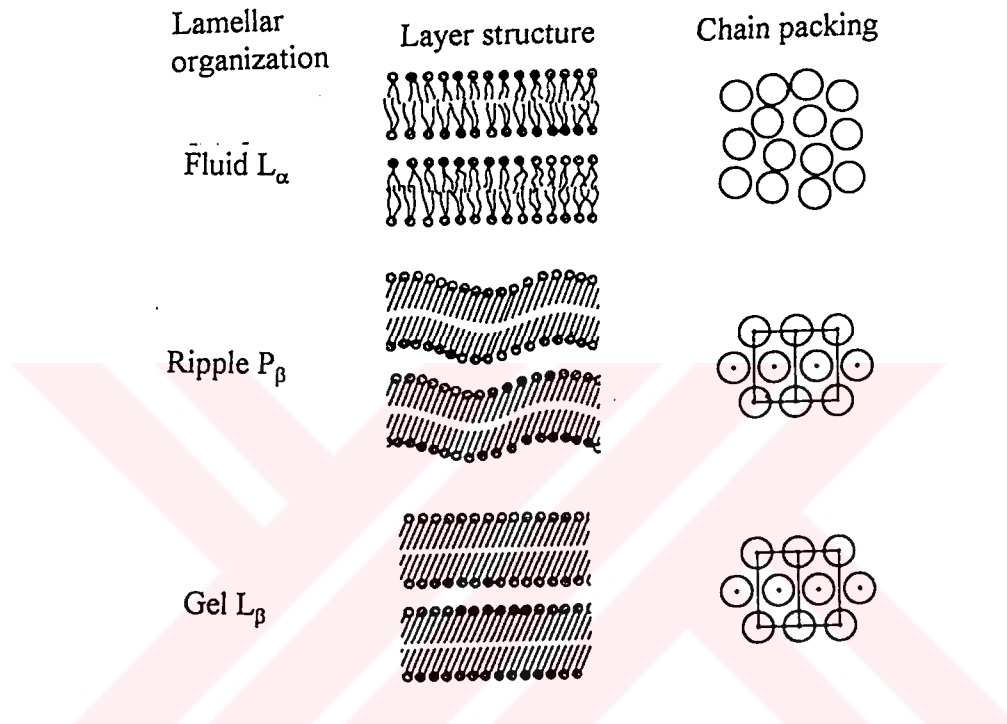


Figure 5. Schematic illustration of the lamellar bilayer phases.

### 1.2.2 Lipid Asymmetry and Lateral Phase Separation

When a bilayer is composed of more than one kind of lipid, more complex structures are possible. Fig.6 illustrates schematically a few cases of a spherical bilayer composed of two lipid types. The simplest imaginable structure is a completely

homogenous vesicle (Fig.6a). Both surfaces have the same lipid composition, and lipid types are randomly distributed in each phase.

However, because of bilayer curvature or the presence of different solutions inside and outside, it is possible that lipids might segregate preferentially into two surfaces (Fig.6b). Such an asymmetric distribution of lipids could be the result of a difference in the thermodynamic stability of each lipid type in a monolayer of given curvature and type of solvent. It could also result kinetically in a biological cell. In lipid bilayers, there is an additional possibility of asymmetry through lateral phase separations (Fig.6c,d)[1].

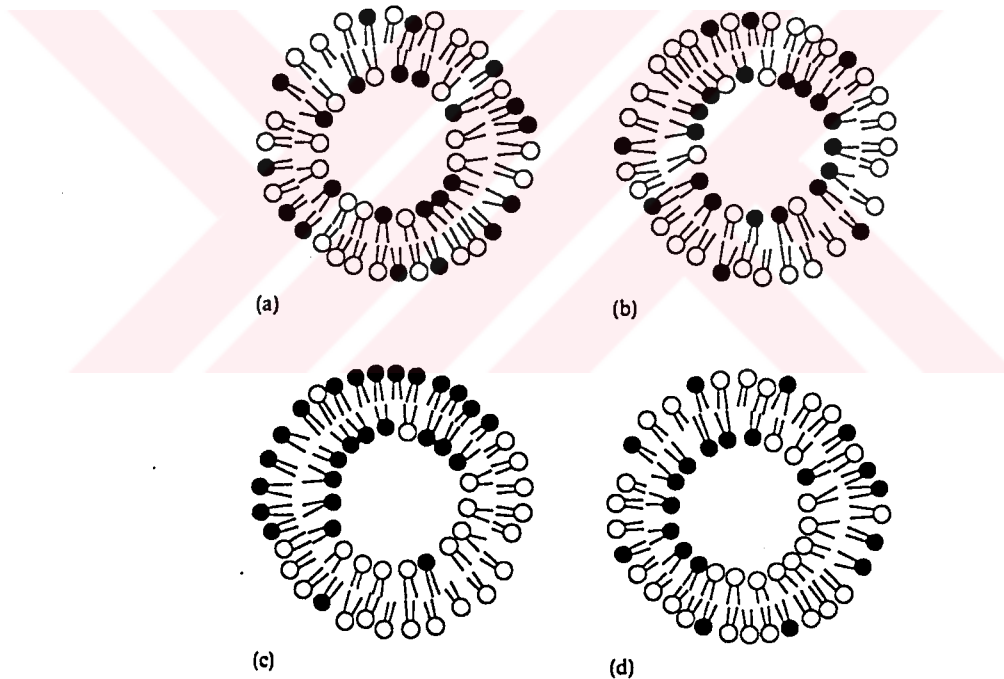


Figure 6. Schematic illustration of possible structures of a spherical bilayer composed of two types of lipids (a) A homogeneous bilayer. (b) Asymmetric compositions of two surfaces. (c) Lateral phase separations of both surfaces. (d) Lateral phase separation of the inner surface only.

Phospholipid molecules in the fluid state (above the hydrocarbon melting temperature) undergo rapid lateral diffusion. Any binary mixture of the two phospholipids differ significantly in their physical properties (e.g., melting temperatures); they often exhibit solid-phase immiscibility, even though the fluid phases are homogeneous. From examination of the effects of temperature on mixtures of phospholipids, one is led to the idea that these systems should exhibit lateral phase separations within the plane of the membrane as illustrated schematically in Fig. 7[17].

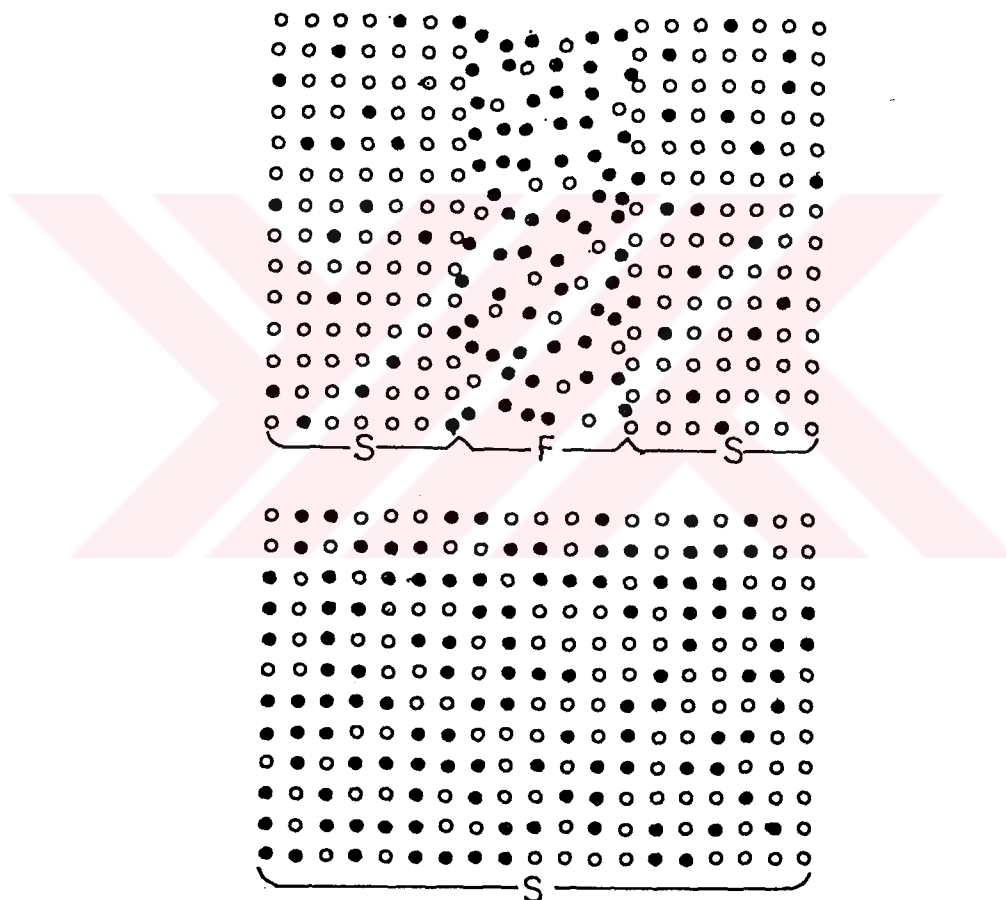


Figure 7. Schematic illustration of lateral phase separations in the plane of a lipid bilayer membrane consisting of two hypothetical lipids, black lipids and white lipids. The bilayer is seen from above, in one case a solid domain (S) is rich in a higher melting white lipid and is in equilibrium with the fluid domain (F), which is rich in the lower melting black lipid.

### 1.3 Structure and Function of Cholesterol

Cholesterol is the sterol which is a major constituent of the plasma membrane of many of the cells of higher organisms, making up as much as 50 wt% of the lipid fraction in the case of the human erythrocyte membrane. It is believed that cholesterol is a primary modulator of the properties of bilayers. Plasma membranes of mammalian cells require cholesterol for normal functions and bacterial membranes do not. The cholesterol requirement in mammalian cells is fulfilled by endogenous biosynthesis and by extracellular supply. Low-density and high-density lipoproteins are the two major carriers of cholesterol in human blood, and high concentrations of cholesterol are found in plaques formed in arteries of patients suffering from atherosclerosis. The cholesterol content of endoplasmic reticulum (ER) (about 12%) and other organelle membranes (less than 20%) is considerably smaller than that of plasma membranes (about 30- 50 mole%).

Endogenous cholesterol is synthesized in ER from squalene epoxide by enzymes that are localized in membranes. The main role of cholesterol in biomembranes is in modulating the conformational state of acyl chains (fluidity), stability, permeability, and utilization of unsaturated fatty acids. Besides this, cholesterol also modifies the functions of several membrane-bound enzymes, and acts as a precursor for bile acids, steroidal hormones, and vitamin D.

Cholesterol is an alicyclic lipid molecule whose structure includes four fused rings, a single hydroxyl group at C-3, and an unsaturation at C-5,6. The conformation of the four fused rings of cholesterol gives rise to a flat amphipathic structure (Fig.8) with angular methyl groups on the  $\beta$ -face, thus making the  $\alpha$ -face

planar and smooth. The cholesterol molecule is predominantly hydrophobic and therefore it is only slightly soluble in water (<30 nM).

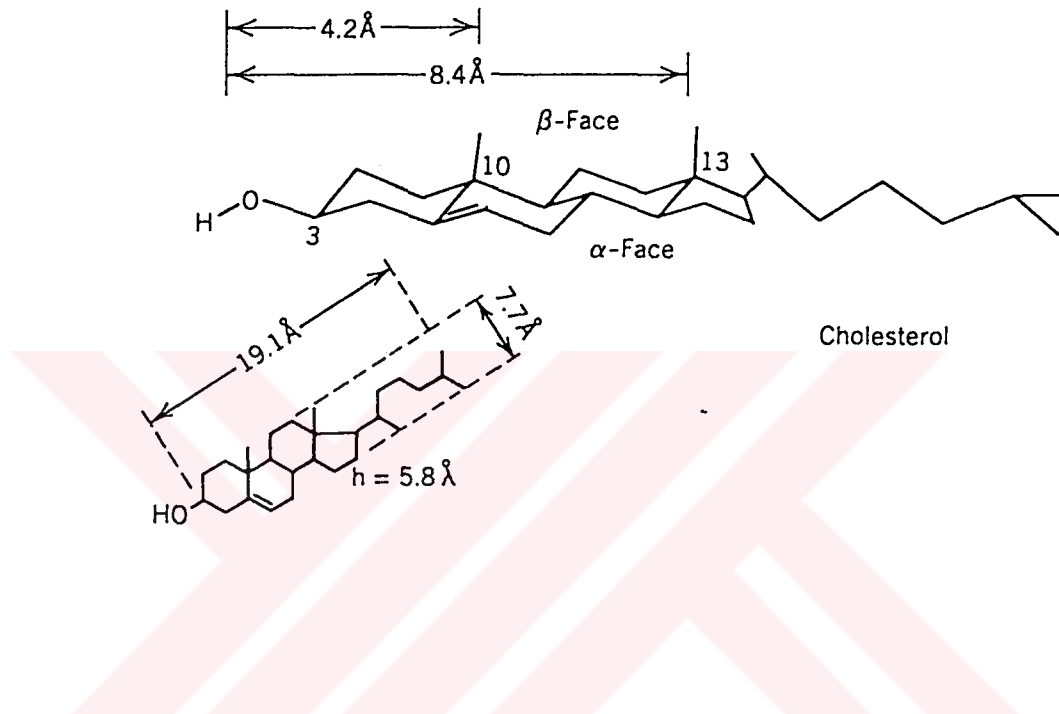


Figure 8. Structure of cholesterol shown in two different conventions .

Physical studies show that cholesterol incorporated into phospholipid bilayers as well as biomembranes is oriented as the long axis of the molecule perpendicular to the plane of the membrane, and parallel with the acyl chains of conjugated membrane lipids[2]

Cholesterol, up to 50 mole% can be dissolved in phosphatidylcholine membranes. Below this limit cholesterol and lecithin form complexes of varying mole ratios. Beyond this limit cholesterol is separated from phospholipid bilayers[18].

The effect of cholesterol on phospholipids has been well documented by many investigators from measurements of phospholipid behavior. These effects include the broadening and eventual elimination of the phase transition[19], suppression of pretransition[20], condensation of the bilayer surface, causing a decrease in surface area per phospholipid molecule[21], interruption of phospholipid headgroup interactions[22]. Below the temperature of the gel liquid-crystal transition of pure lipid ( $T_m$ ), cholesterol has the effect of disrupting the close packing of the fatty acid hydrocarbon chains and thus fluidizing the bilayer, whereas above  $T_m$  it inhibits chain motion and thus rigidifies the bilayer[23]. There are conflicting results in the literature about the effect of cholesterol on order and dynamics of phospholipid membranes in the liquid crystalline phase. Although it is commonly believed that in the liquid crystalline phase cholesterol increases the order of phospholipid chains and decreases the fluidity of the membrane[24]. Deinum et al.[12] showed that with the addition of cholesterol, order increases and at the same time dynamics also increases.

There is a wide range of contradicting results obtained by various experimental techniques about the hydrogen bonding between cholesterol and phospholipids. Previously Brockerhoff [25] suggested that hydrogen bonding between cholesterol's  $\beta$ -OH and the carbonyl groups of phospholipids is responsible for cholesterol's unique effects on lipid bilayer membranes. This idea was justified by Huang [26,27] theoretically. However, other studies [28,29] have shown that the carbonyl oxygens of phosphatidyl choline are not necessary for cholesterol interactions. The possibility of hydrogen bonding between the sterol hydroxyl and the phosphate region of the lipid head group was excluded by  $^{31}\text{P}$  NMR spectroscopic studies[4]. Presti et al. [30] proposed that cholesterol forms associations with phospholipids with stoichiometries of both 1:1 and 1:2. A hydrogen bond between the  $\beta$ -OH of cholesterol and the glycerol ester oxygen of a phospholipid is suggested for

tight binding in a 1:1 complex (Fig.9). A second phospholipid molecule is loosely associated with the complex, probably simply by van der Waals interactions, to form domains of 1:2 stoichiometry, which may coexist with pure phospholipid domains.

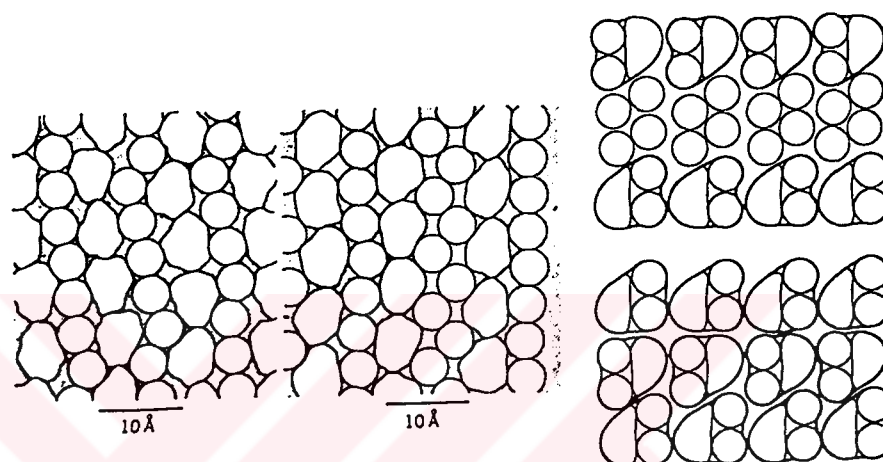


Figure 9. Possible models for the lateral packing of phospholipid + cholesterol 1:1 (left) and 1:2 (right) viewed perpendicular to the plane of the lamellar phase. These arrangements emphasize long-range order of acyl chains (circles) which are closely packed near cholesterol (irregular shapes).

Interfacial boundary phospholipid separates these two domains. At about 20 mol% cholesterol content, free phospholipid domains disappear and interfacial phospholipid is maximal. The existence of domain formation in cholesterol containing PC membranes, such as cholesterol rich and cholesterol poor, was also proposed by Plachy et al. [31] and Recktenwald and McConnell[32]. The phase diagram proposed by Reckstenwald and McConnell [32] was later developed by Vist and Davis (Fig.10)[33].

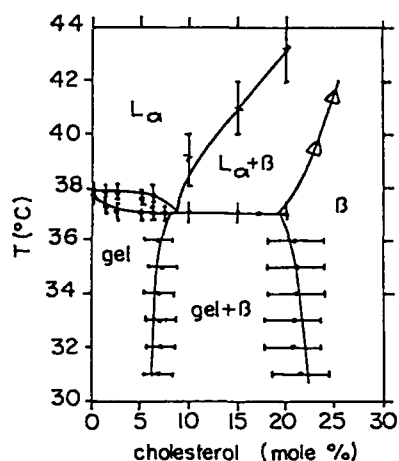


Figure 10. Partial phase diagram for cholesterol/DPPC mixtures. The phases are labelled as follows:  $L_{\alpha}$ , the fluid or liquid crystalline phase; G the gel phase;  $\beta$ , the high cholesterol content phase characteristic of biological membranes.

Properties of these subphases, which have different dynamics, were reported by Severcan et al. [34] Severcan and Plachy[35]. Although much effort has been devoted to the study of the location and interaction of cholesterol with lipid bilayers, its functional role within the membrane is not yet understood clearly because of the complexity of these systems.

#### 1.4 Structure and Function of Vitamin E

Vitamin E was discovered at the university of California, Berkeley in 1922 in the laboratory of Herbert M. Evans. From its initial discovery as an anti-fertility agent, it was given the name of tocopherol meaning child birth (tocos)+ carry (pherin). Vitamin E is the generic name of a mixture of lipid-soluble phenols,



tocopherols and tocotrienols possessing general structural features: an aromatic chromanol head and a 16-carbon tail (Fig.11).

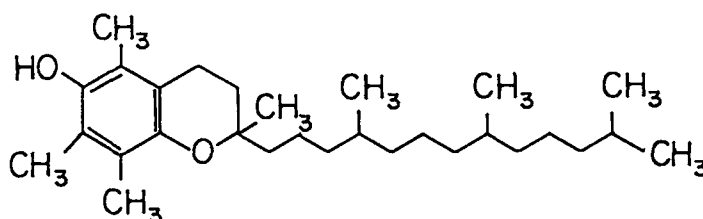


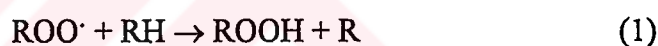
Figure 11. Schematic illustration of  $\alpha$ -Tocopherol.

The amount of methyl substituents in the chromanol nucleus gives rise to alpha-, beta-, gamma-, and delta isomers, whereas the saturation of the hydrocarbon chain constitutes tocopherol (with saturated chain) or tocotrienol (with unsaturated chain) forms of vitamin E. The alpha form of vitamin E with three methyl groups on the chromanol nucleus, d-alpha tocopherol, has generally been considered as the most active naturally occurring form. Alpha-tocopherol is also the most common form of vitamin E found in human diet[36].

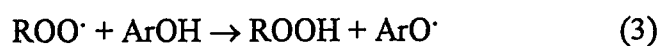
$\alpha$ T is an indispensable component of relatively low concentration ( $\leq 1$  mol% with respect to phospholipid) in the membrane of subcellular organelles such as mitochondria and in the plasma membrane of cells[36].

Vitamin E molecules possess a unique ability to act as membrane free radical harvesting centers which collect their antioxidant power from other intramembrane and cytosolic reductants[37].

The biological activity of vitamin E is generally believed to be due to its antioxidant action to inhibit lipid peroxidation in biological membranes by scavenging the chain-propagating peroxy radicals. The antioxidant function of vitamin E is localized in the chromanol nucleus, where the phenolic hydroxy group donates an H-atom to quench lipid radicals[38]. These can be summarized in the following way: An extremely high antioxidant efficiency of tocopherols may be explained by the functioning of the vitamin E cycle in which chromanoxyl radicals can be reduced by ascorbate, NADPH-, NADH- and succinate-dependent electron transport in microsomes and mitochondria, whereas glutathione, dihydrolipoate and ubiquinols synergistically enhance vitamin E regeneration in membranes and lipoproteins. This was explained by the following reaction sequence and also shown schematically in Fig.12[39]. The peroxy radicals, ROO<sup>·</sup>, are formed deep within the bilayers by the reaction sequence:



where RH represents a polyunsaturated fatty acid moiety and the transferred hydrogen atom comes from the center of a -CH=CHCH<sub>2</sub>CH=CH- unit. The peroxy radical center has quite a large dipole moment[40,41] and should therefore be relatively hydrophilic; as a consequence it may tend to float towards the surface of the bilayers[40].  $\alpha$ T, ArOH, reduces the rate and extent of peroxidation by interacting with the peroxy radicals:



It is probable that for peroxidation occurring in vivo the  $\alpha$ -tocopheroxyl radical formed in reaction 3 is very largely converted back to the  $\alpha$ T by water-soluble reducing agents (such as ascorbate (vitamin C))[42].

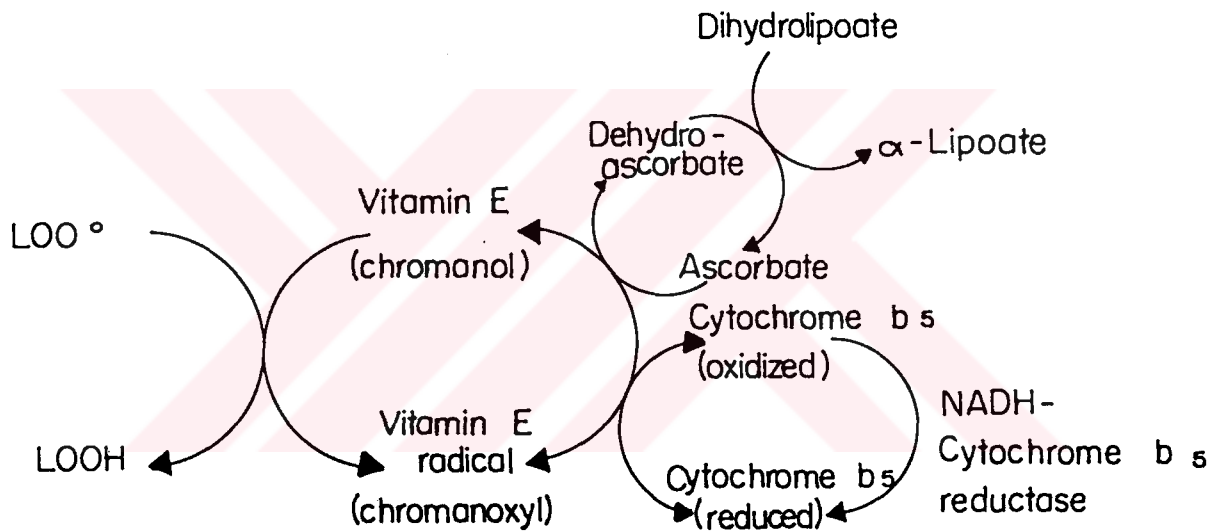
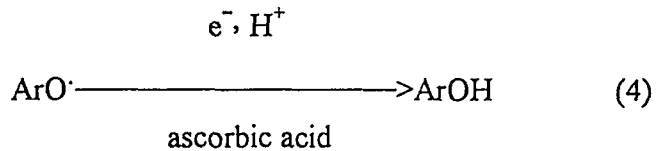


Figure 12. The vitamin E cycle enzymic and non-enzymic recycling interactions of water and lipid soluble antioxidants with vitamin E radicals in human erythrocyte membranes.

Fig.13 shows the various modes of action attributed to vitamin E (tocopherols) in membrane[43].

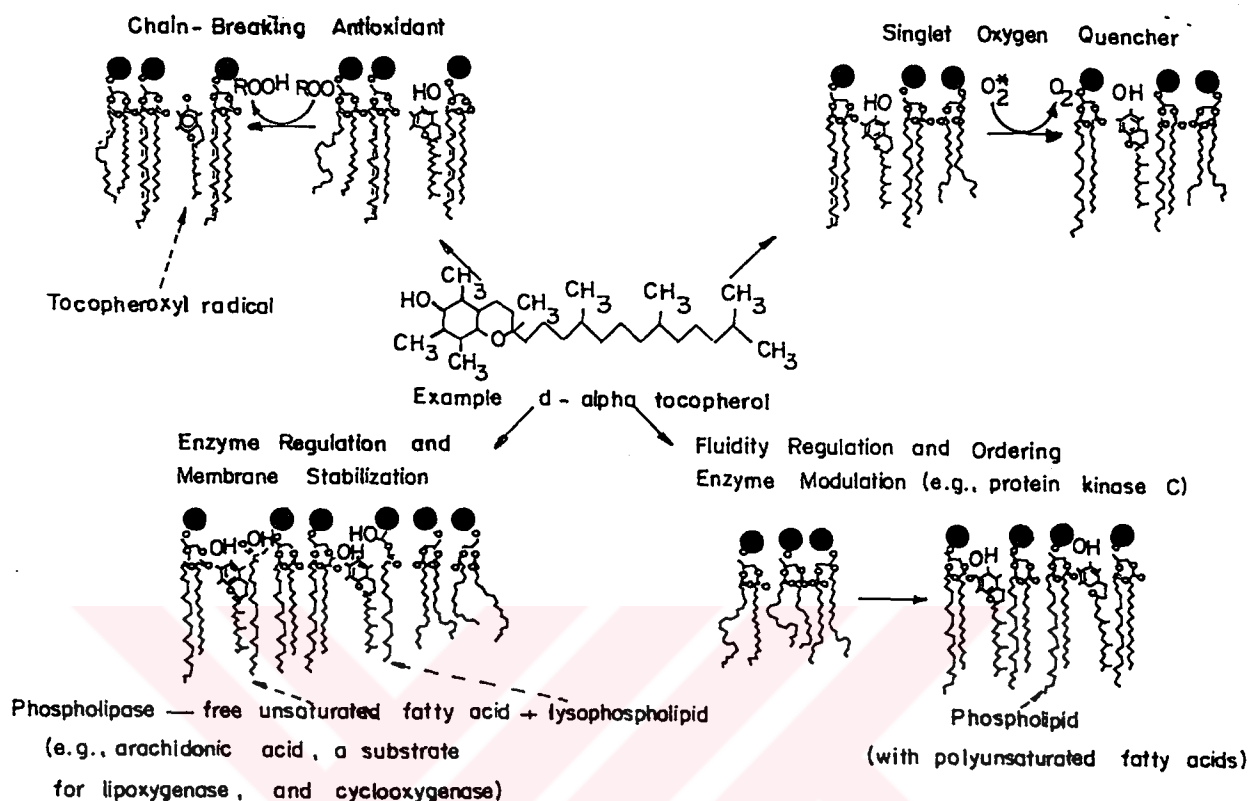


Figure 13. Vitamin E as a biological response modifier.

It is generally known that the stabilizing effect of tocopherols on biological membranes lies in their ability to inactivate free lipid radicals[44], to quench singlet molecular oxygen[45] and to stabilize the membrane lipid bilayer via a van der Waals interaction with unsaturated fatty acid chains of phospholipids[46,47]. It has been demonstrated that  $\alpha$ T can protect biological membranes against the damaging action of free fatty acids[48] whose concentration is sharply elevated under some biological conditions, such as ischemia, stressory damages, hypoxia, etc[49-51]. The molecular mechanism of membrane protection against structural and functional

damage induced by fatty acid is their interaction with  $\alpha$ T with formation of  $\alpha$ T fatty acid complexes[52].

Several vitamin E deficiency diseases mainly affecting newborns or young babies were discovered. Many of these diseases are based upon either inadequate amounts of vitamin E in the diet or defect in the transport of vitamin E to the tissues (such as abetalipoproteinemia). Defects in bile mediated absorption also lead to impaired vitamin E uptake, and may cause muscular dystrophy in children.

Typical severe deficiencies of vitamin E seen in young babies and children have never been observed in adult experimental animals or humans. However, there has been a whole host of literature ranging from epidemiological, clinical and biochemical studies which have provided strong circumstantial evidence that higher levels of vitamin E in the diet have beneficial health effects[36].

The protective role and requirements for vitamin E similar to other antioxidants in prevention or minimization of free-radical damage associated with specific diseases and life style patterns and processes, including cancer, aging, circulatory conditions, arthritis, cataract, pollution, and strenuous exercise have been reviewed by Packer[53].

The antioxidant potency of  $\alpha$ T in vivo depends much on the surrounding environment; for example, fluidity of the organized structures such as membranes and lipoproteins. Recent studies indicate the possible role of vitamin E-membrane interactions in the mechanisms of antioxidant action and membrane protection[54].

It has been suggested that  $\alpha$ T might stabilize biological membranes by restricting the molecular mobility of their components[5,6]. Recently, correlation has been reported between structural and dynamical membrane properties of vitamin E and its antioxidant potency [7,39].

In order to understand the molecular mechanism of action of  $\alpha$ T, several studies have been performed to investigate the interaction of  $\alpha$ T with natural and model membranes. It has been shown that  $\alpha$ T induces phase separation in phospholipid membranes[8,55]. It is found that, with the addition of  $\alpha$ T, the phase transition curve broadened, the main gel to liquid crystalline phase transition is lowered and pretransition is suppressed[9,57]. It has also been shown that  $\alpha$ T induces a decrease of order and an increase in fluidity in the gel phase while an indication of a slight increase in ordering and a decrease in fluidity are registered in the liquid crystalline phase[5,58]. The viscosity of the lipid site of the phospholipid membrane is also reported in the liquid crystalline phase in the absence and in the presence of  $\alpha$ T[5]. The influence of vitamin E on motional anisotropy in phospholipid membranes has also been reported[5,7,59].

### 1.5 Responsible Forces Governing the Bilayer Formation

Biological membranes essentially consist of a two-dimensional matrix made up of a phospholipid bilayer interrupted and coated by proteins. Thus the interior of the membrane is much less polar than the interfacial region. Such an organization is a direct consequence of the hydrophobic effect, whereby the apolar acyl chains of lipids and the side-chains of the nonpolar amino acid residues in proteins tend to be squeezed away from the aqueous phase[2].

To understand the mechanism of formation of membranes, we need to understand the interaction of nonpolar molecules, especially those which are partially polar and partially nonpolar with respect to solvent water. Water is essential for membrane formation. A nonpolar molecule can be defined as an electrically neutral molecule in which the centers of positive and negative charges coincide with each other. In polar molecules, on the other hand, these two centers are asymmetrically arranged, thus creating a positive and negative pole that give rise to what is called a dipole moment. The dipole moment of a nonpolar molecule is very weak. Therefore the forces operating between nonpolar molecules are mainly the van der Waals forces that arise when a pair of any atoms or molecules come close together and induce fluctuating charges upon each other. The van der Waals forces are much weaker than the hydrogen or ionic bonds found between polar molecules. But, in the presence of water, nonpolar molecules are found preferentially associated with one another, rather than with water, which has been called the hydrophobic bond . Since then the term has found widespread usage, although its validity has been questioned[60].

The components in a bilayer matrix are held together largely by noncovalent forces. The hydrophobic effect accounts for most of the interaction energy that stabilizes the bilayer organization; however hydrogen bonding and electrostatic interactions are significant in the polar group regions.

Alignment of the zwitterionic head groups of phospholipids is determined by electrostatic (PC) and H- bonding interactions (for PE) between the N-H and P=O moieties. In crystals of DMPC, two water molecules located between the PC molecules form a hydrogen-bonded phosphate-water-phosphate ribbon. Two other water molecules are H-bonded to one lipid phosphate and to another molecule. This H-bonded network of the head group and water molecules provides stabilization of

the interface. In PC's restriction in the head group conformation is imposed by the tendency of the zwitterionic head groups to optimize their intra and inter molecular interactions, as well as by steric factors that determine conformations about the P-O ester bonds.

Today it is known that the hydrophobic effect arises from the molecular and physical characteristics of water. Hydrophobic substances cannot interact favorably with water via ionic, polar, or hydrogen-bonding interactions. Amphipathic molecules aggregate in water so as to maximize appropriate interactions, i.e., the interactions that maximize orientational configurational entropy. Interactions of acyl chains with water as well as with the polar groups is, for example, minimized in the aggregates. Two factors are at work:

1. The net free energy change for the removal of methylene groups from water to an apolar environment, which is always negative and about 2500-3500 J/mole. The gain in the free energy arising from the hydrophobic effect increases linearly with the chain length. These values suggest that the head group repulsions, branching, extent of chain-chain interactions, and interfacial area influence the configurational entropy of methylene groups.

2. The electrostatic energy change for the removal of a charged group from water to an apolar environment is given by the Born equation. The difference in electrostatic free energy required to transfer ions of radius  $r$  (in Å) and charge  $q$  from vacuum ( $\epsilon_v=1$ ) to a solvent of dielectric constant  $\epsilon_s$  is

$$\begin{aligned}\Delta F &= -q^2/2r[(1/\epsilon_v)-(1/\epsilon_s)] \\ &= -1.4 \times 10^6/2r[1-(1/\epsilon_s)] \text{ J/mole(1)}\end{aligned}$$



For most polar solvents  $\epsilon_s \gg 1$  ( $\epsilon_s=80$  for water). Note that  $\Delta F$  will be the same for the transfer of ions of the same radius. For the transfer of the point charge from the medium of dielectric constant 80 (water) to 2 (hydrocarbon), the overall change in the free energy is about  $6.3 \times 10^4$  J/mole.

Thus, the overall gain in the free energy for the transfer of a phospholipid molecule from water or from a hydrocarbon medium to a nonpolar interface is -  $6.3 \times 10^4$  J/mole.

The hydrocarbons are only slightly soluble in water, and the polar solutes are not soluble in hydrocarbons. That's why amphipaths form aggregates to lower the total free energy[2]. The unwillingness of such aggregates to break up in water has been attributed in part to this hydrophobic force. The most popular qualitative explanation is in terms of an increase in ordering of those molecules of water that are in the vicinity of the hydrophobic portion of the amphiphile. It has been proposed that a microscopic iceberg forms around nonpolar molecules. Since at the hydrocarbon-water surface only weak dispersion forces restrain these molecules, they will, on heating, absorb energy into rotational and translational modes of motion more easily than bulk water. This accounts for the observed increase in their heat capacity[60].

The van der Waals type of attractive dispersion interactions between hydrophobic solutes will also contribute to the formation of aggregates. However, the extent of such contributions remains to be established in most cases. Since few H bonds are actually broken during hydrophobic interactions, the main contribution to the free energies comes from packing, configurational and orientational factors. The entropic interactions are significantly longer range than any typical bonding interactions, but they decay exponentially with distance. Also the attractive

interactions due to hydrophobic effect would become stronger at higher temperatures, as the contribution of TAS term would make the overall free energy more negative[2].

The hydrophobic effect's contribution to the stability of a bilayer in water can be imagined as equivalent to a lateral pressure squeezing the phospholipids together and thus preventing the hydrocarbon chains from coming into contact with water[61].

## 1.6. Infrared Spectroscopy

### 1.6.1. The Basic Theory

Infrared spectroscopy is based on the measurement of vibrational transitions, generally between the ground state and the first excited state. This process is ruled by the laws of quantum mechanics, and the total energy of the molecule is increased or decreased by one or more quanta depending, respectively, upon whether absorption or emission takes place.

It is a useful approximation to consider that the total energy of a molecule is the sum of four contributions, i.e. electronic, vibrational, rotational, and translational energies, which may be considered separately; that is

$$E_{\text{total}} = E_e + E_v + E_r + E_t$$

Changes in vibrational energy lead to infrared vibrational spectra brought about by mid-infrared radiation.

The change in molecular vibrational energy after infra red absorption or emission is given by Bohr equation

$$\Delta E = E_2 - E_1 = h\nu = hc\bar{\nu}$$

where  $E_1$  is the initial energy,  $E_2$  is the final energy,  $h$  is the Planck's constant,  $c$  is the velocity of the light,  $\nu$  is the vibrational frequency in  $\text{sec}^{-1}$  and  $\bar{\nu}$  is the number in  $\text{cm}^{-1}$ . When vibrational transitions are considered, it is convenient to describe the radiation by its wavenumber,  $\bar{\nu}$ , rather than by its frequency,  $\nu$ . Infrared spectra are usually recorded on a linear wavenumber scale, which is sometimes referred to as a frequency scale, although its unit is the reciprocal of a wavelength( $\text{cm}^{-1}$ )[62].

The infrared spectrum is conveniently divided into near-, mid-, and far-infrared regions. The majority of analytical applications have been confined to a portion of the mid-infrared region extending from 4000 to 400  $\text{cm}^{-1}$ .

In order to absorb infrared radiation, a molecule must undergo a net change in dipole moment as a consequence of its vibrational and rotational motion. Only under these circumstances can the alternating electrical field of the radiation interact with the molecule and cause changes in the amplitude of its motions. For example, the charge distribution around a molecule such as hydrogen chloride is not symmetric, because the chlorine has a higher electron density than the hydrogen. Thus hydrogen chloride has a significant dipole moment and is said to be polar. The dipole moment is determined by the magnitude of the charge difference and the distance between the two centers of charge. As a hydrogen chloride molecule vibrates, a regular fluctuation in dipole moment occurs, and a field is established that can interact with the electrical field associated with radiation. If the frequency of the

radiation exactly matches a natural vibrational frequency of the molecule, a net transfer of energy takes place that result in a change in amplitude of the molecular vibration; absorption of the radiation is the consequence. Similarly, the rotation of asymmetric molecules around their centers of mass results in a periodic dipole fluctuation that can interact with radiation.

No net change in dipole moment occurs during the vibration or rotation of homonuclear species such as  $O_2$ ,  $N_2$  or  $Cl_2$ ; consequently, such compounds cannot absorb in the infrared.

Quantum mechanics allows only certain values of the energy. These values are represented by the horizontal line on the Morse curve in Fig.14. Values of energy

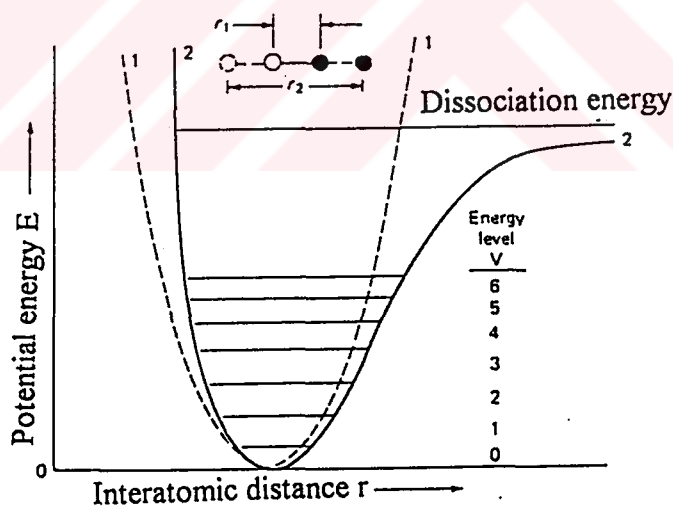


Figure 14. Potential energy diagrams. (1) Harmonic oscillator, (2) anharmonic oscillator.

between these energy levels are not permitted and the spacing between energy levels becomes smaller at higher energy values. As the energy increases, the atoms move farther from their equilibrium positions and hence enter a nonparabolic region of the Morse curve. Therefore, the vibrations can no longer be treated as simple harmonic but are described as anharmonic oscillations[63].

A molecule with N atoms has  $3N-6$  ( $3N-5$  for a linear molecule) normal modes of vibration, each of which occurs with a definite vibrational frequency. Vibrational frequency increases with bond strength (force field) and varies as the inverse of the square root of the reduced mass of two vibrating atoms that are held together by a force constant

$$\nu = c\nu = 1/2\pi(k/\mu)^{1/2}$$

where the fundamental frequency  $\nu$  is related to the reduced mass  $\mu$  and the Hooke's law force constant  $k$ . A consequence of this relation is that vibration of heavy atoms occurs at lower wavenumbers than that of light atoms. The difference is clearly seen upon isotopic exchange; for example, C-D vibrates at a wavenumber approximately 1.3 times lower than C-H. Characteristic vibrations of covalently bonded atoms can be classified as stretching which involves changes in bond lengths, and bending corresponding to changes in bond angles. The various types of vibrations are shown schematically in Fig.15[62].

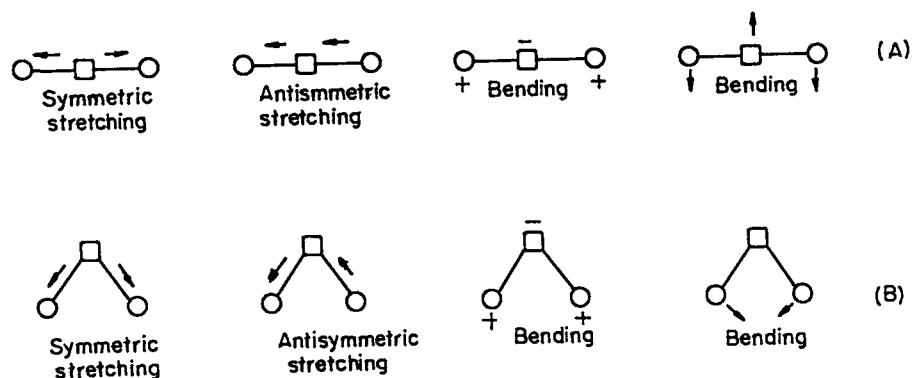


Figure 15. Types of normal vibration in a linear (A) and a non-linear (B) triatomic molecule. Atomic displacements are represented by arrows (in plane of page) and by + and - symbols (out of plane page).

The value of infrared spectral analysis comes from the fact that the modes of vibration of each group are very sensitive to changes in chemical structure, conformation, and environment[63].

Infrared spectroscopy has been a late addition to the spectroscopic inventory of the membrane biophysicist. The reason for this lies in the presence of water in the system. Biomembranes like all biological structures, require an aqueous environment, whereby water is not only the solvent of choice, but often part of the molecular structure itself. Since water is a strong infrared absorber, the application of conventional infrared spectroscopy to the study of biological membranes has been severely limited. This problem is solved by using Fourier transform infrared spectrometers[64].

### 1.6.2 Advantages of FTIR Spectroscopy to Other Biophysical Techniques

Different physical, chemical and spectroscopical techniques are utilized to probe various characteristics of membranes.

The techniques of X-ray diffraction, which yield for the most part time-averaged electron density maps of structure, are poorly suited for the detailed study of disordered phases and also it has disadvantages of working with crystals which contains very little amount of water. Most widely used are electron paramagnetic resonance and fluorescence spectroscopy. These techniques, although, extremely sensitive, generally require incorporation of reporter groups into the membrane component or phase of interest. The presence of probe molecules produces several complicating factors for data analysis. First their structure and polarities differ from those of phospholipids into which they are inserted. Thus they may perturb the environment. Second, the probe molecules may partition into particular domains of the membrane. Third, the probe molecules produce spectral parameters from which it is non-trivial to extract direct structural or dynamic information about the membrane component under investigation. Infrared spectroscopic technique is a non-perturbing technique which also provides investigation of hydrated samples.

Deuterium NMR has been the technique most effectively used to date for studies of the motion of membrane lipid components. The sets of motion includes trans-gauche isomerization, acyl chain vibrations and whole body rotations, among others. To extract the contribution of any single motion to the measured spectral order parameter requires mathematical modeling (of indeterminate accuracy) of all other motions[65].

Infrared spectroscopy is inherently well-suited to the problem of conformational order in phospholipid acyl chains.

1. Structural and dynamic data arise directly from the molecules under study without requiring the use of spectroscopic probes in the case of FTIR spectroscopy.

2. Infrared spectroscopy may be termed as a sub-molecular probe in that vibrations can be observed (and hence structural information gathered) from diverse regions of a lipid molecule.

3. Lipids are easily studied in the gel or liquid-crystalline phases. Since the vibrational spectrum of the acyl chains and head groups is a function of physical state, conformational transitions between the two forms may be monitored by measuring the dependence on temperature of the vibrational spectrum.

4. In vivo membrane studies are also possible.

The above mentioned advantages make FTIR well suited for membrane studies. The major disadvantage is that water, which is always present in biological samples, absorbs substantially in many regions of the infrared spectrum. In order to overcome the problems arising from this fact, subtraction techniques are used to remove most of the interference from water bands or  $D_2O$  can be used as a solvent[64]. However this time D-H exchange should be taken into account. The next section will discuss more about these disadvantages and the methods used to overcome them.



## CHAPTER II

### MATERIALS AND METHODS

#### 2.1 Reagents:

Dipalmitoyl-L- $\alpha$ -phosphatidylcholine (DPPC), dimyristoyl -L- $\alpha$ -phosphatidylcholine (DMPC), dl- $\alpha$ -tocopherol and cholesterol (5(6)-cholesten-3-ol) were obtained from Sigma Chemical Company, USA, and used without further purification.

#### 2.2 Model Membrane Preparations:

Multilamellar liposomes were prepared according to the procedure reported by Severcan and Cannistraro[8]. To prepare multilamellar liposomes, 10 mg of phospholipid were dissolved in 150 $\mu$ l chloroform in a round-bottomed flask. Aliquots of chloroform solutions of lipids were subjected to a stream of nitrogen to form uniform thin films of the lipid on the walls of the container. Residual solvent was removed by subjecting the films to vacuum drying for at least 8 hours. Thin films were hydrated by adding 40  $\mu$ L of 10 mM phosphate buffer (pH 7.1) (80% hydration). Multilamellar liposomes were formed by vortexing the mixture for 20 min at a temperature about 20°C above the  $T_m$  of the corresponding lipid.  $\alpha$ T-, cholesterol-, and  $\alpha$ T and cholesterol containing liposomes were prepared with exactly the same procedures but in this case the dried films were obtained by mixing chloroform-phospholipid solution with the required amount of  $\alpha$ T dissolved in ethanol

and cholesterol dissolved in chloroform.  $\alpha$ T containing flasks require protection from light due to light sensitivity throughout the drying procedure.

DPPC liposomes contain 20 mol% cholesterol (the lipid-to-cholesterol molar ratio is 4:1) and different mol%  $\alpha$ T. The maximum concentration of  $\alpha$ T mol% (the lipid-to- $\alpha$ T molar ratio is 4:1). In tertiary mixture of cholesterol and  $\alpha$ T, for maximum  $\alpha$ T and cholesterol incorporation (20 mol%  $\alpha$ T and 20 mol% cholesterol) the corresponding lipid-to- $\alpha$ T-to-cholesterol molar ratio is 4.25:1:1.

Additionally, pure and  $\alpha$ T containing liposomes were prepared with D<sub>2</sub>O instead of water in order to compare the results with previous FTIR study [66]. The results of the experiments will be given in chapter III.

## 2.3 Instrumentation

### 2.3.1 Dispersive Instruments

Conventional dispersive infrared instruments consisted of an infrared source that was focused on the sample. The output infrared beam was dispersed by a grating or a prism onto a slit that blocked all but a narrow range of frequencies from reaching the detector; therefore, resolution was dependent upon the width of the slit. Hence, to obtain a complete spectrum, the angle of the grating had to be continuously changed with respect to the incident infrared beam; thereby, only the region corresponding to the spectral resolution could be measured at a time. The result was a low energy spectrum because of (i) the necessary proximity of the sample to the source limited its power in order to avoid sample heating, and (ii) only a fraction of the infrared beam coming out from the source reached the detector. Spectra acquisition was then very

slow and dependent on several mechanical devices that make accuracy not very reliable and sample stability a problem[62].

These disadvantages have been overcome by using FTIR spectrometers.

### 2.3.2 Fourier Transform Infrared (FTIR) Spectrometer

Infrared radiation can be analyzed by means of a scanning Michelson interferometer. The Fourier transform is carried out by a computer, which is essential part of the spectrometer, by means of the fast Fourier algorithm developed by Cooley and Tukey.

This technique has several distinct advantages over the conventional dispersive techniques. (a) The detector observes all the frequencies simultaneously and can give a complete spectrum in less than 1 sec. The interferogram signal is termed multiplexed and the consequence is a greater signal-to noise ratio in the same spectral acquisition time ( Fellgett Advantage) and the possibility of performing kinetic measurements. (b) The IR beam impinges fully on the sample without the need of a slit to define resolution or to limit the amount of energy reaching the detector. Thus, more energy is admitted to flow through the system, allowing greater sensitivity and the use of special sampling techniques (Jacquinot Advantage). (b) FTIR instruments use an internal laser reference to facilitate digitisation of data and for frequency calibration. Since the laser frequency is accurately known, any measured data point is calibrated by the system to better than  $0.001 \text{ cm}^{-1}$  (Connes Advantage).

## 2.4 Sample Handling

$\text{CaF}_2$  is used in the present study as window material. It is insoluble in water.

Fig. 16 shows the infrared spectrum of  $\text{CaF}_2$  alone. As seen from the figure it is not transparent in the wavenumber region lower than  $1200\text{ cm}^{-1}$ . It is evident from the figure that there are weak O-H stretching and O-H scissoring bands in the region of around  $3409\text{ cm}^{-1}$  and  $1645\text{ cm}^{-1}$  respectively. They are not so strong. The appearance of these bands is due to the presence of water molecules in the form of vapor in the air.



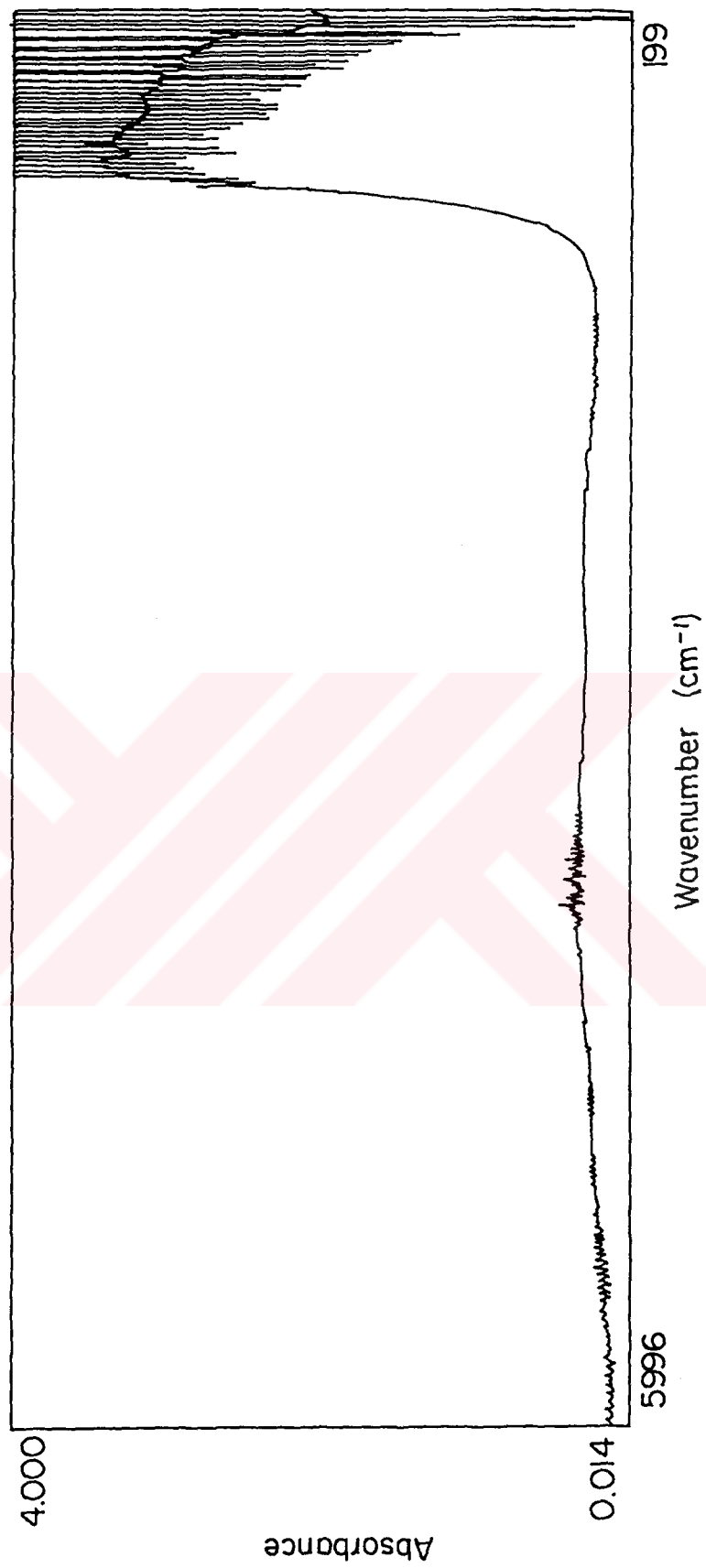


Figure 16. Infrared spectrum of CaF<sub>2</sub>.

20 $\mu$ l of liposomes were placed between CaF<sub>2</sub> windows. Due to the strong absorption of water in the samples, very thin spacers between windows are needed. Alternatively, samples were placed between windows without spacer which enable us to examine sample thickness less than 25  $\mu$ m.

Fig.17a and b show the infrared spectrum of DPPC liposomes without spacer and with spacer of 0.1 mm thickness respectively. As seen from the figure, infrared spectrum of DPPC multibilayer liposomes without spacer is much better.

Temperature is regulated by Unicam Specac digital temperature controller unit and a thermocouple which is located against the cell windows. The range of temperatures studied was from 20°C to 60°C. The samples were then incubated for 10 minutes at each temperature before the spectrum acquisition. Spectra were recorded on a Perkin Elmer 16 PC FTIR, Nicolet 510 FTIR and Bomem FTIR spectrometer at different times. Spectra obtained in all three machines are identical. Typically, 20 scans at 2 cm<sup>-1</sup> resolution were averaged for each sample.

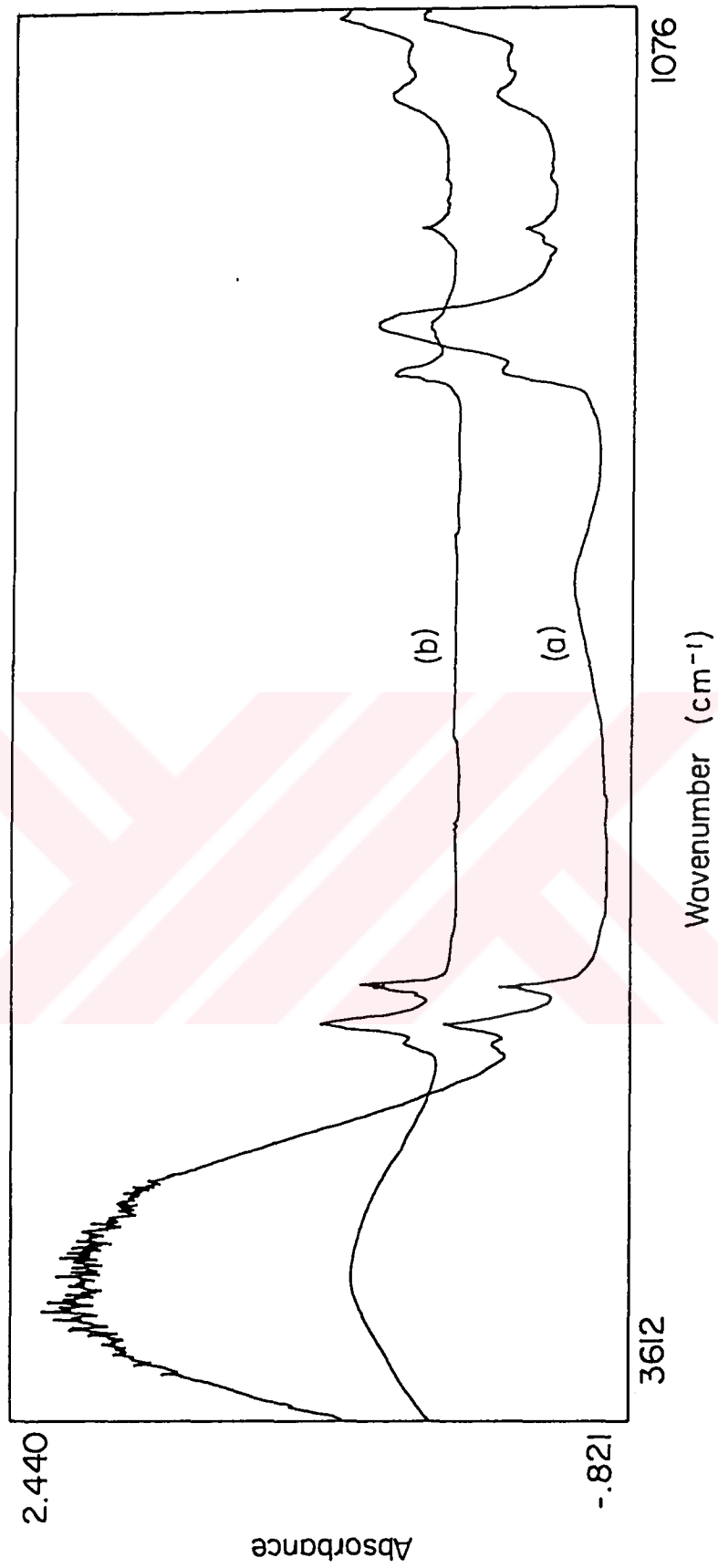


Figure 17. Infrared spectrum of DPPC multilayer liposomes with (a) and (b) without spacer.

## 2.5 Infrared Spectral Regions Used In This Study:

The FTIR studies of reconstituted systems have used primarily the CH<sub>2</sub> stretching vibrations which are the most intense in infrared spectra.

The hydrocarbon chain modes often used in the study of aqueous lipid assemblies are summarized in Table 2.

Table 2. The hydrocarbon chain modes.

FREQUENCY RANGE	DESCRIPTION OF VIBRATION	SYMBOL
2956±1	CH <sub>3</sub> asymmetric stretch	$\gamma$ (CH <sub>3</sub> )
2920±3	CH <sub>2</sub> antisymmetric stretch	$\gamma_{as}$ (CH <sub>2</sub> )
2973±1	CH <sub>3</sub> symmetric stretch	$\gamma_s$ (CH <sub>3</sub> )
2851±2	CH <sub>2</sub> symmetric stretch	$\gamma_s$ (CH <sub>2</sub> )
1735±3	ester carbonyl stretch	$\gamma$ (C=O)
1468±1	CH <sub>2</sub> scissoring	$\delta$ (CH <sub>2</sub> ) <sub>n</sub>

The carbon-hydrogen stretching vibrations give rise to bands in the spectral region 3100 to 2800 cm<sup>-1</sup>. The CH<sub>2</sub> antisymmetric and symmetric stretching modes 2900 and 2850 cm<sup>-1</sup>, respectively, are generally the strongest bands in the spectra of lipids. The frequencies of these bands are conformation-sensitive and, respond to changes of the trans/gauche ratio in acyl chains. This is also the case, although to lesser extent, for the vibrational modes due to the terminal CH<sub>3</sub> groups found at 2956 cm<sup>-1</sup> (asymmetric stretch) and 2870 cm<sup>-1</sup> (symmetric stretch).

The most useful infrared bands for probing the interfacial region lipid assemblies are the ester group vibrations, particularly the double bond C=O stretching bands in the 1750-1700 cm<sup>-1</sup> region.



The infrared bands due to bending vibrations of the methylene and methyl groups occur in the 1500-1350  $\text{cm}^{-1}$  region. The  $\text{CH}_2$  bending (or scissoring) modes give rise to bands around 1470  $\text{cm}^{-1}$ ; the number of these bands as well as their exact frequencies are dependent on acyl chain packing and conformation[64].

The  $\text{CH}_2$  rocking band progression in 700-1200  $\text{cm}^{-1}$  region can not be observed completely in Fig.16 since the  $\text{CaF}_2$  window which we used does not permit investigation of all these bands. The rocking bands are extremely weak and their observation and study are difficult due to overlap with many other vibrational modes. However, the head group vibrational band of this progression which is the most intense band in this region can be used to characterize the nature of the packing of long methylene chains.

## 2.6 Spectrum Handling

Fig.18 shows the infrared spectrum of air. Strong absorptions due to the presence of molecules ( $\text{H}_2\text{O}$  and  $\text{CO}_2$ ) in air appear in the spectrum. It is necessary to subtract these absorptions from the sample spectrum. The spectrum of the air is recorded as reference and subtraction process is done using appropriate software.

Water is the solvent for the lipid dispersions. The infrared absorption of water overlaps with the lipid bands in the region of  $\text{CH}_2$  and  $\text{C}=\text{O}$  stretchings.

Fig.19 illustrates the infrared spectrum of liquid water. Strong absorption bands were observed around 3409 $\text{cm}^{-1}$  and 1645 $\text{cm}^{-1}$  which reflects the water stretching and scissoring modes respectively.

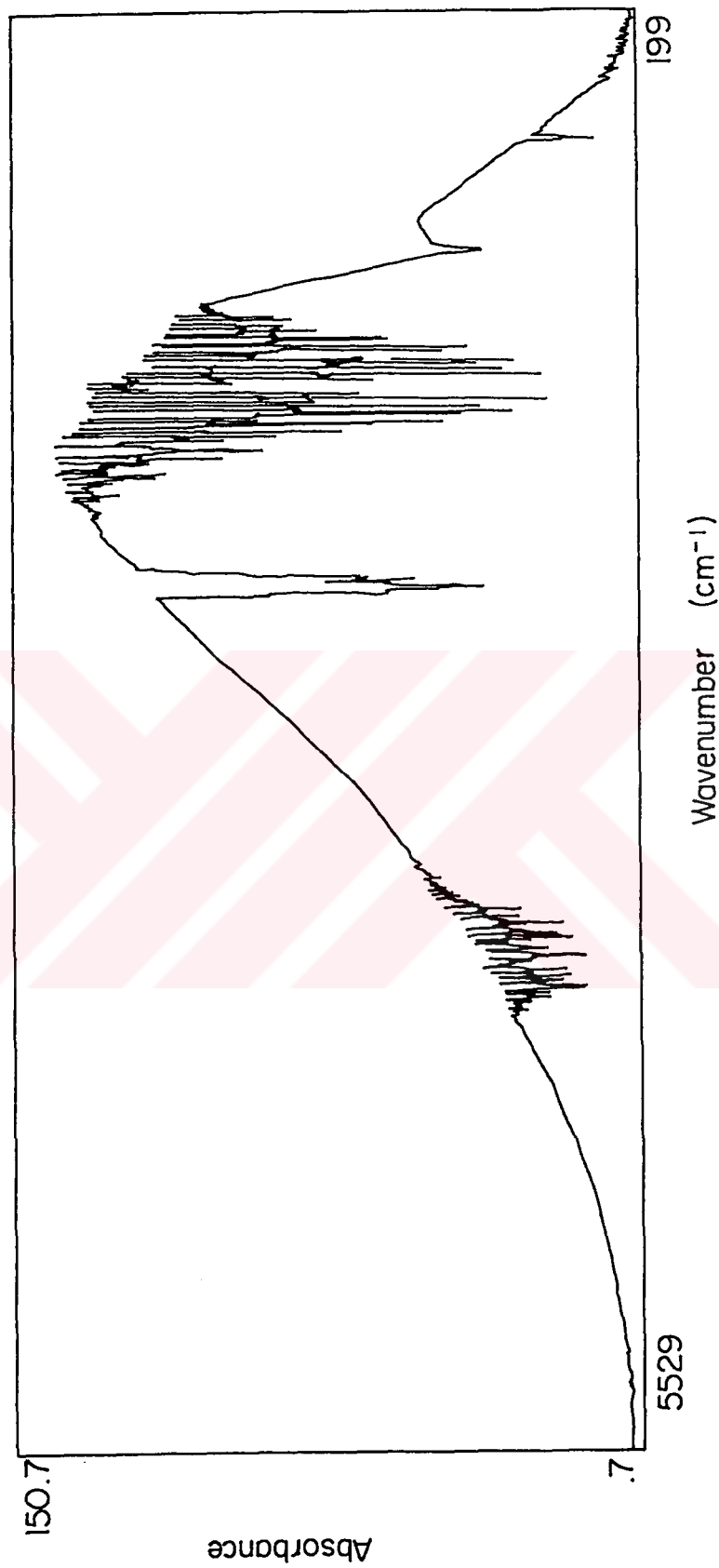


Figure 18. Infrared spectrum of the air.

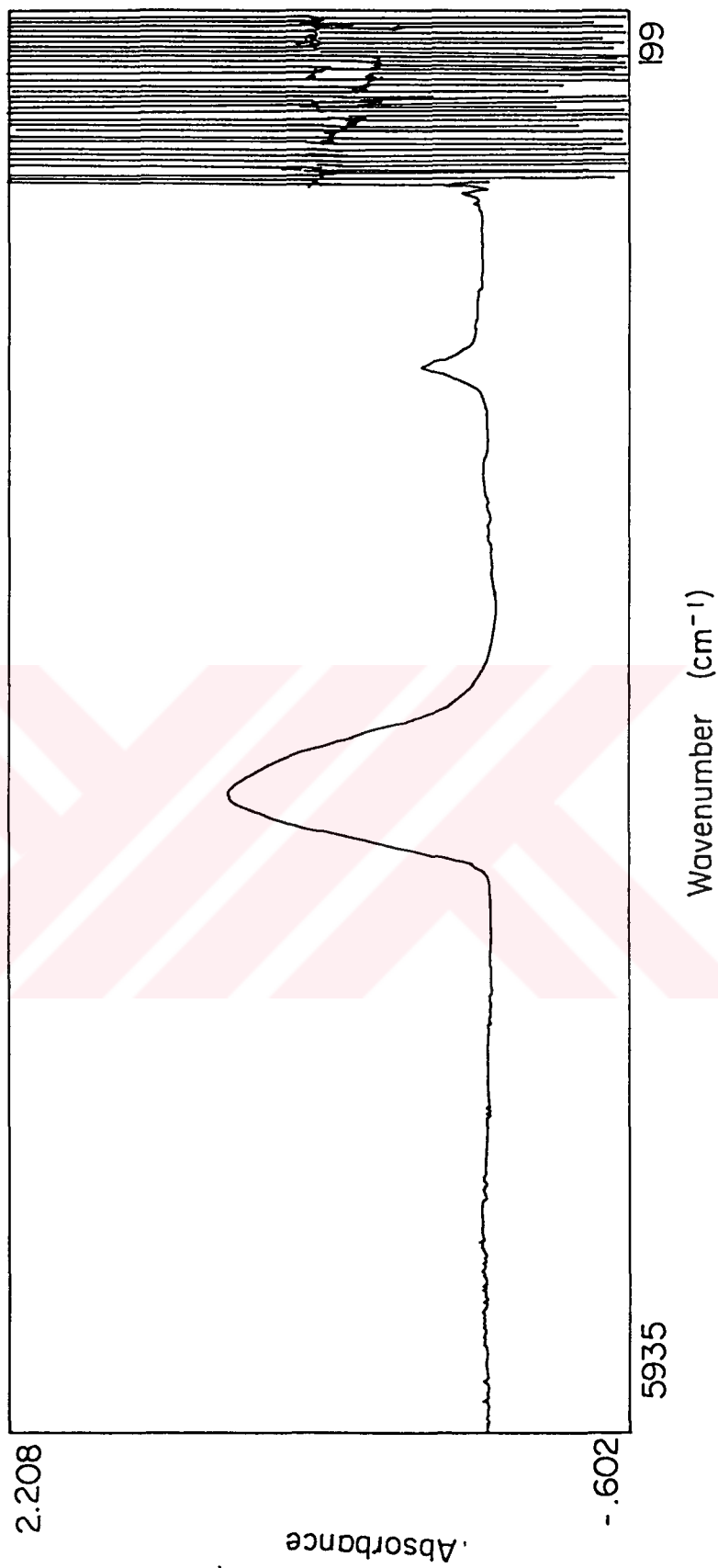


Figure 19. Infrared spectrum of liquid water.

Fig.20 shows the water vapor bands on DPPC infrared spectrum of C=O stretching band. It is shown in the figure that presence of water vapor in the air has an unwanted effect on the spectrum. This means that having a good spectrum depends on the level of humidity or the procedure for subtracting these.

Water is the solvent for the lipid dispersion. Fig.21a shows the infrared spectrum of DPPC multibilayer liposomes in excess water. Strong infrared absorption of water is observed in the same region as mentioned above which overlaps with the lipid bands in the region of CH<sub>2</sub> and C=O stretching. Water bands should be subtracted from the spectrum of multilamellar bilayers. It is not an easy problem to overcome. We have to find the most suitable water spectrum to do the process of water subtraction without destroying the sample spectrum. Absorbance subtraction is a routine operation for all modern infrared spectrometers[67,68]. Two main precautions should be considered, namely (i) the water spectra must be recorded with the cells of identical pathlength and window materials and (ii) they must be recorded at the same temperatures as that of the sample in order to take into account temperature-induced changes in the water spectrum[69]. Fig.21b shows the FTIR spectrum of the same sample after water subtraction. As one can see from the figure, this time C=O bending mode is clearly observed.

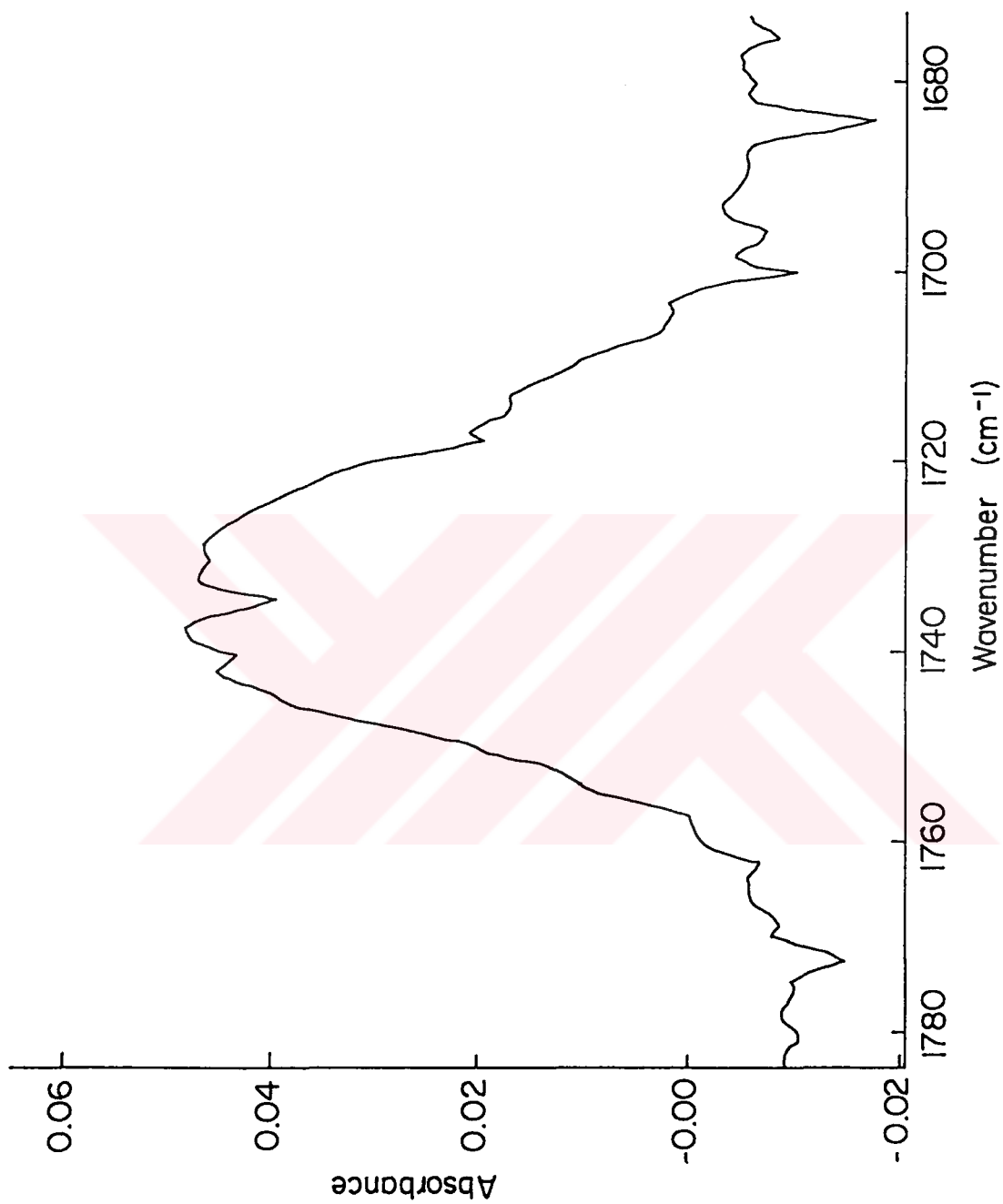


Figure 20. Water vapor bands on the infrared spectrum of a DPPC sample in the region of C=O stretching mode at 50°C.

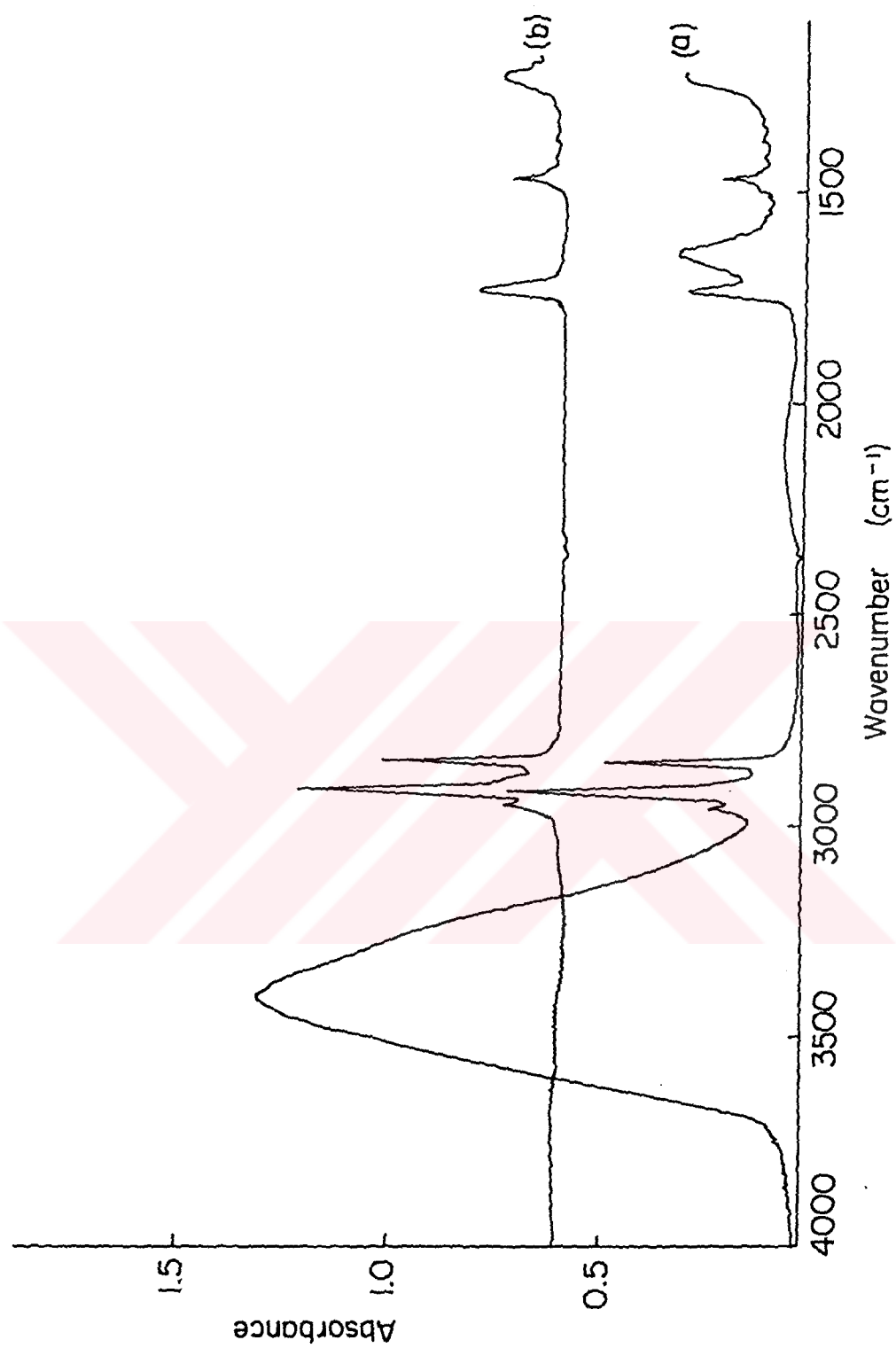


Figure 21. FTIR spectrum of aqueous DPPC multilamellar liposomes at 30°C (a) before and (b) after water subtraction.

In order to eliminate the disadvantages of working with water, generally samples are prepared with less content of water such as 50 % hydration (50% lipid w/v) for infrared spectroscopy. Since biological membranes contain excess water. It was not desired to prepare the samples at that concentration. It was tried to find out the most suitable concentration which contained excess water and also permitted one to investigate the infrared bands. Although, we succeeded to work with 90% hydration (10% lipid w/v), it was decided to work with 80% hydration to reduce the difficulties on water subtraction in the C=O stretching region. Fig.22a and b shows the FTIR spectra of DPPC multilamellar liposomes at 90% and 80% hydration respectively. As seen from the figure the clearest spectrum is observed when the hydration level is decreased.

The other method is to use D<sub>2</sub>O instead of water for hydration process to get rid of disadvantages of water. Fig.23 shows the FTIR spectrum of DPPC liposomes in excess D<sub>2</sub>O. Since the infrared absorbance of D<sub>2</sub>O is outside the wavenumber range of interest, a smoother spectrum is observed. However there are disadvantages of using D<sub>2</sub>O. Samples must be prepared in closed containers to eliminate D-H exchange with air. In addition to this, D-H exchange between sample and D<sub>2</sub>O should also be considered. Therefore this has not been extensively used in this study.

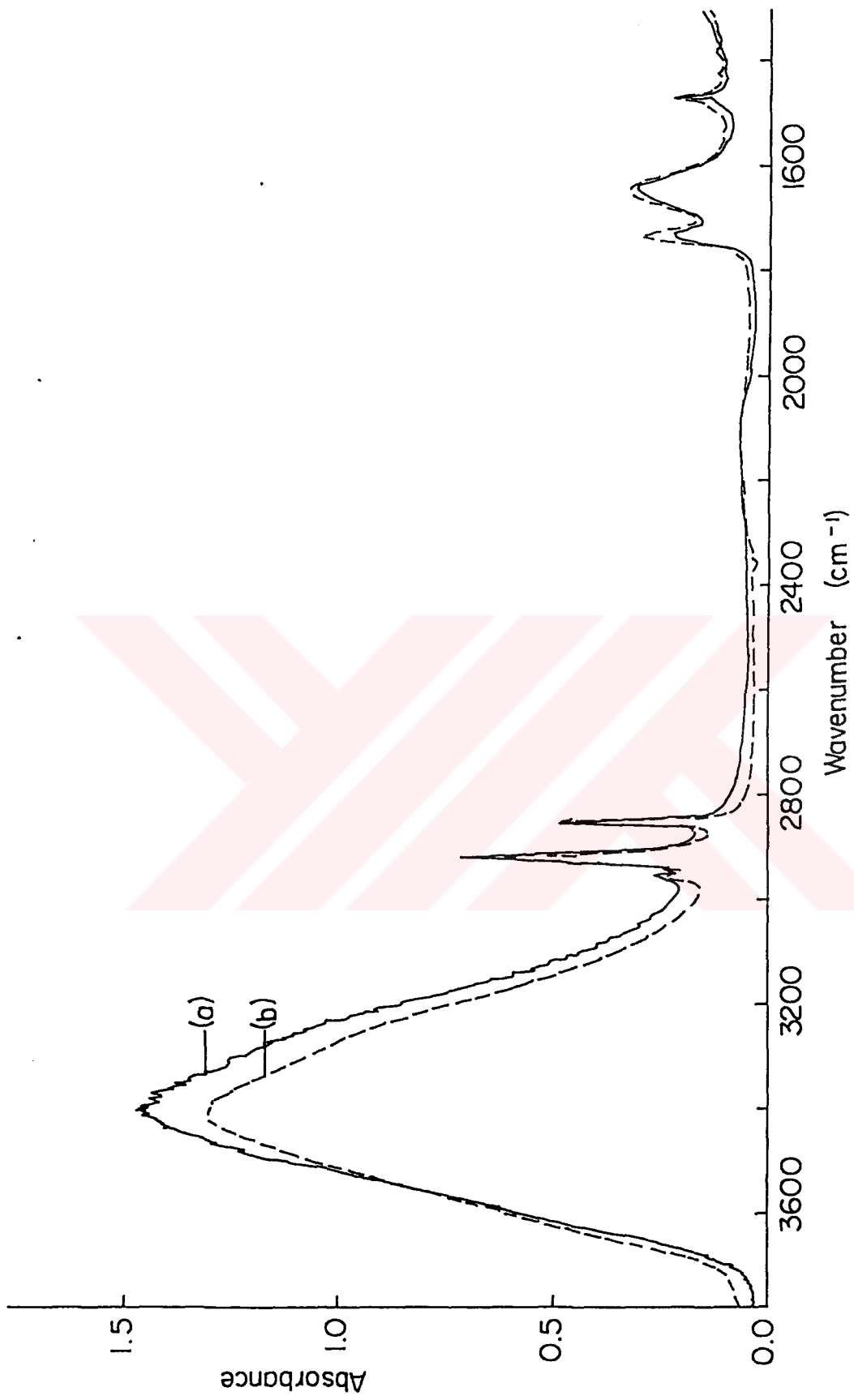


Figure 22. FTIR spectra of DPPC liposomes at different water concentration. (a) 90%, (b) 80% hydration



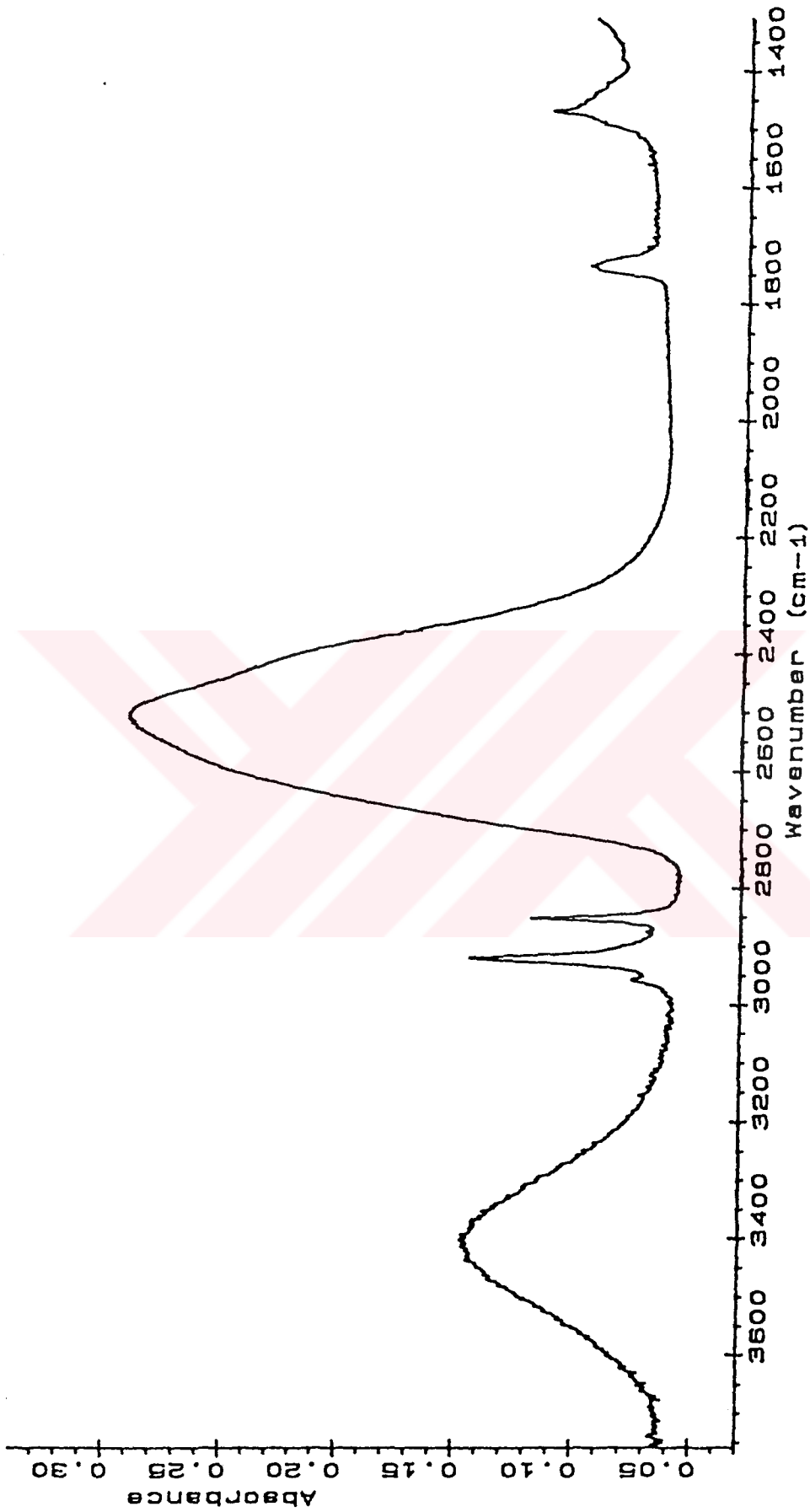


Figure 23. FTIR spectrum of DPPC multilamellar liposomes in D<sub>2</sub>O

## 2.7. Empirical Rules Used in FTIR Spectroscopic Membrane Research:

All the bands given in section 2.5 exhibit temperature-dependent variations in frequency and in bandwidth which can be related to structural changes at the molecular level.

The frequency of CH<sub>2</sub> antisymmetric and symmetric vibrational mode changes give knowledge about the conformational structure of phospholipid acyl chains. The frequency values below the phase transition temperature are characteristic of conformationally highly ordered acyl chains as found in solid hydrocarbons, whereas the values above phase transition are characteristic of conformationally disordered acyl chains with high content of gauche conformers such as those found in liquid hydrocarbons.

The frequencies of the CH<sub>2</sub> stretching bands of acyl chains depend on the degree of conformational disorder hence can be used to monitor the average trans/gauche isomerization in the systems. The shifts to higher wavenumbers correspond to an increase in number of gauche conformers.

The temperature-dependent variations in bandwidth reflect changes in vibrational and torsional motion. As the bandwidth increases, mobility of the phospholipid acyl chains increases, and also the reverse of this statement is true. In short, bandwidth gives dynamic information about the system[70].

Frequencies of CH<sub>3</sub> asymmetric stretching mode give information about dynamics of the deep interior of the bilayer[71]. A decrease in frequency corresponds to stiffness of the bilayer.

The change in the bandwidth of the CH<sub>2</sub> scissoring mode reflects both conformational disorder and chain rotation[69]

A red shift in frequency of C=O stretching mode reflects the existence of hydrogen bonding [13]. Changes in the bandwidth of C=O stretching mode reflect the changes in librational and torsional motion of the interfacial region[71].



## CHAPTER III

### RESULTS AND DISCUSSION

In conceiving the present study and during the analysis of the results, we have been particularly careful to make a distinction between structural parameters (such as order) and dynamic parameters (such as bandwidth). On the other hand the correlation between chain order and chain motion is not well understood to date[5,7,12].

The infrared spectra of lipids have been studied at two spectral regions which originate from molecular vibrations of different molecular moieties which can be referred to (i) head-group and (ii) hydrocarbon tail spectral characteristics.

#### 3.1 Spectral Characteristic of the Acyl Chains

Fig.24 displays the spectrum of DPPC multilamellar bilayers in the C-H stretching region at different temperatures. This figure illustrates that variations in temperature produce significant changes in peak position, peak height and the bandwidth of the C-H stretching bands. In general peak height decreases with increasing temperature. In the gel phase, the CH<sub>2</sub> antisymmetric and symmetric stretching bands are relatively sharp and are observed near 2918 cm<sup>-1</sup> and 2849 cm<sup>-1</sup> respectively; on conversion to the liquid crystalline phase, these bands broaden and their absorption maximum shifts to the higher wavenumbers, 2923 cm<sup>-1</sup> and 2852 cm<sup>-1</sup> respectively. As mentioned in the introductory part, the most common structure of aqueous lipid assemblies is the well

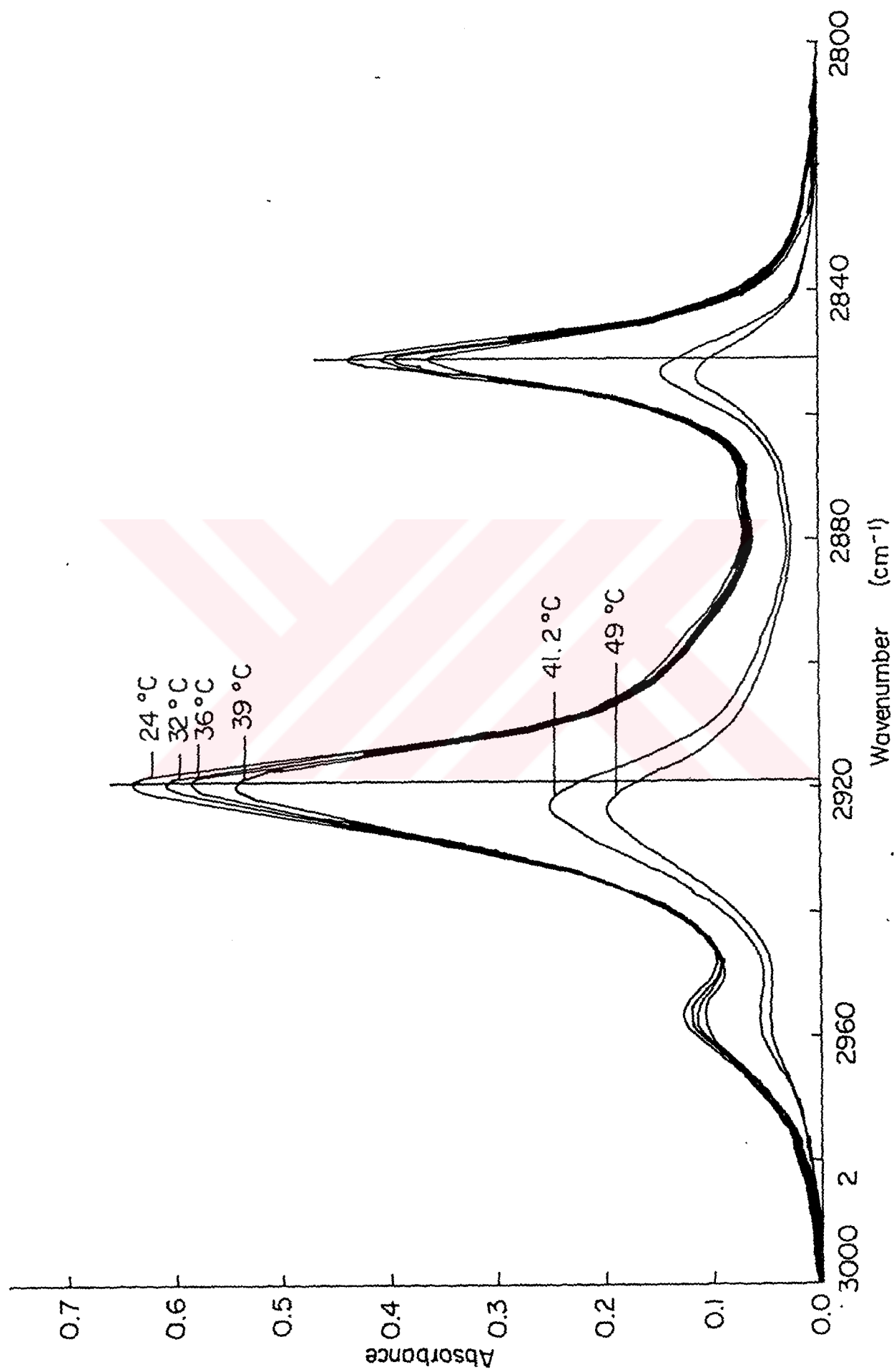


Figure 24. Temperature dependence for the C-H stretching region of the FTIR spectrum of pure DPPC multilamellar liposomes at different temperatures.

investigated multibilayer structure, which can exist in two physical states; the ordered, rigid gel phase and the more fluid, disordered liquid crystalline phase. The temperature-induced transition between these two states, i.e., the gel-to-liquid crystal phase transition, produces considerable changes in the infrared spectrum. It is evident from Fig.24 that abrupt increases in peak position and bandwidth and an abrupt decrease in peak height are observed around 41.2°C, which is consistent with those reported in other studies [69]. This transition corresponds to the melting of the hydrocarbon chains, therefore, it is sometimes referred to as the chain melting phase transition. It involves the introduction of conformational disorder (i.e., gauche conformers) in the acyl chains, and changes in bandwidths can be related to variations in the rates of motion of the acyl chains[72,73]

### 3.1.1 Vitamin E-Membrane Interactions

The peak frequency of the CH<sub>2</sub> antisymmetric stretching vibration versus temperature is plotted in Fig.25, for pure DPPC liposomes and DPPC liposomes containing different mol%  $\alpha$ T. As shown in the figure, the phase transition for the multilamellar suspension occurs over a narrow range of temperatures centered at  $\approx 41^\circ$  C and is completed within about 1°C. The phase transition of DPPC liposomes is altered drastically in the presence of  $\alpha$ T. Increasing concentrations of  $\alpha$ T produce a progressive broadening of the phase transition curve and lowering of  $T_m$  which are consistent with other studies[5] At temperatures below the phase transition, with the addition of  $\alpha$ T, an increase in frequency is observed which corresponds to the progressive increase in the gauche rotamer. On the other hand, above the phase transition the effect of  $\alpha$ T is negligible. These are also valid for the CH<sub>2</sub> symmetric stretching vibration frequencies which is shown in Fig.26.

CH<sub>2</sub> ANTISYMMETRIC STRETCHING

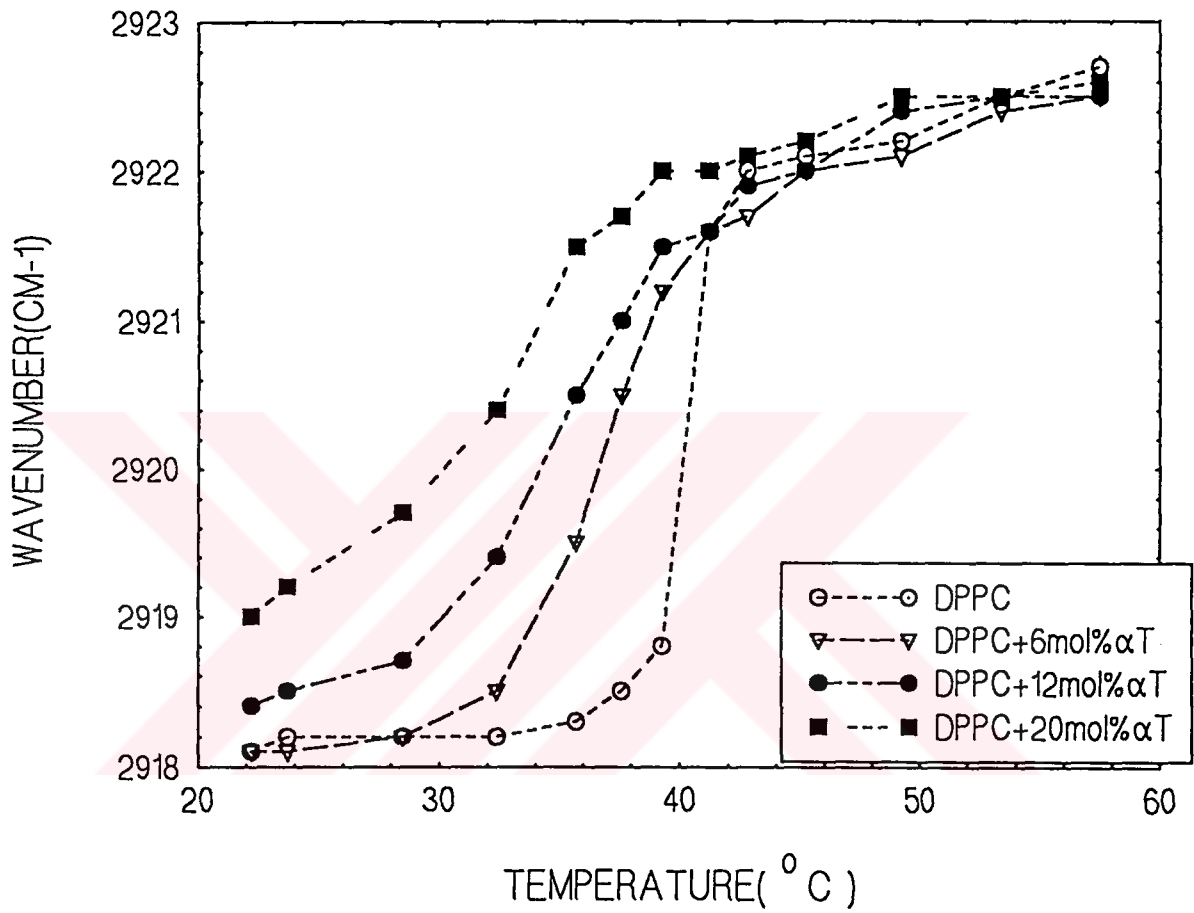


Figure 25. Frequency of the CH<sub>2</sub> antisymmetric stretching mode of DPPC multilamellars versus temperature for DPPC multilamellar liposomes-containing 0 mol% αT, 6mol% αT, 12 mol% αT, and 20 mol% αT.

### CH<sub>2</sub> SYMMETRIC STRETCHING

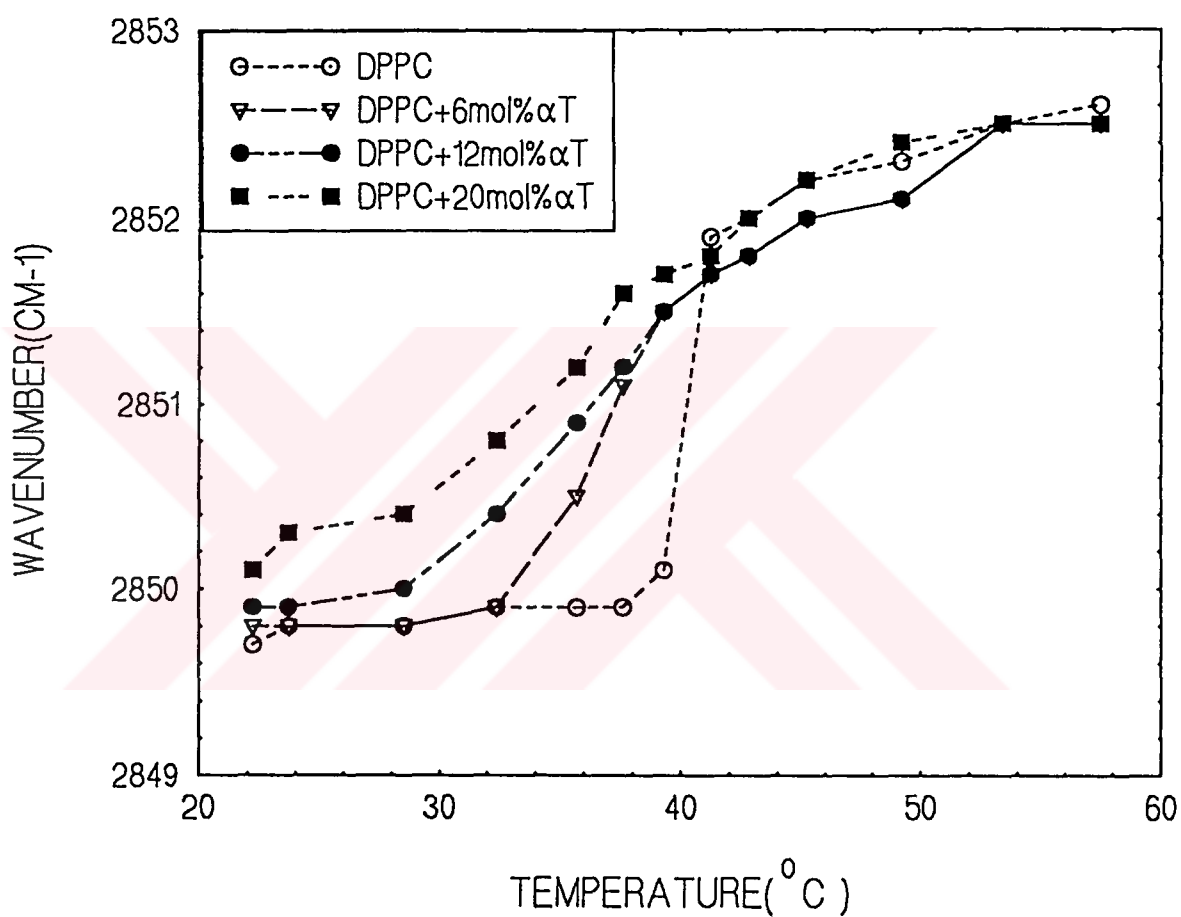


Figure 26. Frequency of the CH<sub>2</sub> symmetric stretching of DPPC multilayers versus temperature for DPPC multilamellar liposomes-containing 0 mol%  $\alpha$ T, 6 mol%  $\alpha$ T, 12 mol%  $\alpha$ T, and 20 mol%  $\alpha$ T.



In structural studies, previous FTIR results of  $\alpha$ T-phospholipid membrane interaction [66] show some discrepancies with other spectroscopic results such as ESR, STESR and deuterium NMR[8,56,57]. Previous FTIR results are also different from our present FTIR results. In a previous FTIR study [66], it was reported that, in the gel and in the liquid crystalline phase,  $\alpha$ T increases order whereas previous ESR, STESR,  $^2$ H-NMR studies and our FTIR studies report that with the addition of  $\alpha$ T ordering of the membrane decreases in the gel state and negligible effect is observed in the liquid crystalline state.

Since FTIR studies of  $\alpha$ T containing phospholipid liposomes are our control studies, we repeated the FTIR spectroscopic investigation of  $\alpha$ T containing DPPC membranes by using the same experimental conditions that Villian et al.[66] used in order to understand the reason for this discrepancy. In that study  $D_2O$  was used instead of  $H_2O$  for hydration process. We repeated the experiments by using both  $H_2O$  and  $D_2O$  for hydration. The comparison of the results is shown in Fig.27 and Fig.28 for  $CH_2$  antisymmetric stretching mode of pure and 20 mol%  $\alpha$ T-containing DPPC liposomes for  $H_2O$  and  $D_2O$  hydration respectively. As seen from Fig.27 and Fig.28 similar results are obtained, which conflicts with Villain's result[66] but is, however, in agreement with ESR and NMR results. In the gel phase  $\alpha$ T again induced the formation of gauche rotomers, while it exhibited negligible effect in the liquid crystalline phase. As expected, red shifts in frequencies are also observed when  $D_2O$  is used as a solvent. It was reported earlier by Gallagher [74] that  $H \rightarrow D$  isotopic exchange may lead to a decrease of interatomic distances in crystals. The reduced mass also increases with deuterium substitution. This implies a decrease in frequency. DPPC phase transition curve in Fig.28 shows this property. From Fig.28 it is also observed that addition of  $\alpha$ T inhibits  $H \rightarrow D$  exchange.

### CH<sub>2</sub> ANTISYMMETRIC STRETCHING

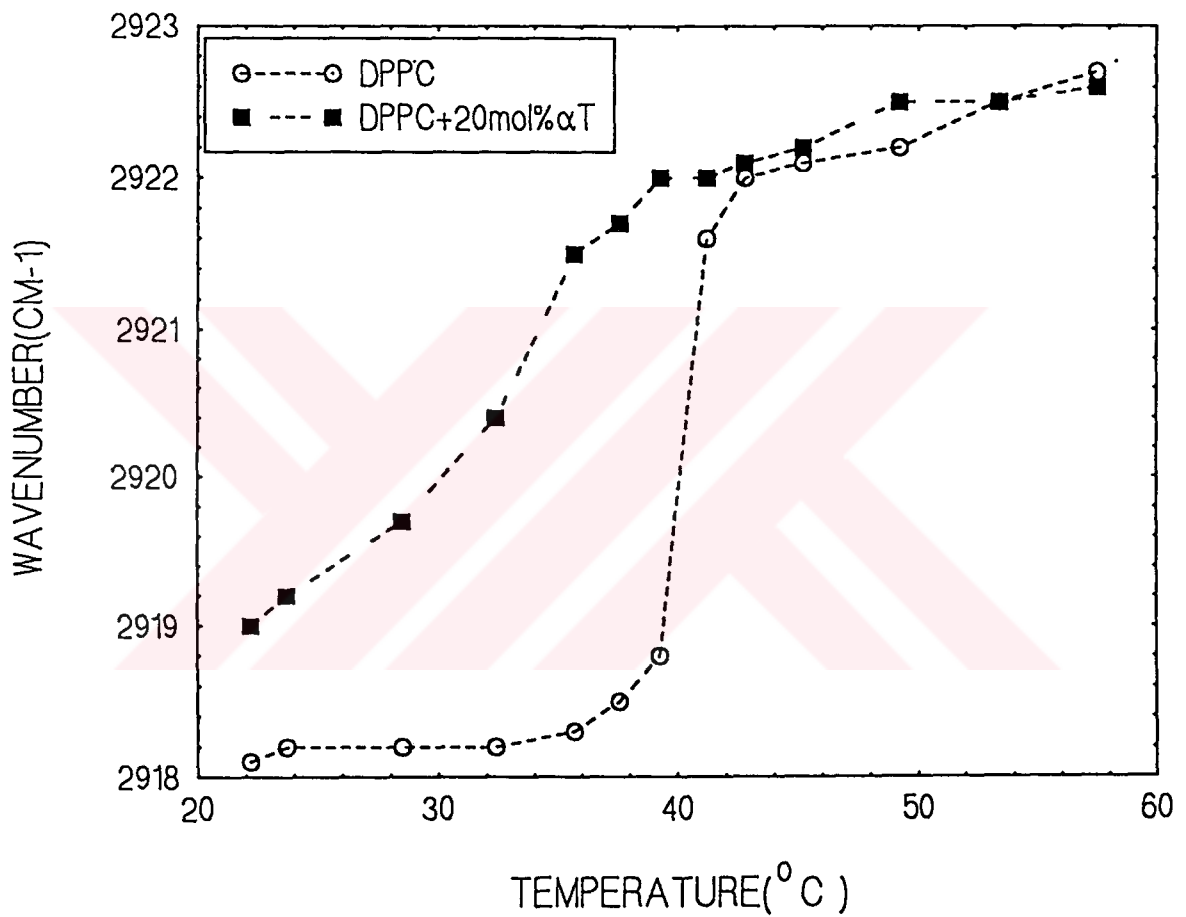


Figure 27. Temperature dependence frequency of CH<sub>2</sub> antisymmetric stretching mode of DPPC liposomes in the absence and in the presence of 20 mol% αT for H<sub>2</sub>O hydration.

### CH<sub>2</sub> ANTISYMMETRIC STRETCHING

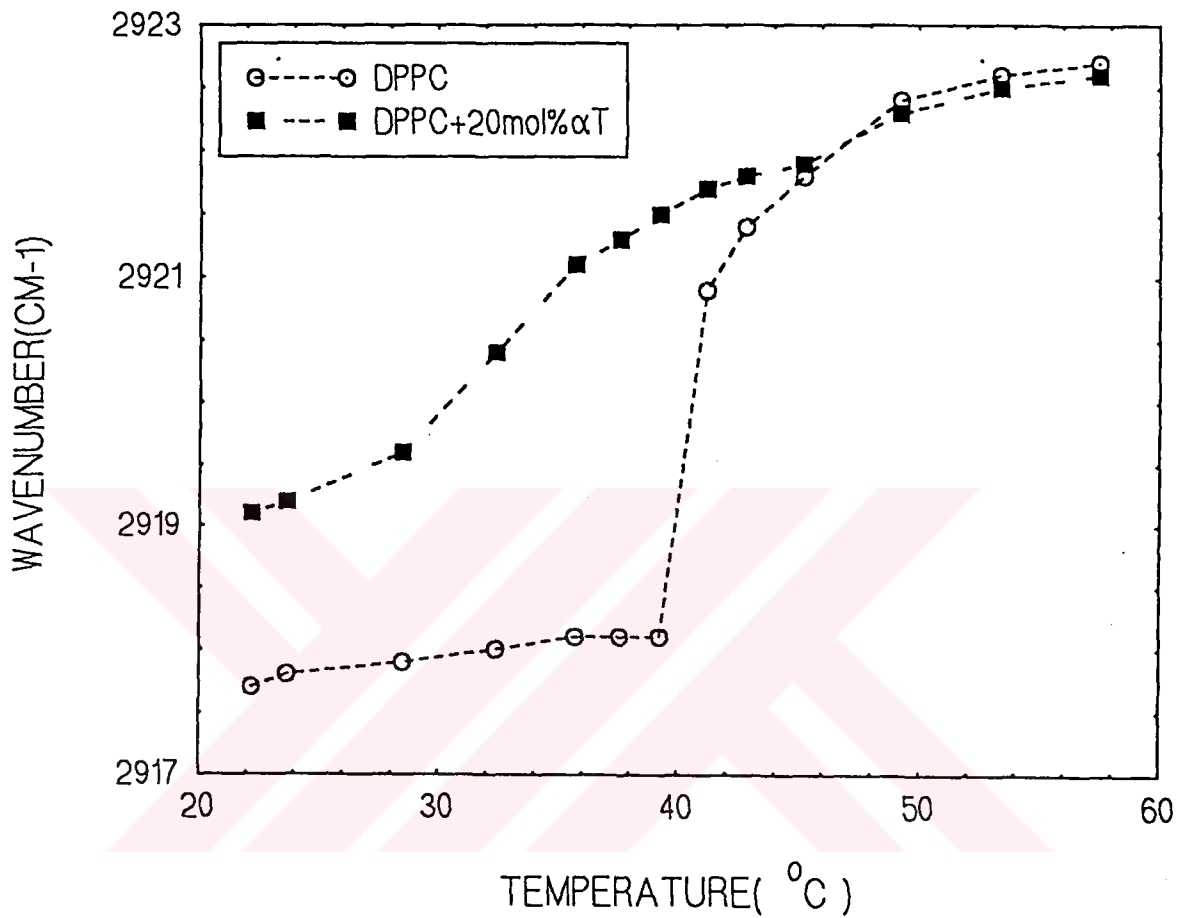


Figure 28. Temperature dependence frequency of CH<sub>2</sub> antisymmetric stretching mode of DPPC liposomes in the absence and in the presence of 20 mol% αT for D<sub>2</sub>O hydration.

Fig.29 and Fig.30 illustrate bandwidth changes of CH<sub>2</sub> antisymmetric and symmetric stretching modes respectively as a function of temperature. At any given temperature, the bandwidth progressively increases with increasing  $\alpha$ T concentration. Bandwidth was measured at 0.75x peak height position. However, qualitatively similar results are also obtained at 0.50x peak height position. Considerable insight is obtained into the various types of motion performed by the fatty acyl chains due to the different responses of the several IR spectral parameters to motional effects. One of them is half-bandwidths of the CH<sub>2</sub> stretching mode. The half-bandwidth monitors the freedom of motion of the absorbing group i.e., the amplitudes and rates of motion within its immediate environment. The half-bandwidth will therefore reflect the main thermal transition where a considerable change in its environment occurs. It is also sensitive to other changes which do not introduce gauche conformers, such as decreased freedom of librational or torsional motion of the chains[73,75]. Fig.29 and Fig.30 demonstrate that  $\alpha$ T increases the motional freedom of lipid acyl chains by increasing the bandwidth both in the gel and in the liquid crystalline phase. The antisymmetric and symmetric methylene bands show identical behaviour. Although in the liquid crystalline state our results conflict with the previous NMR and ESR results where it was stated that  $\alpha$ T decreases membrane fluidity [6,5], our results agree with previous FTIR results[66]. As previously reported [66], this discrepancy between FTIR and other techniques can be due to the existence of subphases occurring in vitamin E-phospholipid binary mixtures which are named as vitamin E poor and vitamin E rich phases[8]. We know that conventional ESR and NMR studies monitor the overall dynamic effect of these subphases[5]. On the other hand FTIR may monitor dominantly one of these subphases. This might be the reason of this discrepancy.

### CH<sub>2</sub> ANTISYMMETRIC STRETCHING

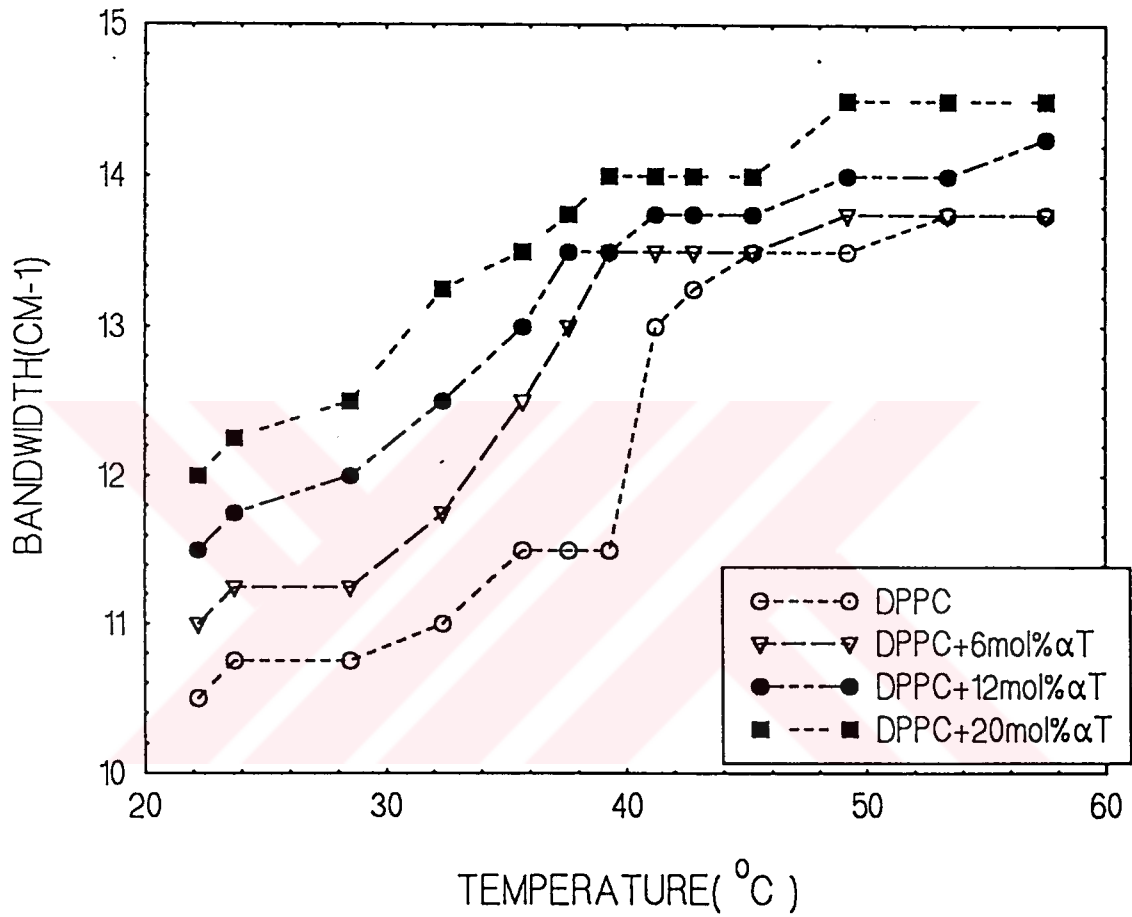


Figure 29. Temperature dependence of the bandwidth at 0.75x peak height of the CH<sub>2</sub> antisymmetric stretching mode of DPPC multilamellar liposomes containing 0 mol% αT, 6 mol% αT, 12 mol% αT, and 20 mol% αT.

CH<sub>2</sub> SYMMETRIC STRETCHING

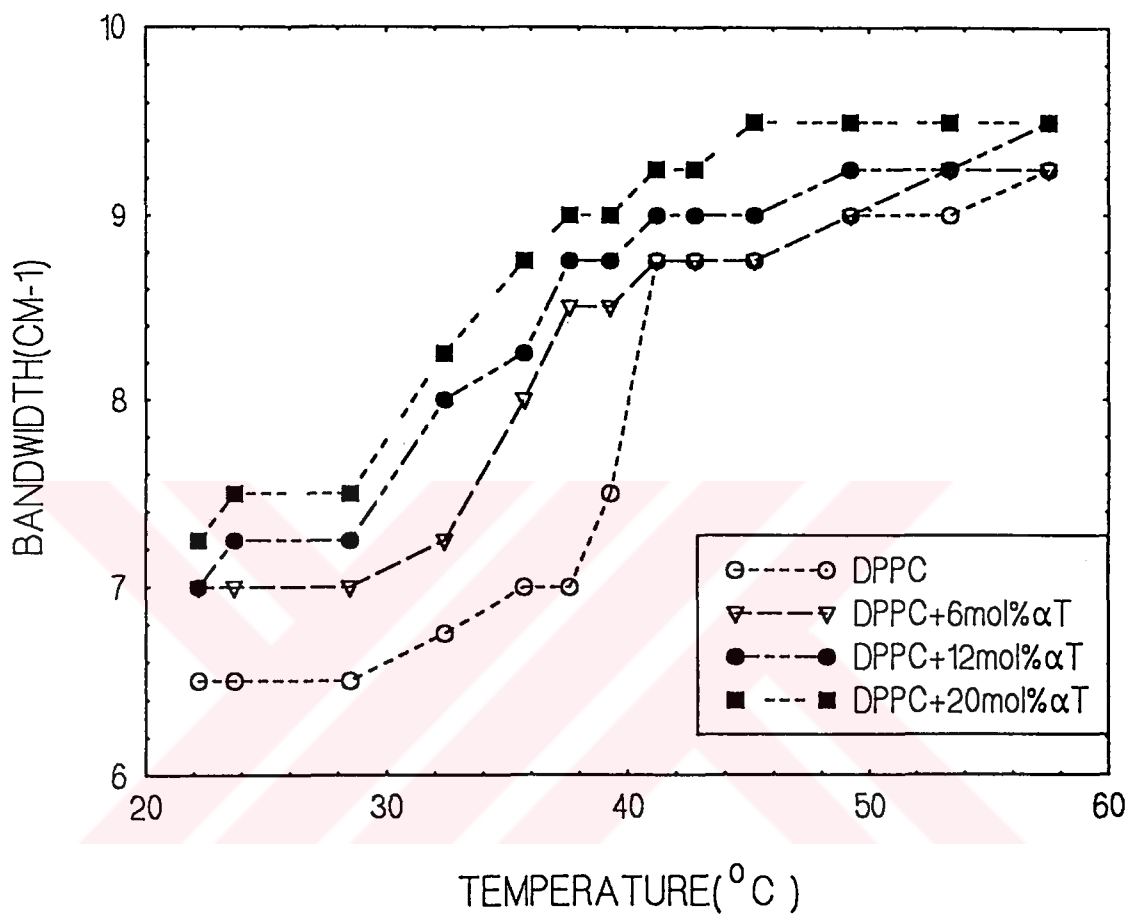


Figure 30. Temperature dependence of the bandwidth at 0.75x peak height of the CH<sub>2</sub> symmetric stretching mode of DPPC multilamellar liposomes containing 0 mol% αT, 6 mol% αT, 12 mol% αT, and 20 mol% αT.

### 3.1.2 Cholesterol-Membrane Interactions

The individual effect of cholesterol on pure DPPC phospholipid bilayers was also investigated in detail. The temperature dependence of the frequencies of the symmetric  $\text{CH}_2$  stretching mode in pure DPPC, and in different mol% cholesterol-containing systems are shown in Fig.31. With the incorporation of cholesterol the following changes are observed: Introduction of gauche conformers occurs over a wider temperature range. In the gel phase, frequencies of the C-H stretching modes follow the order: pure < DPPC+20 mol% cholesterol < DPPC+40 mol% cholesterol. This demonstrates that cholesterol increases the average number of gauche conformers in the gel phase. In the liquid crystalline phase, the order of frequencies has changed in the reverse direction and the number of gauche conformers decreases with increasing cholesterol concentration. Fig.32 shows the variation of bandwidth of the  $\text{CH}_2$  symmetric stretching mode as a function of temperature for different mol% cholesterol-containing DPPC liposomes. These results were confirmed by antisymmetric  $\text{CH}_2$  stretching mode frequencies and bandwidth measurements. These observations are also in agreement with the results of  $^2\text{H}$ -NMR. [76] and Raman spectroscopic studies [77].

CH<sub>2</sub> SYMMETRIC STRETCHING

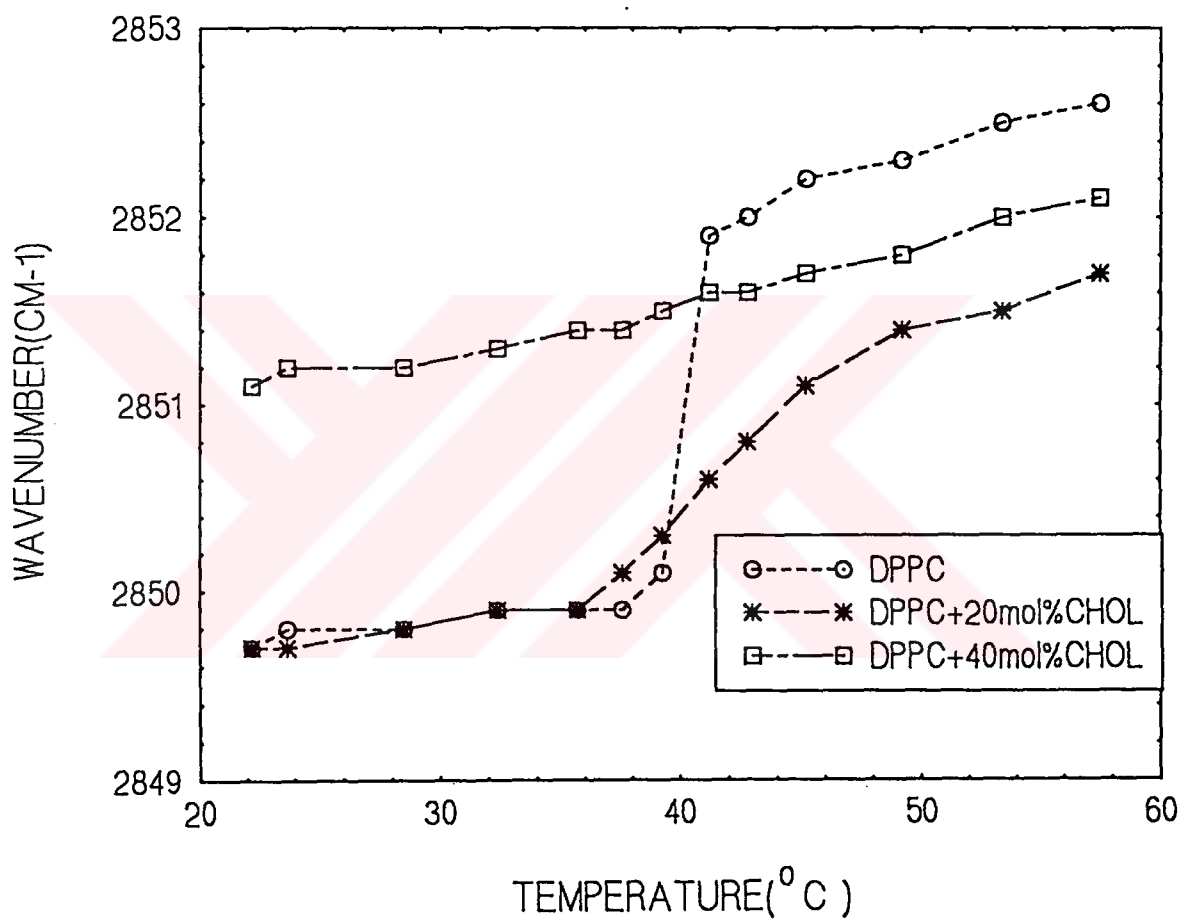


Figure 31. Temperature dependence frequency of CH<sub>2</sub> symmetric stretching mode of DPPC multilamellar liposomes containing-0 mol% cholesterol, 20 mol% cholesterol, and 40 mol% cholesterol.



CH<sub>2</sub> SYMMETRIC STRETCHING

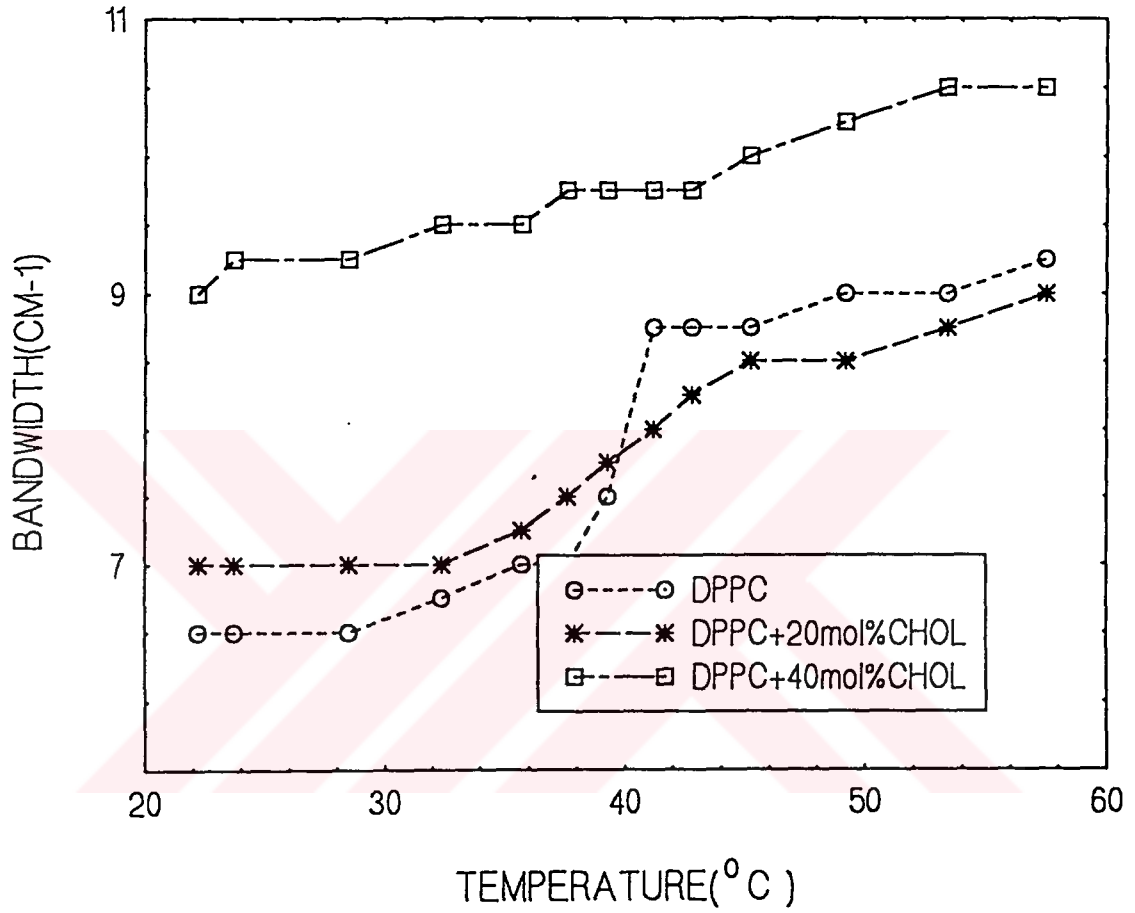


Figure 32. Temperature dependence of the bandwidth at 0.75x peak height of the CH<sub>2</sub> symmetric stretching mode of DPPC multilamellar liposomes containing 0 mol% cholesterol, 20 mol% cholesterol, and 40 mol% cholesterol.

### 3.1.3 Vitamin E-Cholesterol-Membrane Interactions

#### 3.1.3.1 CH<sub>2</sub> Stretching Modes

Fig.33 shows the temperature dependence of the CH<sub>2</sub> antisymmetric stretching mode for pure DPPC, 20 mol% cholesterol-containing DPPC, 20 mol%  $\alpha$ T-containing DPPC and DPPC multibilayers containing both 20 mol%  $\alpha$ T and 20 mol% cholesterol. As illustrated in Fig.33,  $\alpha$ T has paramount effect on cholesterol-containing multibilayers both in the gel and liquid-crystalline phases. As seen from the figure, cholesterol increases slightly and  $\alpha$ T increases significantly the frequency in the gel phase. When both of them are present in the system, the frequency increases additively. In the liquid crystalline phase cholesterol decreases (red shift), but  $\alpha$ T slightly increases (blue shift) the frequency. When  $\alpha$ T is added to cholesterol-containing DPPC liposomes, the effect of cholesterol on frequency decreases and wavenumbers shifts to higher values. These results imply in the gel phase that when both cholesterol and  $\alpha$ T are present together in the system, they exhibit an additive effect on the acyl chain organization, by increasing the number of gauche rotamers. On the contrary, in the liquid crystalline phase  $\alpha$ T reduces the effect of cholesterol by increasing the number of gauche rotamers in the system. Similar results were obtained from the analysis of CH<sub>2</sub> symmetric stretching mode frequencies (see Fig.34).

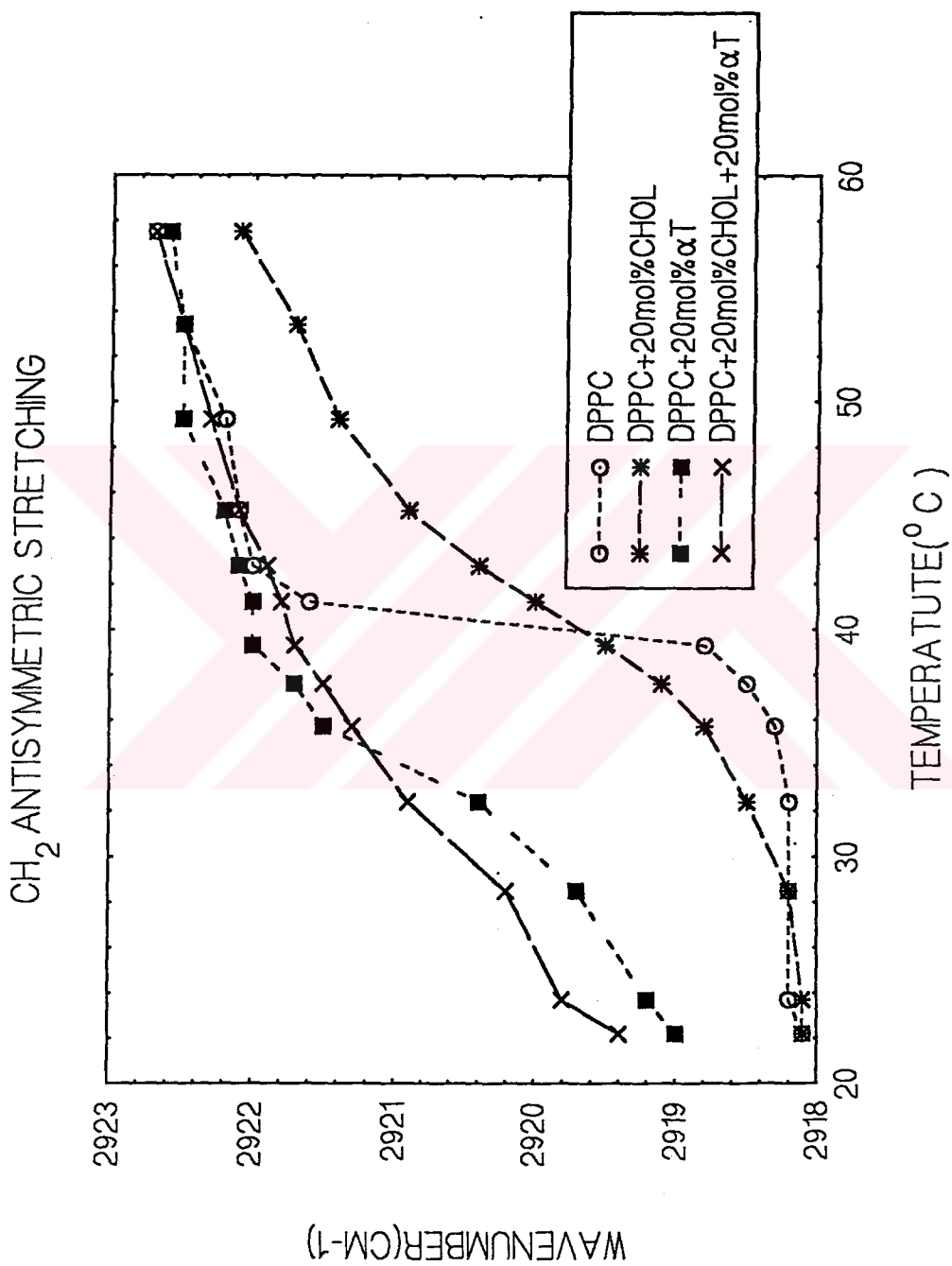


Figure 33. Temperature dependence frequency of CH<sub>2</sub> antisymmetric stretching mode of DPPC multilamellar liposomes containing 0 mol% cholesterol + 0mol% αT, 20 mol% cholesterol, 20 mol% αT, 20 mol% cholesterol + 20 mol% αT.

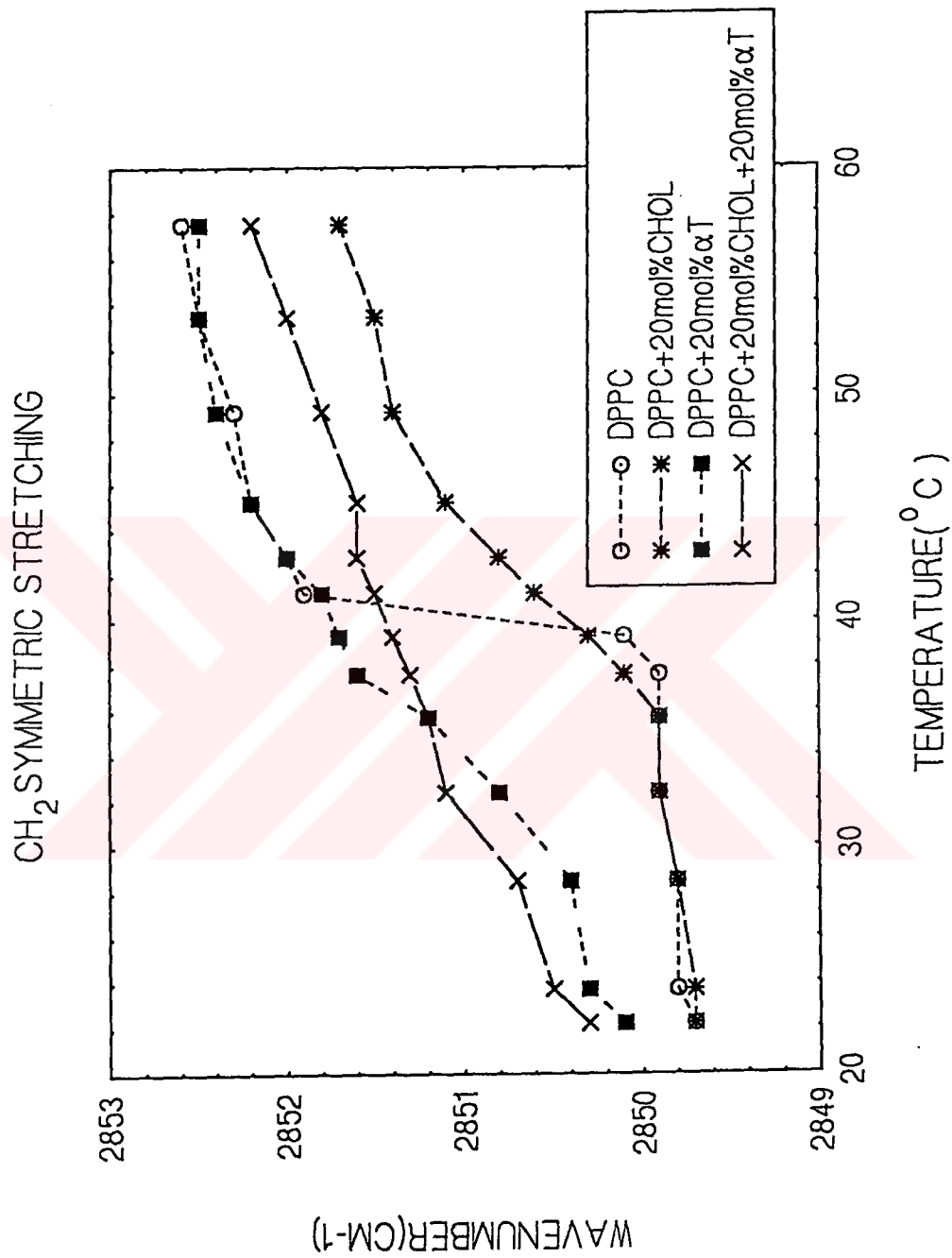


Figure 34. Temperature dependence frequency of CH<sub>2</sub> symmetric stretching mode of DPPC multilamellar liposomes containing-0 mol% cholesterol + 0mol% αT, 20 mol% cholesterol, 20 mol% αT, 20 mol% cholesterol + 20 mol% αT.

The temperature dependence of the bandwidths of CH<sub>2</sub> antisymmetric and symmetric stretching modes are shown at 0.75x height in Fig.35 and Fig.36 respectively. The bandwidth data of the CH<sub>2</sub> symmetric stretching mode in the presence of cholesterol indicates that cholesterol increases bandwidth (mobility) in the gel and decreases bandwidth (mobility) in the liquid crystalline phase. On the other hand, αT increases mobility both in the gel and in the liquid crystalline phase. However, when cholesterol and αT are present in the system together, the bandwidth increment is more than the bandwidth increment when they are present individually. It is certain that the presence of αT and cholesterol affect the mobility of the system additively in the gel phase or synergistically in the liquid crystalline phase. Similar results are gathered from the CH<sub>2</sub> antisymmetric stretching bandwidth(Fig.35). It is proposed that the CH<sub>2</sub> symmetric stretching near 2850cm<sup>-1</sup> is of special significance because of its sensitivity to the changes in mobility and in conformational disorder of the hydrocarbon chains. It is also overlapped with other vibrational modes[69]. The bandwidth parameter measured from the CH<sub>2</sub> symmetric stretching region reflects the changes in the system better than the CH<sub>2</sub> antisymmetric region[70]

### CH<sub>2</sub> ANTISYMMETRIC STRETCHING

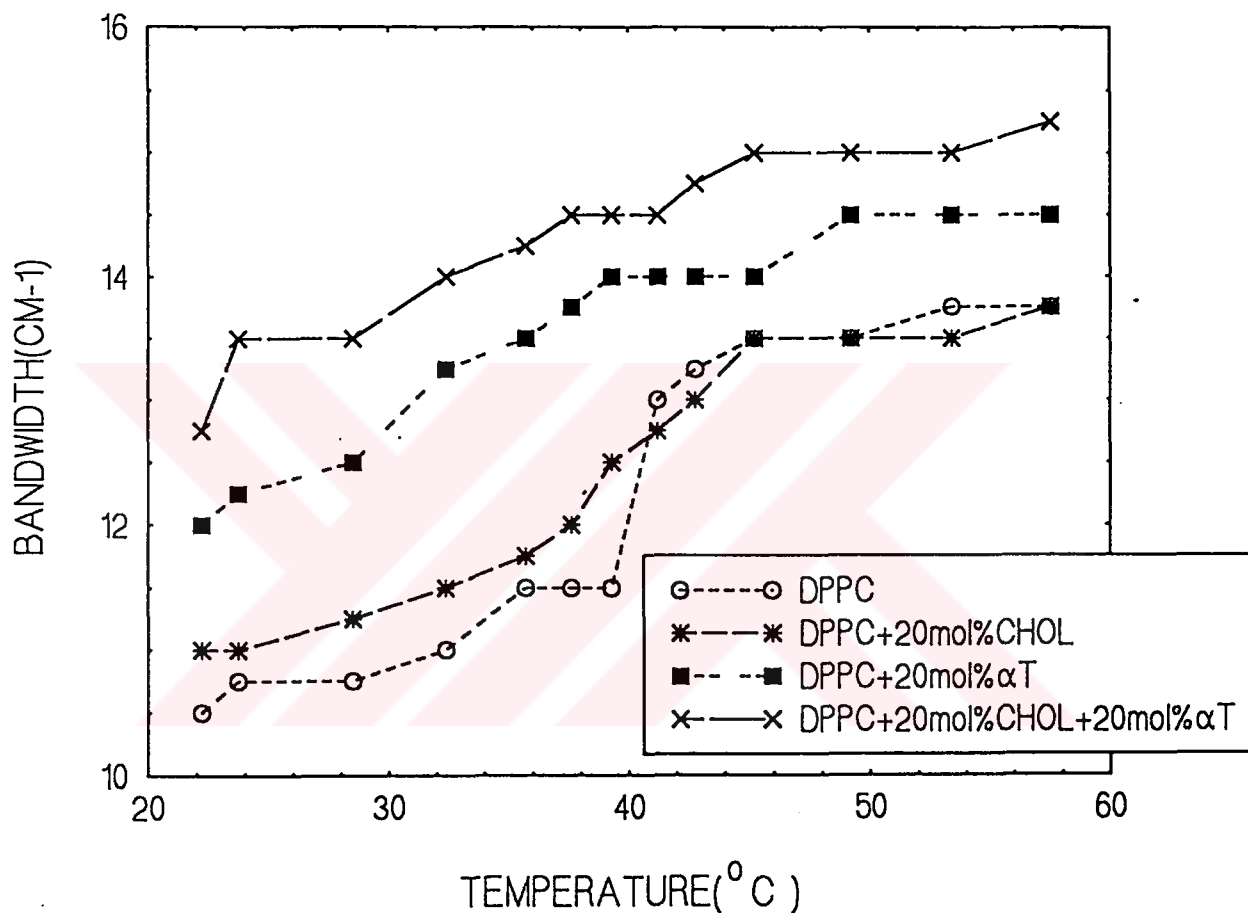


Figure 35. Temperature dependence of the bandwidth at 0.75x peak height of CH<sub>2</sub> antisymmetric stretching mode of DPPC multilamellar liposomes containing-0 mol% cholesterol + 0 mol% αT, 20 mol% cholesterol, 20 mol% αT, 20 mol% cholesterol + 20 mol% αT.

### CH<sub>2</sub> SYMMETRIC STRETCHING

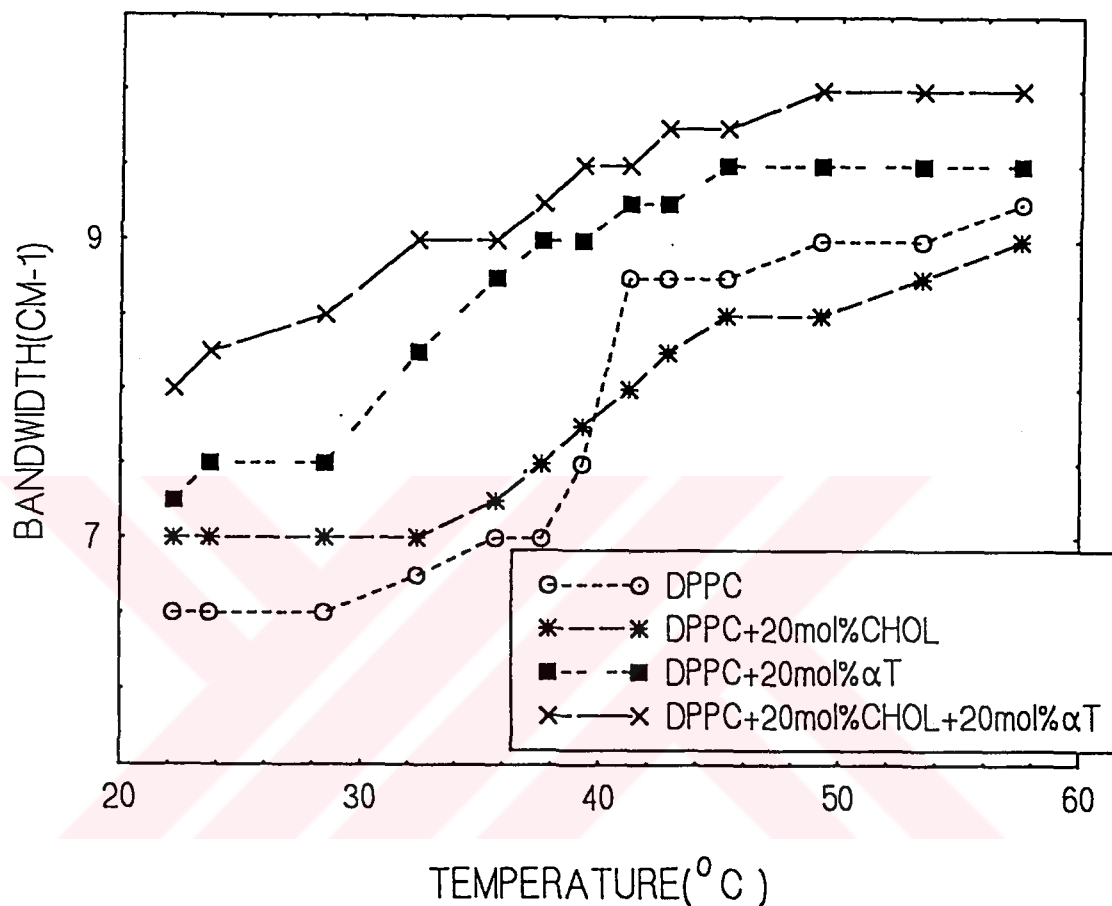


Figure 36. Temperature dependence of the bandwidth at 0.75x peak height of CH<sub>2</sub> symmetric stretching mode of DPPC multilamellar liposomes containing-0 mol% cholesterol + 0 mol% αT, 20 mol% cholesterol, 20 mol% αT, 20 mol% cholesterol + 20 mol% αT.

Fig.37 and Fig.38 reflect the effect of  $\alpha$ T concentration on cholesterol-containing multilamellar bilayers. In these figures the frequencies of the  $\text{CH}_2$  antisymmetric and symmetric stretching vibrations versus temperature are plotted for increasing  $\alpha$ T concentration in the system. As seen from Fig.37 and Fig.38 at any given temperature, the effect of cholesterol on DPPC liposomes decreases gradually with increasing  $\alpha$ T concentrations. Above the main phase transition temperature, addition of  $\alpha$ T to cholesterol-containing DPPC liposomes increases the frequency i.e., increases the number of gauche rotamers. At 20 mol%  $\alpha$ T concentration in 20 mol% cholesterol-containing liposomes effect of cholesterol on DPPC liposomes significantly decreases. Below the main phase transition temperature an increase in the number of gauche rotamers is observed with the increasing  $\alpha$ T concentration. Identical results are obtained for the  $\text{CH}_2$  symmetric stretching mode.



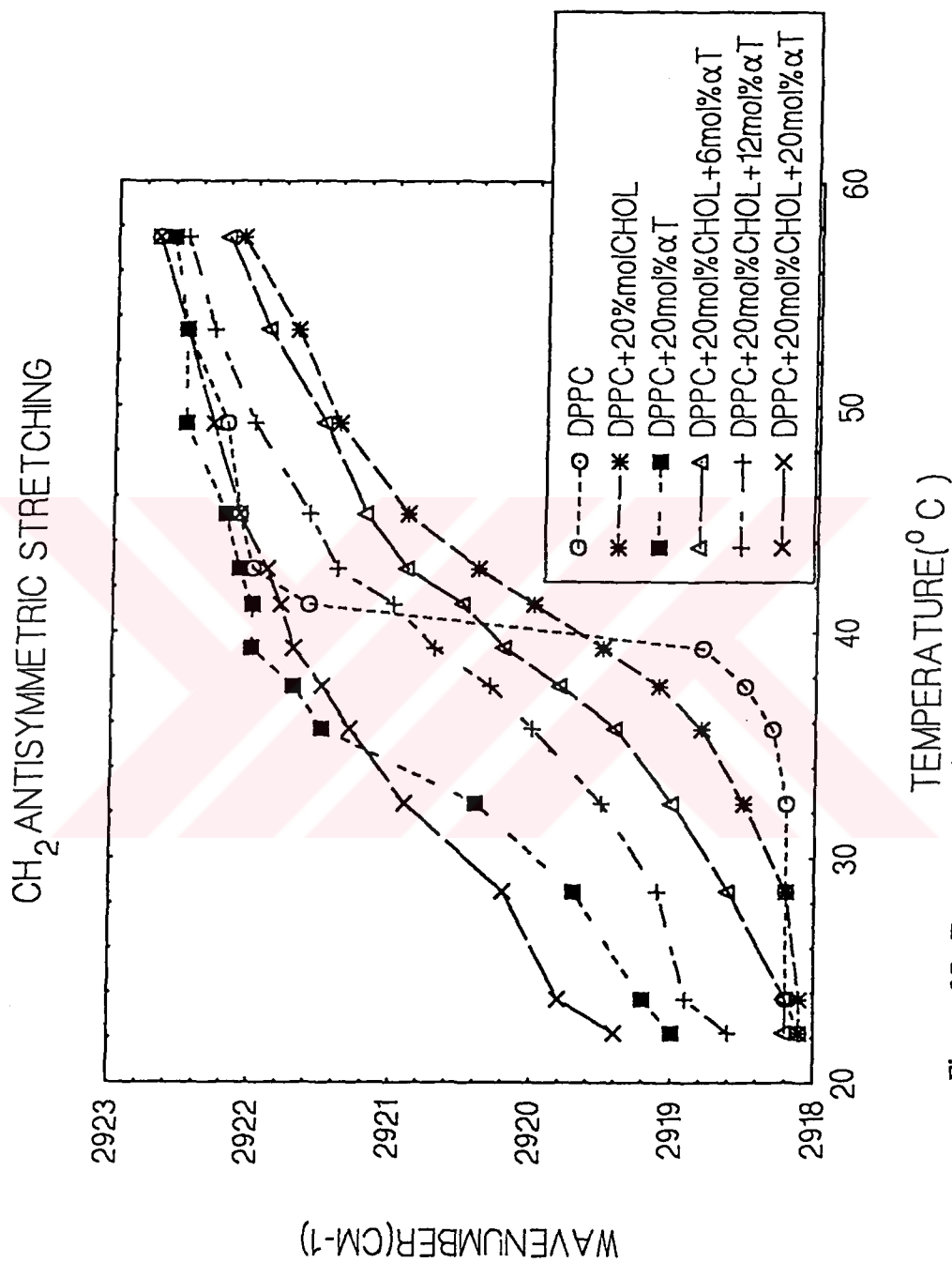


Figure 37. Temperature dependence of the CH<sub>2</sub> antisymmetric stretching mode of DPPC multilamellar liposomes containing-0 mol% cholesterol + 0 mol% αT, 20 mol% cholesterol, 20 mol% αT, 20 mol% cholesterol + 6 mol% αT, 20 mol% cholesterol + 12 mol% αT, 20 mol% cholesterol + 20 mol% αT.

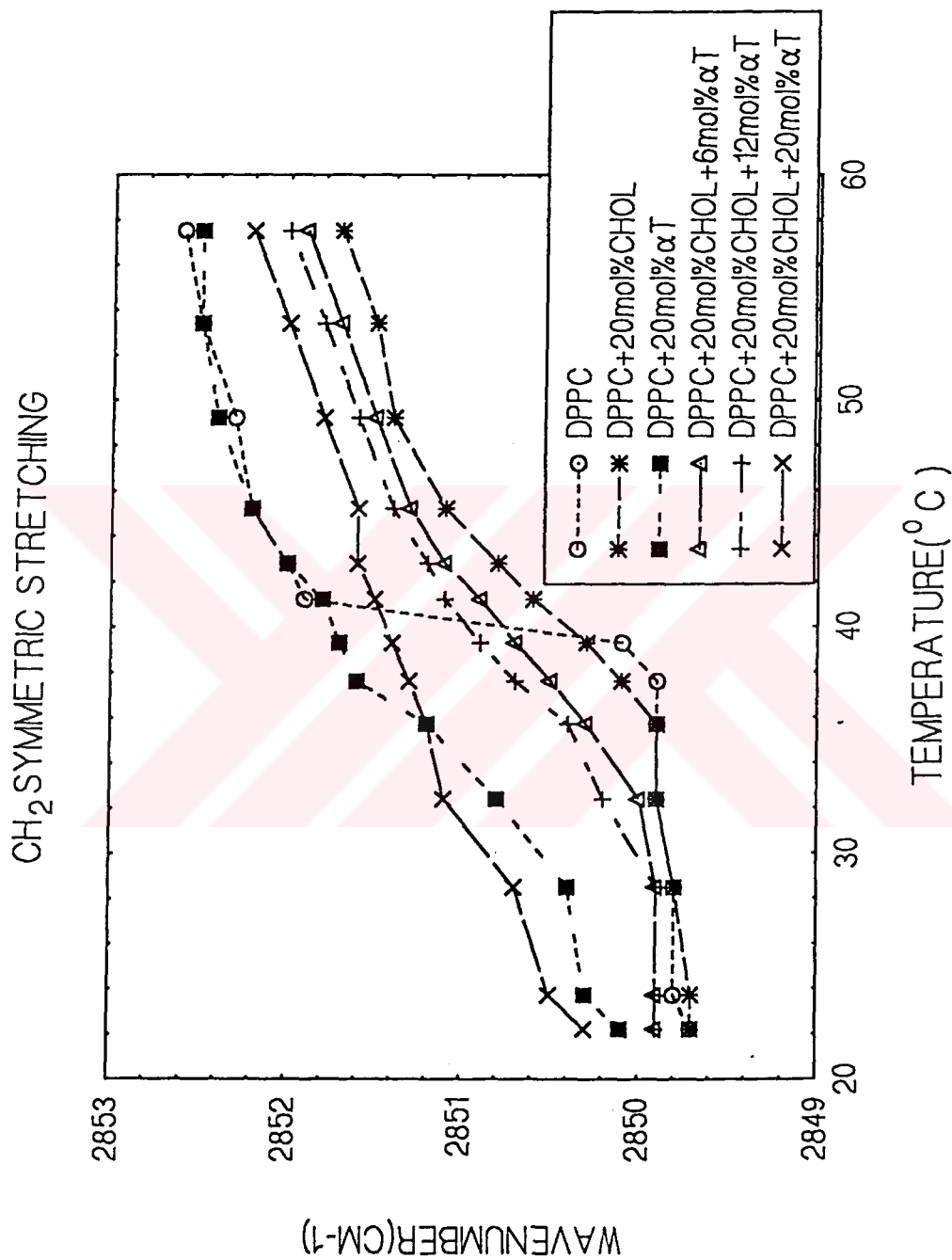


Figure 38. Temperature dependence of the CH<sub>2</sub> symmetric stretching mode of DPPC multilamellar liposomes containing 0 mol% cholesterol + 0 mol% αT, 20 mol% cholesterol, 20 mol% αT, 20 mol% cholesterol + 6 mol% αT, 20 mol% cholesterol + 12 mol% αT, 20 mol% cholesterol + 20 mol% αT.

The bandwidth of the CH<sub>2</sub> symmetric stretching mode at 0.75x peak height as a function of temperature is shown in Fig.39 for DPPC liposomes in the absence and in the presence of 20 mol% cholesterol and different mol% αT. Here again, the figure shows that the effect of increasing concentration of αT on 20 mol% cholesterol containing multilamellar liposomes is an increase in the bandwidth parameter as the temperature increases which implies an increase in acyl chain motion. Fig.39 also shows that the effects of αT on acyl chain motion and gauche/trans isomerization are dominant over those of cholesterol.



### CH<sub>2</sub> SYMMETRIC STRETCHING

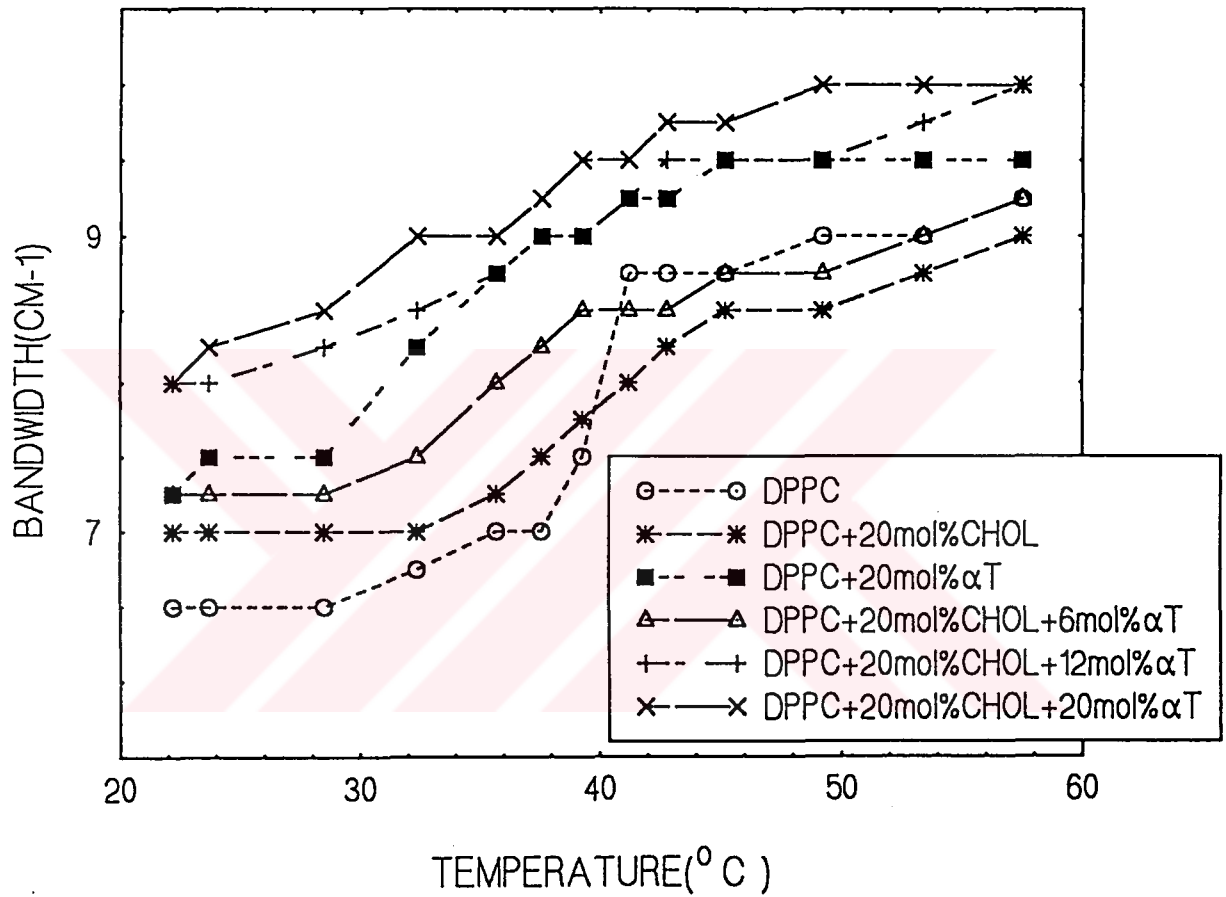


Figure 39. Temperature dependence of the bandwidth at 0.75x peak height of CH<sub>2</sub> symmetric stretching mode of DPPC multilamellar liposomes containing-0 mol% cholesterol + 0 mol% αT, 20 mol% cholesterol, 20 mol% αT, 20 mol% cholesterol+ 6 mol% α, 20 mol% cholesterol + 12 mol%αT, 20 mol% cholesterol + 20 mol% αT.

### 3.1.3.2 CH<sub>3</sub> Asymmetric Stretching

Fig.40 shows the temperature-dependence of CH<sub>3</sub> stretching band of pure and  $\alpha$ T and/or cholesterol containing DPPC liposomes. This band provides a monitor of the center of the bilayer. For DPPC, there is a monotonic increase in frequency with increasing temperature, reflecting increasing librational freedom of the acyl chains in the central area of the bilayer. The melting phenomena are not evident, reflecting the fact that the methyl mode is mechanically decoupled from the methylene mode and hence need not respond to the melting phenomena[73]. In the liquid crystalline phase the frequencies are nearly the same in the pure and  $\alpha$ T-containing DPPC systems, and a decrease in frequency is observed in cholesterol-containing DPPC system. In the gel phase,  $\alpha$ T increases, but cholesterol slightly decreases frequency. These results indicate that in the gel phase,  $\alpha$ T increases and cholesterol slightly decreases the dynamics of the deep interior of the bilayer. In the liquid crystalline phase cholesterol decreases the dynamics and the effect of  $\alpha$ T on dynamics is negligible. All these results are in agreement with the results on the CH<sub>2</sub> stretching bands. With the addition of  $\alpha$ T into cholesterol-containing liposomes, an additional decrease in frequency is observed both in the gel and in the liquid crystalline phase, indicating additional stiffness. This result is different from the result on the CH<sub>2</sub> stretching bands, which implies that effect of  $\alpha$ T on cholesterol-containing liposomes is different for different parts of the membrane.

### CH<sub>3</sub> ANTISYMMETRIC STRETCHING

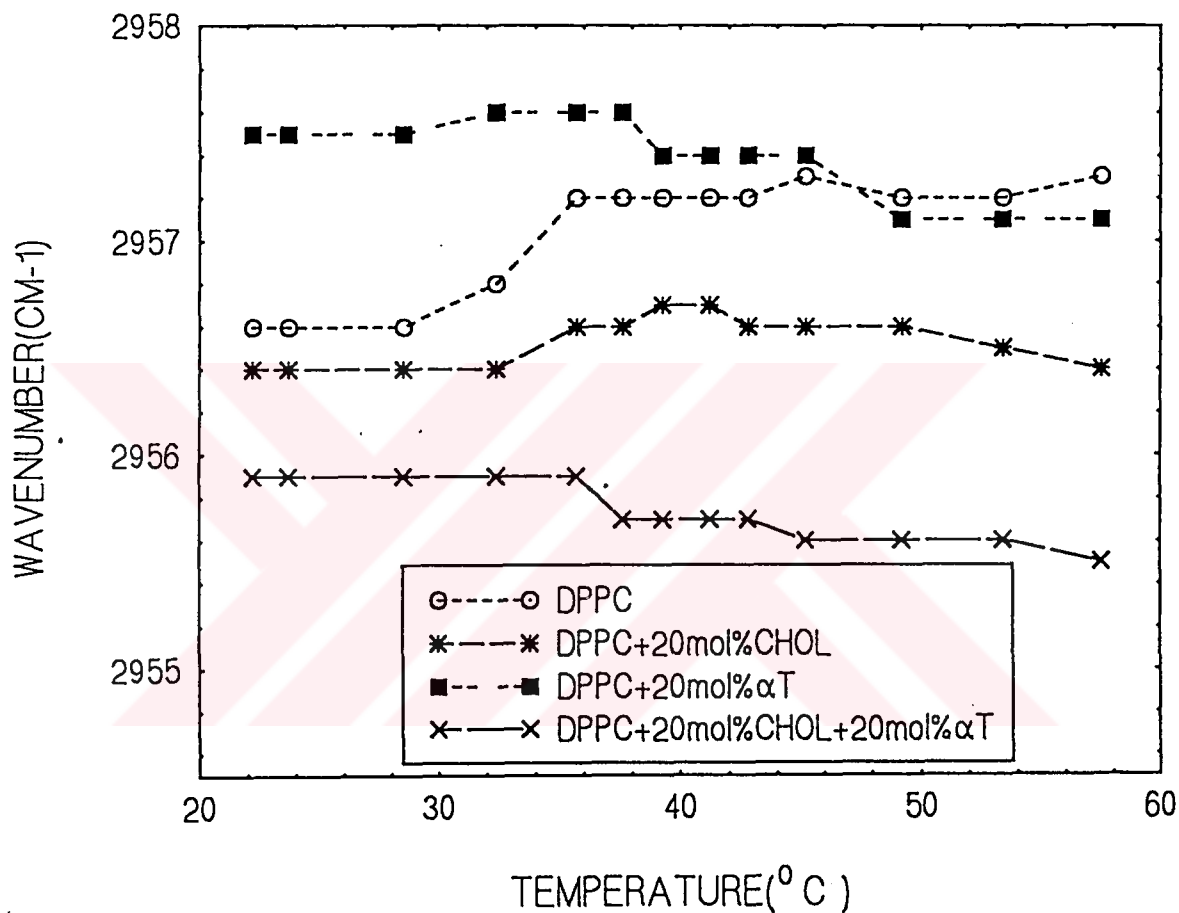


Figure 40. Temperature dependence of the frequency of the asymmetric CH<sub>3</sub> stretching mode of DPPC multilamellar liposomes containing 0 mol% cholesterol + 0 mol% αT, 20 mol% cholesterol, 20 mol% αT, and 20 mol% cholesterol + 20 mol% αT.

### 3.1.3.3 CH<sub>2</sub> Scissoring Mode

Fig.41 shows the infrared spectra of the CH<sub>2</sub> scissoring band of DPPC multibilayers at different temperatures. The spectrum consists of a strong narrow band at 1468 cm<sup>-1</sup>, superimposed on several weak bands. The 1468 cm<sup>-1</sup> band results from the scissoring mode of the methylene groups in all-trans acyl chains in which the phase difference between adjacent group is 180°, while the underlying bands arise from scissoring modes of glycerol and choline methylenes and methyl bending modes [69]. Although the CH<sub>2</sub> scissoring mode is relatively insensitive to temperature variations in the fluid phase, the main transition produces a large decrease in the intensity of the CH<sub>2</sub> scissoring bands along with an increase in bandwidth as seen in Fig.41. As in the case of the C-H stretching bands, the effect is interpreted as arising from the conformational disorder introduced at T<sub>m</sub>. X-ray diffraction studies of DPPC in gel state have shown that at temperatures between the pretransition (T<sub>p</sub>) and T<sub>m</sub>, the acyl chain packing is hexagonal and that below T<sub>p</sub>, a progressive distortion of the lattice occurs which results in a distorted hexagonal subcell [78,79]. Infrared spectra suggest that this distorted hexagonal subcell is orthorhombic-like (ortho hexagonal)[69]. Thus the pretransition can be characterized as a transition from an orthorhombic-like subcell at temperatures below T<sub>p</sub> to one which is characterized by lack of interchain coupling of the CH<sub>2</sub> scissoring modes at temperatures above T<sub>p</sub>. Between T<sub>p</sub> and T<sub>m</sub> the packing is hexagonal, where the acyl chains are generally viewed as behaving like rigid rotors, independently of each other. In fact, NMR studies [80,81] found that at temperature below T<sub>p</sub>, the motional regime in the gel phase of DPPC is such that neighbouring chains make an oscillating disrotatory motion, while above T<sub>p</sub>, a quasi-free chain rotation takes place. These results agree with the infrared and earlier X-ray interpretations[79,82,83]. Fig 42 shows acyl chain crystal-packing patterns[84].

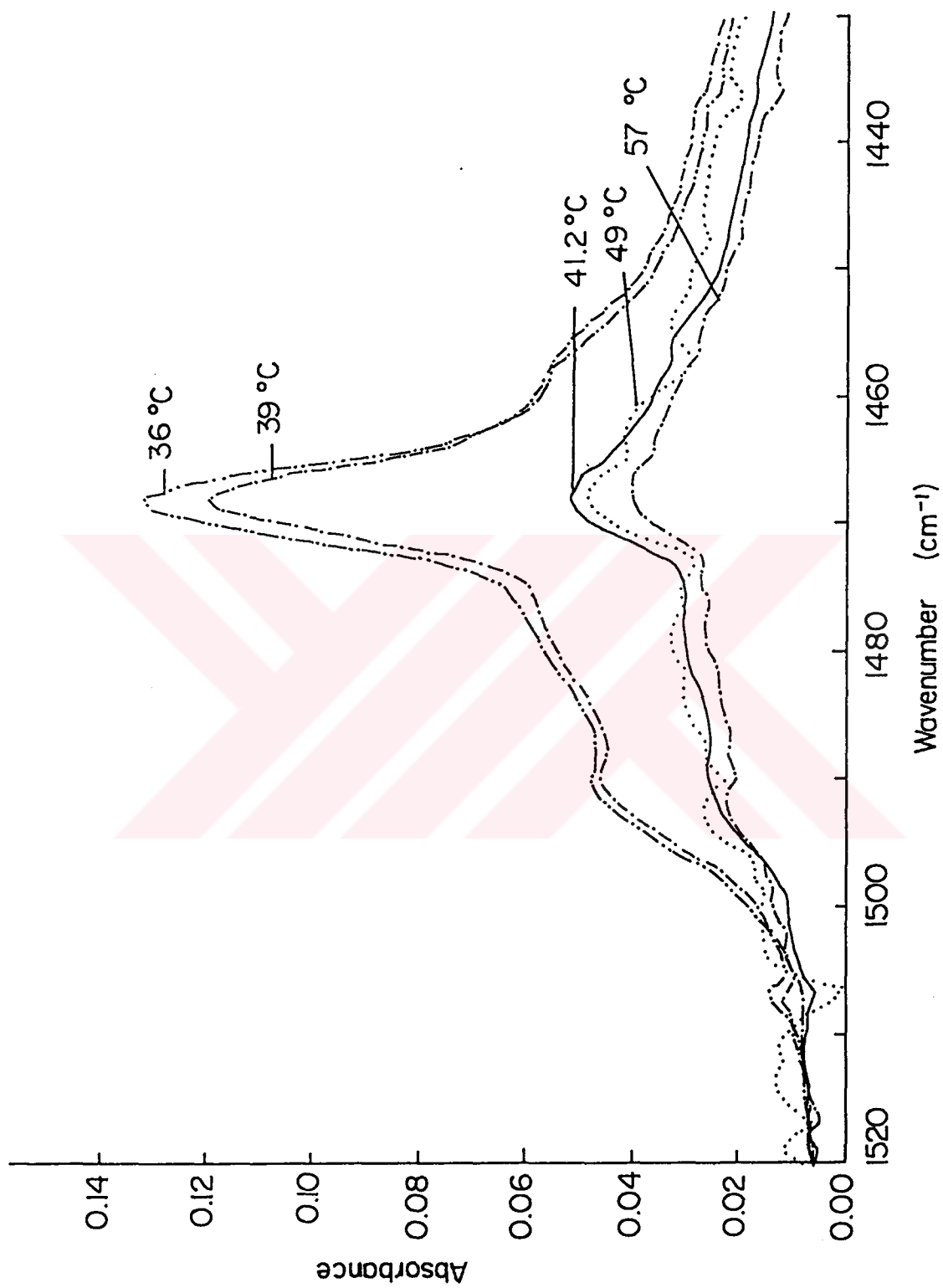


Figure 41. Infrared spectra of the CH<sub>2</sub> scissoring band of DPPC multibilayers at different temperatures.



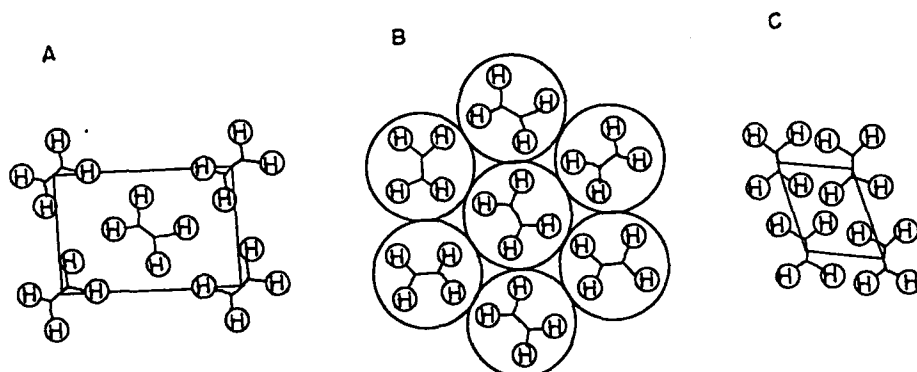


Figure 42. Acyl chain crystal-packing patterns: A, orthorhombic or monoclinic; B, hexagonal and C, triclinic. In all cases, the long axes of the chains are projecting from the page. In the case of hexagonal packing, the torsion about the long axes is such that the orientations of chains relative to each other at a given moment are random

Fig. 43 shows the infrared spectra of the  $\text{CH}_2$  scissoring band of DPPC multibilayers, pure and containing 20 mol%  $\alpha\text{T}$  and /or cholesterol at  $32^\circ\text{C}$ . As can be seen, the inclusion of cholesterol does not make any change in the bandwidth, but the inclusion of  $\alpha\text{T}$  increases the width of the band. When both  $\alpha\text{T}$  and cholesterol are present in the system, an additional increase in bandwidth is observed, suggesting an increase in the conformational disorder and chain rotation in the gel phase.

Fig.44 and 45 show that the infrared spectra of the same system at  $39^\circ\text{C}$  and  $49^\circ\text{C}$ , respectively. Fig.45 shows that  $\alpha\text{T}$  again exhibits a dominant effect on cholesterol containing DPPC multilamellar liposomes. As seen from the figures, cholesterol decreases the bandwidth in the liquid crystalline phase. The figures also indicate that the presence of  $\alpha\text{T}$  individually or with cholesterol cause substantial difference in the shape of the  $\text{CH}_2$  scissoring band counters.

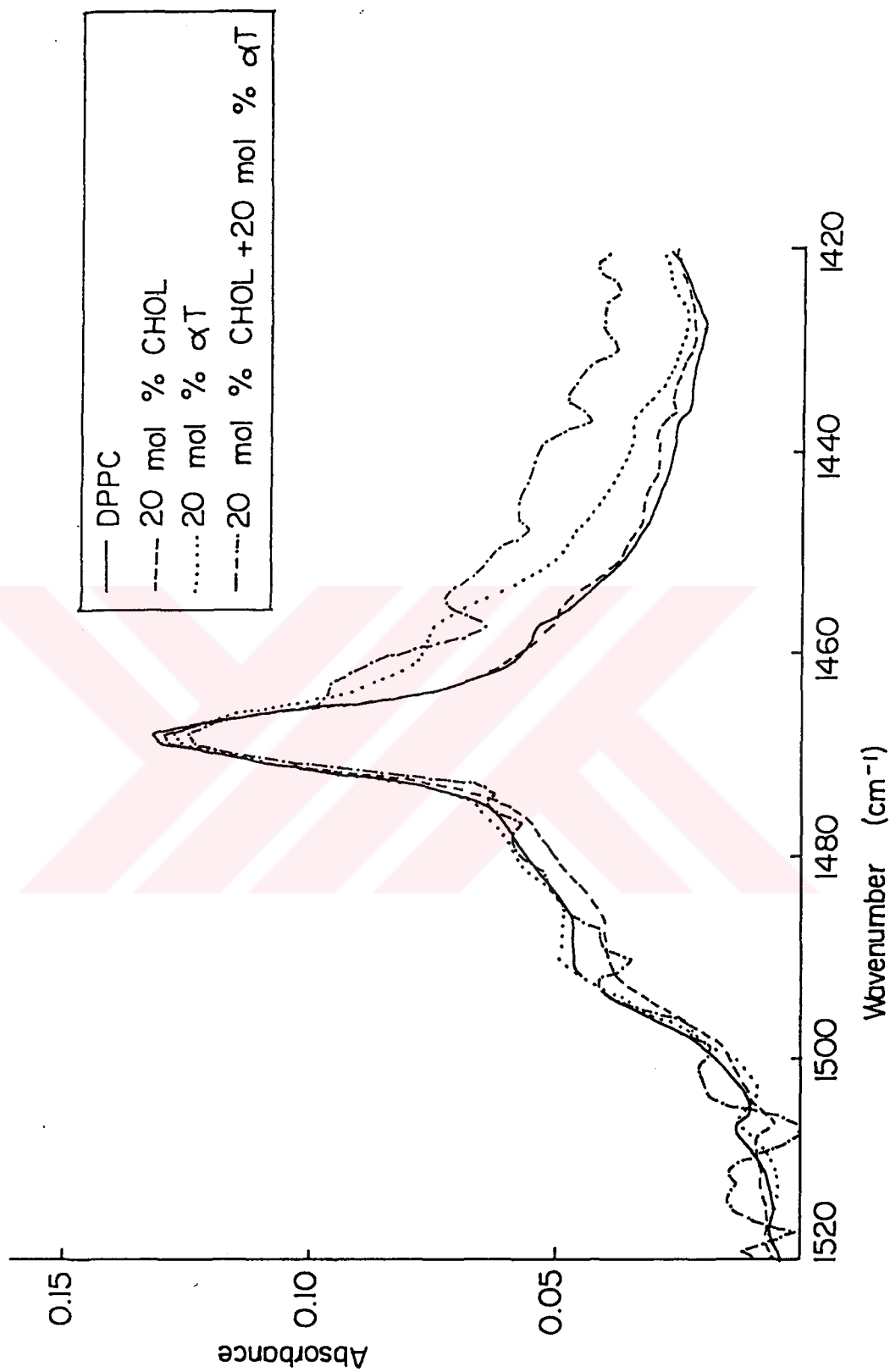


Figure 43. CH<sub>2</sub> scissoring mode of spectra of DPPC multibilayer liposomes containing 0 mol% cholesterol + 0 mol% αT, 20 mol% cholesterol, 20 mol% αT, 20 mol% cholesterol + 20 mol% αT at 32°C.

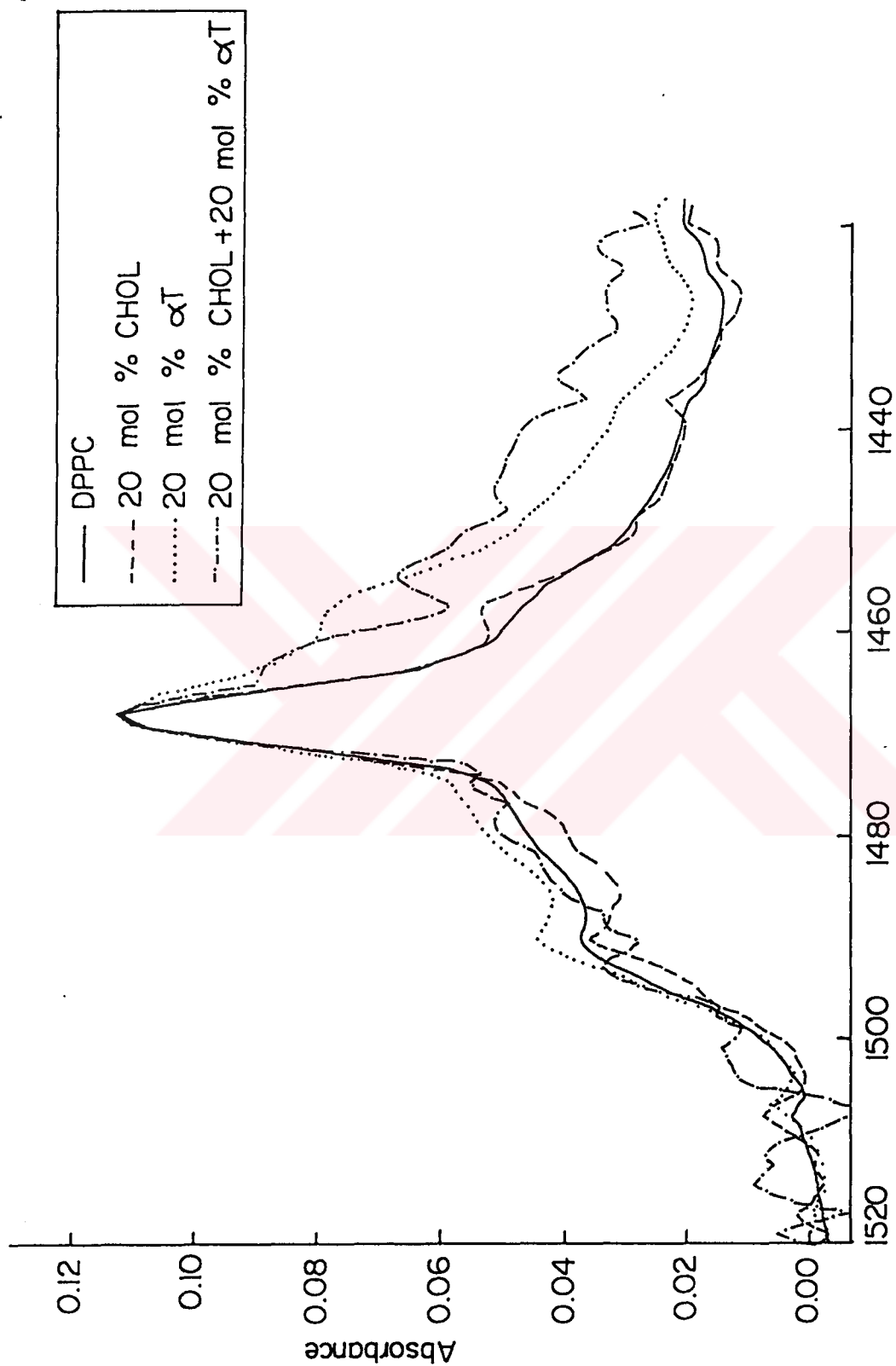


Figure 44. CH<sub>2</sub> scissoring mode of spectra of DPPC multilayer liposomes containing 0 mol% cholesterol + 0 mol% αT, 20 mol% cholesterol, 20 mol% αT, 20 mol% cholesterol + 20 mol% αT at 39°C.

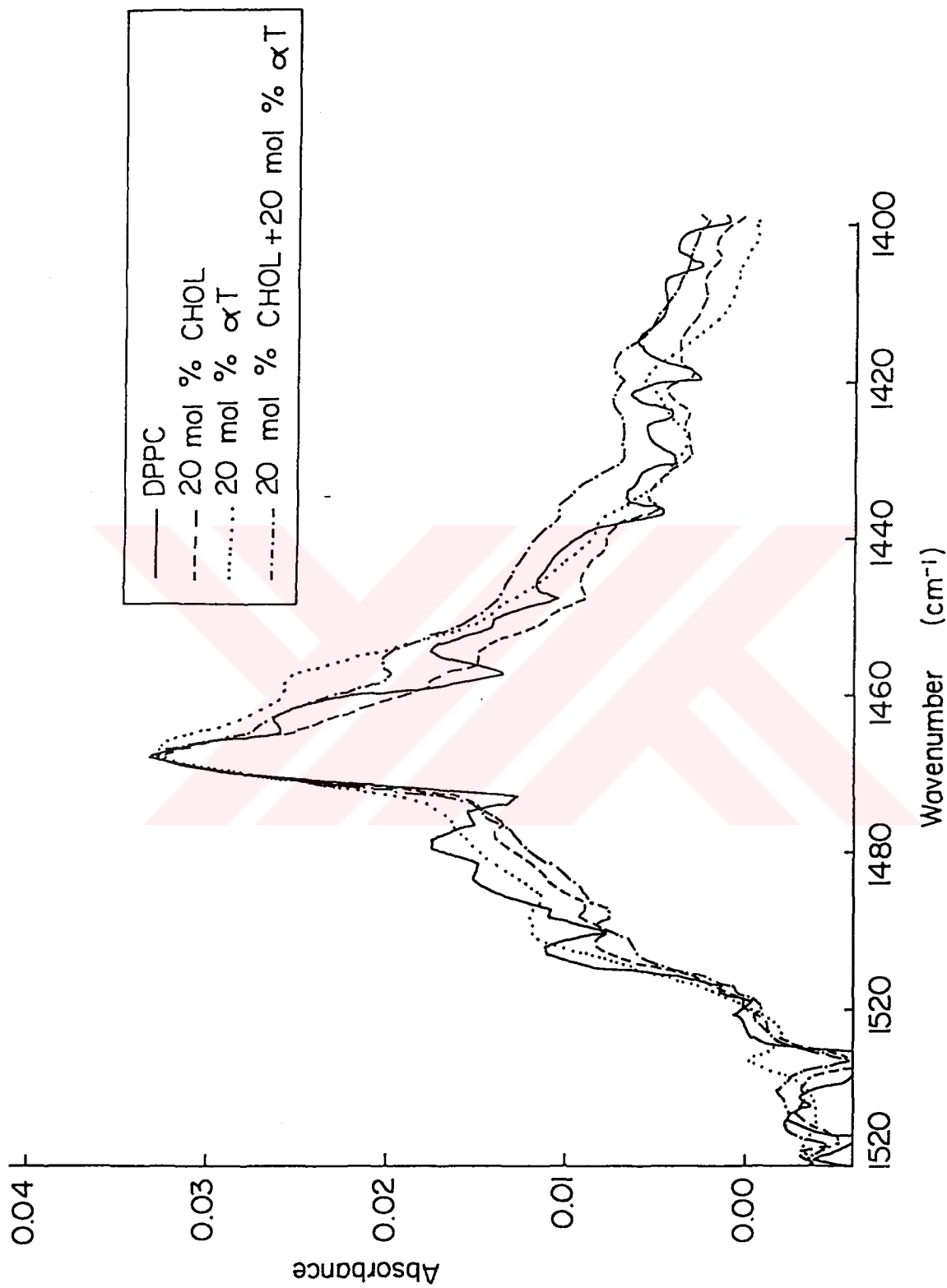


Figure 45.  $\text{CH}_2$  scissoring mode of spectra of DPPC multilayer liposomes containing 0 mol% cholesterol + 0 mol%  $\alpha$ T, 20 mol% cholesterol, 20 mol%  $\alpha$ T, 20 mol% cholesterol + 20 mol%  $\alpha$ T at 49°C.

### 3.1.3.3 Head Group Vibration: C=O Stretching Mode

Fig.46 shows the infrared spectra of the C=O stretching mode of DPPC at different temperatures. The band contours are nearly symmetric and the peak maximum is observed at around  $1735\text{ cm}^{-1}$ . As the temperature is increased this band decreases in intensity and an abrupt decrease in peak height is observed at the main phase transition temperature.

Fig.47 shows the infrared spectra of C=O stretching mode for pure,  $\alpha$ T and/or cholesterol-containing liposomes in the main phase transition region. The frequencies of the peaks follow the order: cholesterol > DPPC >  $\alpha$ T >  $\alpha$ T+cholesterol. Similar results are obtained for the gel and for the liquid crystalline phase which indicate that  $\alpha$ T makes hydrogen bonding with the C=O region of DPPC. We did not observe hydrogen bonding formation between cholesterol and DPPC. The presence of cholesterol in the  $\alpha$ T-membrane system increases the strength of hydrogen bonding. We do not have any explanation for this result.

Fig.48 shows the variation of C=O vibrational frequency as a function of temperature. An abrupt decrease is observed around  $41^\circ\text{C}$  in the DPPC curve which monitors the main phase transition temperature. As seen from the figure, the effects of  $\alpha$ T and cholesterol are opposite both in the gel and in the liquid crystalline phase.  $\alpha$ T decreases, but cholesterol increases the frequency in both. When both of them are present in the system with the same mol%, the frequency decreases more in the gel phase. In the liquid crystalline phase, curves of DPPC liposomes containing only  $\alpha$ T and both  $\alpha$ T and cholesterol overlap completely, indicating that the system behaves as if there is no cholesterol in the system.

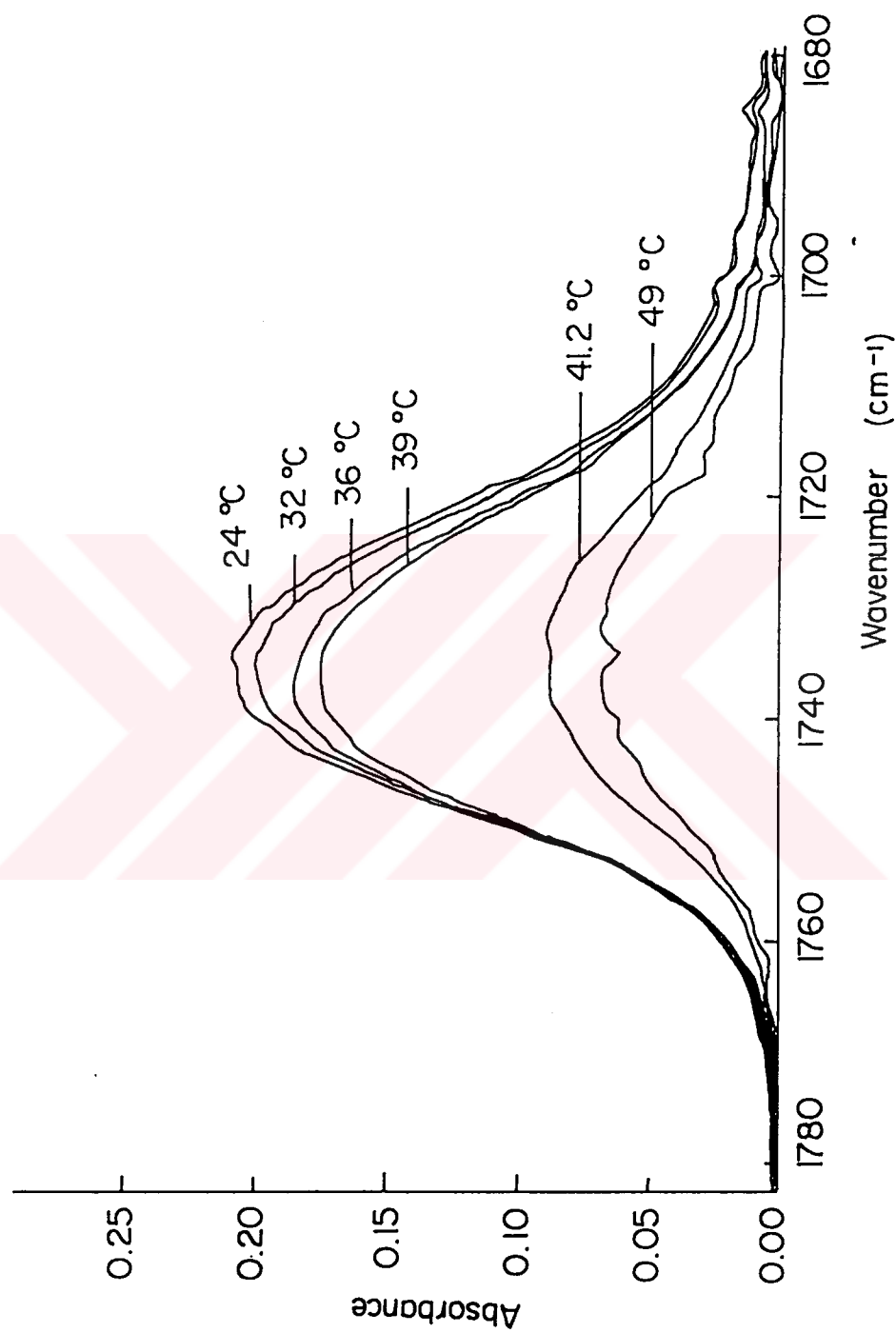


Figure 46. Infrared spectra in the C=O stretching region of DPPC multilamellar liposomes at six temperatures (24, 32, 36, 39, 41.2, and 49°C) in decreasing intensity.

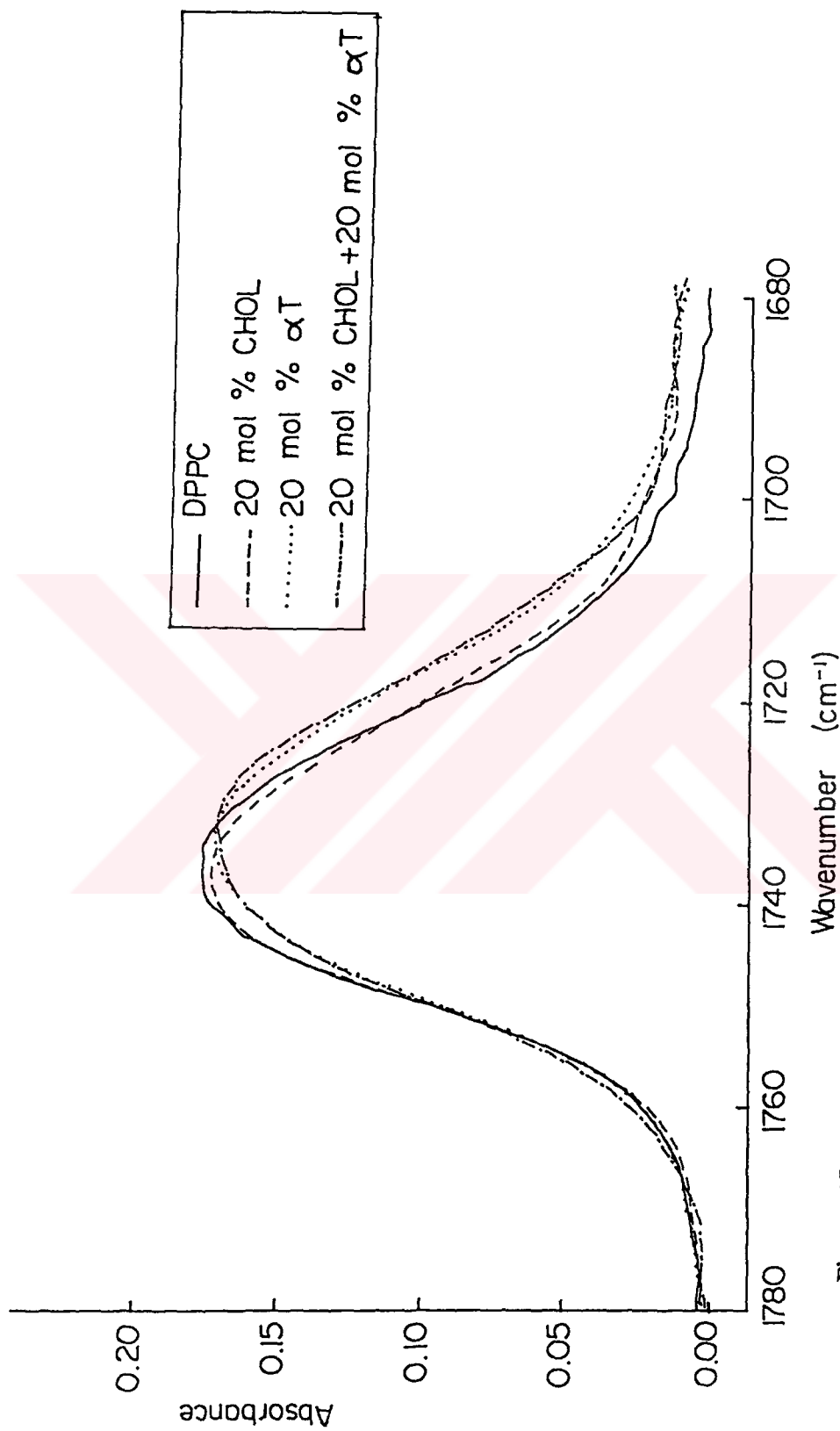


Figure 47. Infrared spectra in the C=O stretching region of DPPC multilamellar liposomes containing 0 mol% cholesterol + 0 mol%  $\alpha$ T, 20 mol% cholesterol, 20 mol%  $\alpha$ T, 20 mol% cholesterol + 20 mol%  $\alpha$ T at 42°C.

C=O STRETCHING

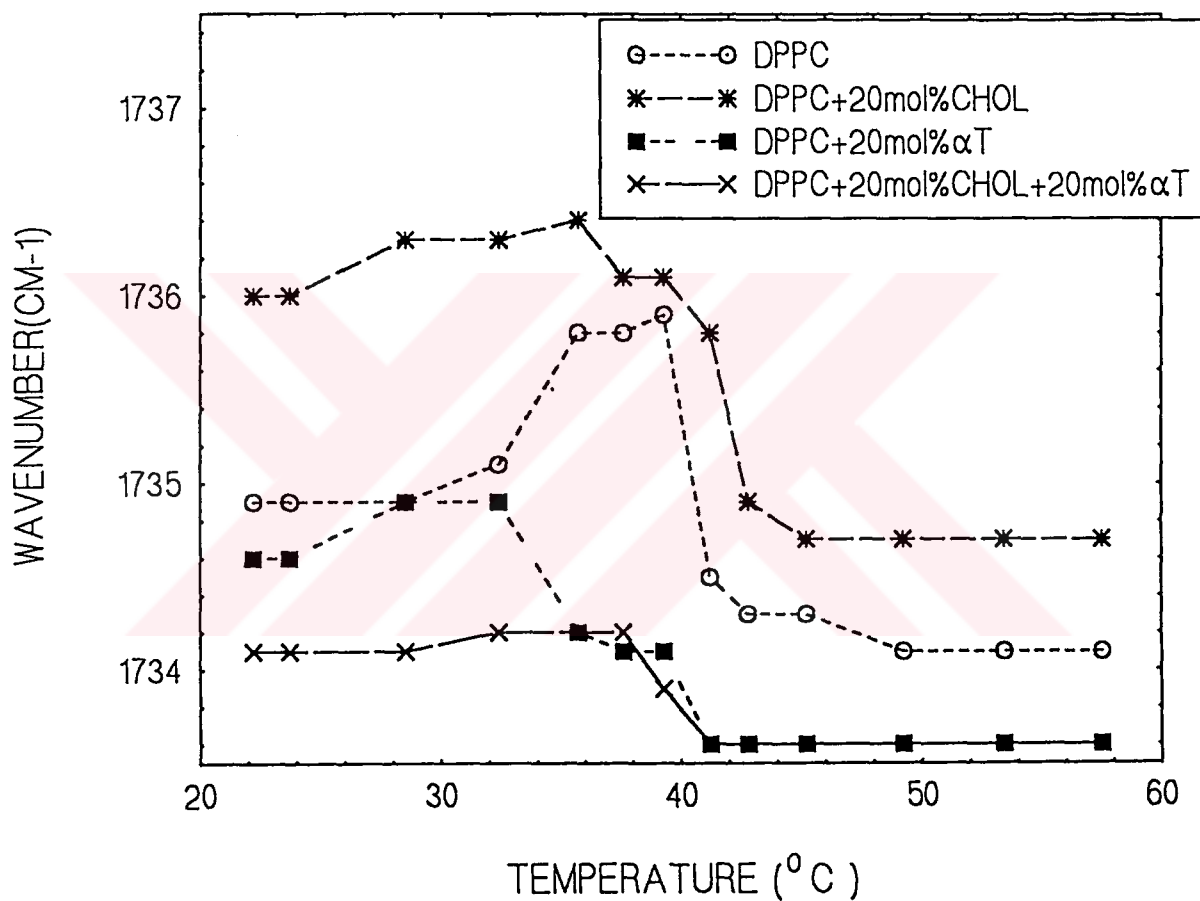


Figure 48. Temperature dependence frequency changes of C=O stretching mode for DPPC multilamellar liposomes containing 0 mol% cholesterol + 0 mol% αT, 20 mol% cholesterol, 20 mol% αT, and 20 mol% cholesterol + 20 mol% αT.



Fig.49 shows the variation of C=O stretching bandwidth as a function of temperature. It is observed that below the main phase transition temperature, the effect of cholesterol is negligible. However, a drastic increase in bandwidth is observed with the addition of  $\alpha$ T in DPPC liposomes. When both  $\alpha$ T and cholesterol are present in the system, bandwidth increases synergistically. In the liquid crystalline phase bandwidth increases by the same amount with the addition of cholesterol and  $\alpha$ T separately into DPPC liposomes. Again a synergistic effect is observed with the addition of both  $\alpha$ T and cholesterol into the system. These results indicate that the joint occurrence of  $\alpha$ T and cholesterol makes a drastic effect on librational and torsional motions of the interfacial region.



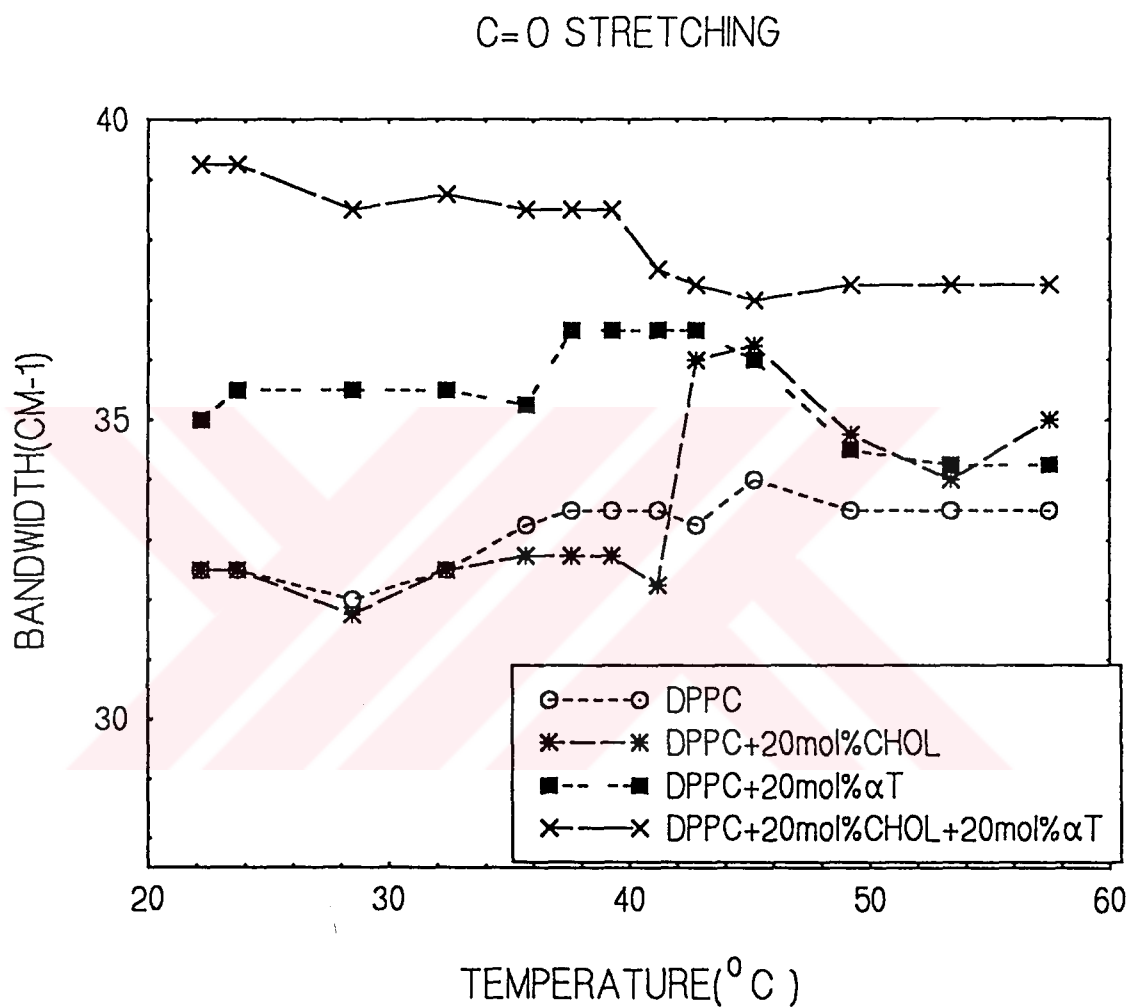


Figure 49. Temperature dependence of the bandwidth at 0.75x peak height of C=O stretching mode of DPPC multilamellar liposomes containing 0 mol% cholesterol + 0 mol%  $\alpha$ T, 20 mol% cholesterol, 20 mol%  $\alpha$ T, 20 mol% cholesterol + 20 mol%  $\alpha$ T.

## CHAPTER IV

### CONCLUSION

From all these results of the present study; it is clear that effect of  $\alpha$ T on DPPC liposomes is more profound than cholesterol. It is also observed that  $\alpha$ T decreases or diminishes the interaction of cholesterol with phospholipid membranes. For the interpretation of the results it will be useful to remember the previous studies related to the location of cholesterol and  $\alpha$ T in the lipid membranes [11,56,85-87].

The polar hydroxyl group of cholesterol at C-3 is located in the aqueous interface and for this reason the polar head group should be localized within a reasonably close lateral distance to the membrane surface. The long axis of the cholesterol molecule is thus perpendicular to the plane of the membrane, and parallel with the acyl chains of conjugated membrane lipids [85]. The cholesterol ring nucleus configuration has been shown by X-ray analysis to be all-trans-anti, which leads to a flat planar structure with a thickness of around 2 Å [86]. Different conformations of a phospholipid and cholesterol molecules were proposed; and energies associated with the conformations were calculated [11]. For  $\alpha$ T, it is known that the 5-CH group in the chromonal nucleus is very close to the surface of membrane [87], whereas its hydrocarbon chain interacts hydrophobically with acyl chains of membrane phospholipid [56]. The average depth to which the head group of  $\alpha$ T is embedded in the membrane is not known to date.

There is wide range of contradictory published results obtained by various experimental techniques about the hydrogen bonding between cholesterol and phospholipids. Previously Brockerhoff [25] suggested that hydrogen bonding between cholesterol's  $\beta$ -OH and the carbonyl groups of phospholipids is responsible for cholesterol's unique effects on lipid bilayer membranes. However other studies [28,29] have shown that the carbonyl oxygens of phosphatidylcholine are not necessary for cholesterol interactions. The possibility of hydrogen bonding between the sterol hydroxyl and the phosphate region of lipid head group was excluded by  $^{31}\text{P}$  NMR spectroscopic studies [22]. Presti et al. [30] proposed that cholesterol forms associations with phospholipids with stoichiometries of both 1:1 and 1:2. A hydrogen bond between the  $\beta$ -OH of cholesterol and the glycerol ester oxygen of phospholipid is suggested for tight binding in a 1:1 complex. A second phospholipid molecule is loosely associated with the complex, probably simply by van der Waals interactions, to form domains of 1:2 stoichiometry, which may coexist with pure phospholipid domains. Interfacial boundary phospholipid separates these two domains. At about 20 mol% cholesterol content, free phospholipid domains disappear and interfacial phospholipid is maximal. The existence of domain formation in cholesterol-containing PC membranes, such as cholesterol rich and cholesterol poor, was also proposed by Plachy et al. [31] and Recktenwald and McConnell [32]. The functional role of cholesterol within the membrane is not understood clearly because of the complexity of these systems.

Vitamin E has been studied extensively. It is not precisely defined whether the hydrogen bonding occurs between the hydroxyl group  $\alpha$ T and the ester carbonyl group of the lipid [25, 88] or with one of the oxygens in phosphate group [34]. Lai et al. showed that the hydroxyl group of tocopherol is more important than the hydroxyl group of cholesterol in influencing their interactions with phospholipids [89]. Severcan

and Cannistraro provided direct ESR evidence that two distinct phases are induced by  $\alpha$ T in phospholipid membranes in the liquid crystalline phase, which are named as  $\alpha$ T poor and  $\alpha$ T rich phases[8]. Reorientational dynamics of the spin probe has a different time scale in the two phases[8]. No information about the existence of subphases is yet available in the gel phase and also there is no phase diagram proposed yet for the binary mixture of  $\alpha$ T and phospholipids.

With our present knowledge, it is quite difficult to account for the reasons for the different joint effect of  $\alpha$ T and cholesterol in the gel and in the liquid crystalline phases. In the triple mixture of cholesterol- $\alpha$ T-DPPC, pair interactions such as cholesterol-cholesterol, cholesterol-phospholipid, cholesterol- $\alpha$ T, etc. should be considered for each phase. It can be concluded that in the gel phase cholesterol or  $\alpha$ T increases fluidity by the same amount and their joint effect is additive. Dominant behavior of  $\alpha$ T is also observed in the ordering effect. In the light of present and previous studies, we can speculate that in the gel phase insertion of  $\alpha$ T and cholesterol molecules into the bilayer could disrupt the tight packing of the phospholipid chains, mainly governed by Van der Waals force; cholesterol-lipid and  $\alpha$ T-lipid interactions might become stronger than the other membrane component's pair interactions; thus an increase of both disordering and fluidity could result in the bilayer.

In the liquid crystalline phase, it can be imagined that packing interactions between the hydrocarbon chains are now less important. Although there is not any model proposed so far for  $\alpha$ T-lipid interactions,  $\alpha$ T may also form complexes with fatty acids in the lipid bilayers as proposed earlier [52,90]. An explanation for the present results related to the disordering effect of  $\alpha$ T on cholesterol-containing liposomes is that  $\alpha$ T may be inserted between phospholipid and cholesterol; thus it

decreases the interaction of cholesterol chains with phospholipid acyl chains, which may increase the probability for trans-gauche isomerisation and a decrease in the bilayer ordering would be registered .

In summary; data presented here show that  $\alpha$ T diminishes or decreases the interaction of cholesterol with phospholipid membranes by forming a suitable complex and stronger interaction. It is also known that, although the processes are poorly understood, cholesterol can spontaneously desorb from membranes and transfer between membranes [91,92]. With all this information given above in mind, the following speculation can be made: Excess content of  $\alpha$ T causes cholesterol to be released from membrane. In the liquid crystalline and in the gel phase, cholesterol can be transferred through the high cholesterol content (cholesterol rich) phase [33]; in this phase at  $\approx 20$  mol% cholesterol it was proposed that there is a percolation process: the cholesterol rich areas suddenly become connected, forming a network that extends over the entire bilayer [93] which allows fast diffusion to occur. The importance of phase domains in mediation of molecular transport is reinforced by kinetic data [91,92] which define two different pools of cholesterol : one of them which is a major portion of cholesterol and is exchangeable, and the other one which is a minor portion and is nonexchangeable. These studies also indicated that the cholesterol desorption rate from membranes may be faster than that previously believed. With the present knowledge it is very difficult to make any speculation about the role of vitamin E rich domains in sterol transport, where enhanced diffusion processes associated with a percolation effect was also proposed [8]. At this moment we do not know the physiological importance of the present results and their relevance to health benefits. The concentrations of  $\alpha$ T used (20 mol%) in the experiments are much higher than physiological levels of vitamin E (0.1-0.2 mol%). The existence of phase domains is also much less clear for biologically relevant

phosphatidylcholines. Much more theoretical and experimental work with model and natural membranes is clearly needed to establish a precise structure-function relationship.



## REFERENCES

- [1] C. R. Cantor and P. R. Schimmel, 1980. Biophysical Chemistry Part I: The conformation of Biological Macromolecules, W. H. Freeman and Co., New York.
- [2] M. Jain, 1988. Introduction to Biological Membranes, John Wiley and Sons Inc., New York.
- [3] M.P. Sheetz and S. I. Chan, Biochemistry, **11**, 4573 (1972).
- [4] P. L. Yeagle et al., Proc. Natl. Acad. Sci., **72**, 3477 (1975).
- [5] F. Severcan and S. Cannistraro, Chem. Phys. Lipids, **53**, 17 (1990).
- [6] S. R. Wassal et al., Chem. Phys. Lipids, **60**, 29 (1991).
- [7] Y. J. Suzuki et al., Biochemistry, **32**, 10692 (1993).
- [8] F. Severcan and S. Cannistraro, Chem. Phys. Lipids, **47**, 129 (1988).
- [9] F. Severcan and S. Canistraro, Biosci. Repots, **9**, 489 (1989).
- [10] E. Serbinova et al., Free Radic. Biol. Med., **10**, 263 (1991).
- [11] H. L. Scott and W. S. McCullough, Biophys. J., **64**, 1398 (1993).
- [12] G. Deinum et al., Biochemistry, **27**, 852 (1988).
- [13] C. Sandorfy and T. Theophanides (eds.), 1984. Spectroscopy of Biological Molecules, D. Rediel Publishing Co., Dordrecht, Holland.
- [14] H. H. Fuldner, Biochemistry, **20**, 5707 (1984).
- [15] M. J. Ruocco and G. G. Shipley, Biochim. Biophys. Acta., **684**, 59 (1982).
- [16] M. J. Ruocco and G. G. Shipley, Biochim. Biophys. Acta., **691**, 309 (1982).
- [17] H. M. McConnell, P. Devaux, and C. Scandella, 1972. Lateral Diffusion and Phase Separations in Biological Membranes, In Membrane Fusion (C. F. Fox, ed), Academic Press, New York.



- [18] H. Lecuyer and D. G. Devirchian, J. Mol. Biol., 45, 39 (1969)
- [19] T. N. Estep et al., Biochemistry, 18, 2112 (1979)
- [20] B. R. Copeland and H. M. McConnel, Biochim. Biophys. Acta, 599, 95 (1980).
- [21] B. De Kruijff et al., Biochim. Biophys. Acta, 307, 1 (1973).
- [22] P. L. Yeagle, Acc. Chem. Res., 11, 321 (1978).
- [23] E. Oldfield and D. Chapman, FEBS Lett., 23, 285 (1972).
- [24] R. A. Demel, K. R. Bruckdorfer, L. L. M. Van Deenen, Biochim. Biophys. Acta, 255, 321 (1972).
- [25] H. Brockerhoff, Lipids, 9, 645 (1974).
- [26] C. H. Huang, Nature, 259, 242 (1976).
- [27] C.H. Huang, Lipids, 12, 348, (1977).
- [28] S. Clejan et al., Biochemistry, 18, 2118 (1979).
- [29] S. Fowlerbush, H. Levin, and I. W. Levin, Chem. Phys. Lipids, 27, 101 (1980).
- [30] F. T. Presti, R. J. Pace, and S.I. Chen, Biochemistry, 21, 3831 (1982).
- [31] W. Plachy et al., Bull. Mag. Res., 2, 399 (1981).
- [32] D. J. Recttenwald and H. M. McConnell, Biochemistry, 20, 4505 (1981).
- [33] M. R. Vist and J. H. Davis, Biochemistry, 29, 451 (1990).
- [34] F. Severcan et al., Xth Int. Conf. on Mag. Res. in Biol. Sys., Stanford, CA, USA (1982).
- [35] F. Severcan and W. Plachy, 1984. Application of Physics to Medicine and Biology, (Eds.: Z. Bajzer, P. Baxa, and C. Franconi), World Scientific Publ. Co.
- [36] L. J. Machlin, 1984. Handbook of Vitamins: Nutritional, Biochemical and Clinical Aspects, Marcel Dekker, Inc., New York.
- [37] V. E. Kagan, E. A. Serbinova, and L. Packer, Arch. Biochem. Biophys., 280, 33 (1990).
- [38] G. W. Burton and K.U. Ingold, J. Am. Chem. Soc., 103, 6472 (1985).
- [39] A. Constantinescu, D. Han, and L. Packer, J. Biol. Chem., 268, 10906 (1993).

- [40] L. R. C. Barclay and K. U. Ingold, J. Am. Chem. Soc., **103**, 6478 (1981).
- [41] R.W. Fessenden, A. Hitachi and V. Nagarajan, J. Phys. Chem., **88**, 107 (1984).
- [42] T. Doba, G. W. Burton, and K. U. Ingold, Biochim. Biophys. Acta, **835**, 298 (1985), and references cited therein.
- [43] L. Packer and S. Landvik, Ann. N. Y. Acad. Sci., **570**, 1 (1989).
- [44] A. L. Tappel, Ann. N. Y. Acad. Sci., **203**, 12 (1972).
- [45] G. W. Grams and K. Eskins, Biochemistry, **11**, 606 (1972).
- [46] J. A. Lucy, Ann. N. Y. Acad. Sci., **203**, 3 (1972).
- [47] A. T. Diplock and J. A. Lucy, FEBS Lett., **29**, 205 (1973).
- [48] L. V. Tabidze et al., Bull. Exp. Biol. Med. (U.S.S.R.), **11**, 48 (1983).
- [49] A. M. Katz et al., FEBS Lett., **67**, 207 (1976).
- [50] D. Kunze et al., Eur. J. Clin. Invest., **56**, 471 (1975).
- [51] M. Tada, T. Yamamoto, and Y. Tonomura, Physiol. Rev., **58**, 1 (1978).
- [52] A. N. Erin et al., Biochim. Biophys. Acta, **774**, 96 (1984).
- [53] L. Packer, Am. J. Clin. Nutr., **53**, 1050S (1991).
- [54] M. Iwatsuki et al., Biochim. Biophys. Acta, **1200**, 19 (1994).
- [55] R. H. Bisby and S. Ahmed, Free Radic. Biol. Med., **6**, 231 (1989).
- [56] S. Srivasta et al., Biochim. Biophys. Acta, **734**, 353 (1983).
- [57] S. R. Wassal et al., Biochemistry, **25**, 319 (1986).
- [58] M. Steiner, Biochim. Biophys. Acta, **640**, 100 (1981).
- [59] F. Severcan, Nanobiology, **1**, 373 (1992).
- [60] D. P. Datta, 1987. Comprehensive Introduction to Membrane Biochemistry, Floral Publishing, Cambridge.
- [61] B. L. Silver, 1985. The Physical Chemistry of Membranes, Publishers Creative Servises Inc., New York.
- [62] J. L. R. Arrondo et al., Prog. Biophys. Molec. Biol., **59**, 23 (1993).

- [63] D. A. Skoog and J. J. Levy (1992). Principles of Instrumental Analysis, Saunders College Publishing, U. S. A.
- [64] A. Watts and J. J. H. H. M. De Pont (eds), 1986. Progress in Lipid- Protein Interactions, Elsevier Science Publishers B. V. (Biomedical Division), New York.
- [65] R. J. H. Clark and R. E. Hester (eds), 1986. Spectroscopy of Biological Systems, John Wiley and Sons Ltd., New York.
- [66] J. Villalain, F. J. Aranda, and J. C. Gomez-Fernandez, Eur. J. Biochim., **158**, 141 (1986).
- [67] D. G. Cameron H. L. Casal, and H. H. Mantsh, J. Biochem. Biophys. Methods, **1**, 21 (1979).
- [68] D. Chapman et al., J. Biochem. Biophys. Methods, **2**, 315 (1980).
- [69] H. L. Casal and H. H. Mantsh, Biochim. Biophys. Acta, **779**, 381 (1984).
- [70] D. G. Cameron and G. M. Charette, Appl. Spectrosc., **35**, 224 (1981).
- [71] J. Umemura, D. G. Cameron, and H. Mantsch, Biochim. Biophys. Acta, **602**, 32 (1980).
- [72] I. M. Asher and I. W. Levin, Biochim. Biophys. Acta, **468**, 63 (1977).
- [73] H. L. Casal, Biochemistry, **19**, 444 (1980).
- [74] K. H. Gallager, 1959. The Isotope Effect in Relation to Bond Length in Hydrogen Bonds in Crystals. In: Hydrogen Bonding (ed. D. Hadzi), Pergamon Press, New York.
- [75] D. C. Lee et al., Biochim. Biophys. Acta, **769**, 49 (1984).
- [76] R. A. Haberkorn et al., J. Am. Chem. Soc., **99**, 7353 (1977).
- [77] J. L. Lippert and W. L. Peticolas, Proc. Natl. Acad. Sci. USA, **68**, 1572 (1968).
- [78] M. J. Janiak, D. M. Small, and G. G. Shipley, Biochemistry, **15**, 4575 (1976).
- [79] M. J. Janiak et al., J. Biol. Chem., **254**, 6068 (1979).
- [80] E. Boroske and L. Trahms, Biophys. J., **42**, 275 (1983).
- [81] L. Trahms, W. D. Klabe, and E. Boroske, Biophys. J., **42**, 285 (1983).

- [82] D. G. Cameron, E. F. Gudgin and H. H. Mantsch, Biochemistry, 20, 4496 (1981).
- [83] H. L. Casal et al., J. Chem. Phys., 77, 2825 (1982).
- [84] D. G. Cameron et al., Biochim. Biophys. Acta, 596, 463 (1980).
- [85] P. S. Coleman and B. B. Lavities, CRC Critical Review in Biochemistry, 341 (1981).
- [86] W. L. Duax and D. A. Norton, Eds, (1975). Atlas of Steroid Structure Vol. 1, Plenum Press, New York.
- [87] B. Perly et al., Biochim. Biophys. Acta, 819, 131 (1985).
- [88] H. Schindler and J. Seeling, J. Chem. Phys., 59, 1841 (1973).
- [89] M. Z. Lai, N. Duzgunes and F. C. Szoka, Biochemistry, 24, 1646 (1985).
- [90] R. J. Cushley and B. S. Forrest, Can. J. Biochem., 55, 220 (1977).
- [91] L. K. Bar, Y. Barenholdz, and F. Schroeder, Biochemistry, 25, 6701 (1986).
- [92] G. Nemezc, R. N. Fontaine, and F. Schroeder, Biochim. Biophys. Acta, 943, 511 (1988).
- [93] B. Snyder and E. Freire, Proc. Natl. Acad. Sci. USA., 77, 4055 (1980).

**T.C. YÜKSEKÖĞRETİM KURULU**  
**BOKÜMANTASYON MERKEZİ**